

**UNIVERSITÀ DEGLI STUDI DI CATANIA**

**DOTTORATO DI RICERCA IN BASIC AND APPLIED BIOMEDICAL  
SCIENCES**

**XXXI CICLO**

**Dipartimento di Scienze Biomediche e Biotecnologiche (BIOMETEC)**

---

---

**Dott.ssa Giulia Russo**

**Novel computational strategies for the identification of new  
therapeutic targets in melanoma and thyroid cancer**

**TESI DI DOTTORATO**

Coordinatore:

Ch.mo Prof. Massimo Libra

Relatore:

Ch.mo Prof. Francesco Pappalardo

---

---

**ANNO ACCADEMICO 2017/2018**

**Novel computational strategies for the identification of new  
therapeutic targets in melanoma and thyroid cancer**

Giulia Russo

SOTTOMESSA IN PARZIALE ADEMPIMENTO AI REQUISITI PER  
IL CONSEGUIMENTO DEL TITOLO DI  
“DOTTORE DI RICERCA”  
ALL' UNIVERSITÀ DEGLI STUDI DI CATANIA  
20 NOVEMBRE 2018, ITALIA, CATANIA

© Copyright Giulia Russo, 2018

# UNIVERSITÀ DEGLI STUDI DI CATANIA

## DOTTORATO DI RICERCA IN BASIC AND APPLIED BIOMEDICAL SCIENCES

Dipartimento di Scienze Biomediche e Biotecnologiche (BIOMETEC)

I sottoscritti certificano che hanno letto e raccomandato alla Facoltà per gli Studi di Dottorato l'accettazione della tesi intitolata “**Novel computational strategies for the identification of new therapeutic targets in melanoma and thyroid cancer**” di Giulia Russo, a parziale adempimento ai requisiti per il conseguimento del titolo di “**Dottore di Ricerca**”.

20 Novembre, 2018

Tutor (Prof. Francesco Pappalardo):

\_\_\_\_\_

Coordinatore (Prof. Massimo Libra):

\_\_\_\_\_

# UNIVERSITÀ DEGLI STUDI DI CATANIA

20 Novembre, 2018

**Autore:** Giulia Russo

**Titolo:** Novel computational strategies for the identification of new therapeutic targets in melanoma and thyroid cancer

**Dipartimento:** Scienze Biomediche e Biotecnologiche (BIOMETEC)

**Grado:** Dottore di Ricerca

L'autore concede il permesso all'Università degli studi di Catania di far circolare e di far ottenere copie della presente tesi di dottorato per soli usi didattici e non commerciali, sia a privati che istituzioni.

Firma dell'autore: \_\_\_\_\_

L'AUTORE SI RISERVA TUTTI GLI ALTRI DIRITTI DI PUBBLICAZIONE. NESSUNA PARTE DELLA TESI O RIASSUNTI ESTESI ESTRATTI DA ESSA POSSONO ESSERE RIPRODOTTI CON QUALUNQUE MEZZO, SENZA LA PREVENTIVA AUTORIZZAZIONE SCRITTA DA PARTE DELL'AUTORE.

# INDEX

SUMMARY .....	6
SOMMARIO .....	7
ACKNOWLEDGEMENTS .....	8
1 INTRODUCTION .....	10
1.1 The importance of signaling pathways and cross-talks in cancer .....	10
1.2 MAPK and PI3K/AKT pathways: common target in cutaneous melanoma and thyroid cancer .....	13
1.3 Target therapy with BRAF inhibitors.....	19
1.4 Computational strategies for signaling networks .....	25
1.4.1 Database and tools for the visualization, simulation and analysis of signaling networks .....	25
1.4.2 Algorithms for Pathway visualization, investigation and prediction .....	27
1.4.3 Software for Pathway Analysis .....	29
1.4.4 Algorithms in finding alternative pathways and new drug targets .....	30
2 AIM OF THE THESIS.....	32
3 COMPUTATIONAL MODELING IN MELANOMA.....	33
3.1 Melanoma background.....	33
3.2 Methods .....	39
3.2.1 Pathway model .....	39
3.2.2 DNA methylation .....	44
3.3 Results and discussion .....	48
3.3.1 Pathway model results .....	48
3.3.2 DNA Methylation results .....	51
4 COMPUTATIONAL MODELING IN THYROID CANCER .....	55
4.1 Thyroid cancer background .....	55
4.2 Methods .....	58
4.3 Results and discussion .....	64
5 CONCLUSIONS .....	71
6 BIBLIOGRAPHY.....	73

## SUMMARY

Cancer signaling pathways have been extensively investigated. However, the way cross-talk processes and integrates pathway responses in cancer is still far from being completely elucidated. Genetic and epigenetic alterations lead cells to aberrant proliferation and escapement from physiological mechanism controlling cell growth, survival and migration. In this context, specific mutations transform cellular proto-oncogenes to oncogenes, triggering hyperactivation of signaling pathways, whereas inactivation of tumor suppressors removes critical negative regulators of signaling. MAPK and PI3K/AKT pathways often present mutated genes in different types of cancer, and are strongly involved in intensive cross-talk.

There is an ever-increasing awareness that computational modeling and simulation are more than helpful in improving the understanding at cellular and molecular levels, in speeding-up the drug discovery process through the identification of alternative strategies with the aim to overcome drug resistance in cancer.

The main objective of this thesis is to reveal biochemical and genetic mechanisms underlying drug resistance in melanoma and thyroid cancer through the application of ordinary differential equations based models coupled with algorithmic approaches. These tumors share both MAPK and PI3K/AKT signaling pathway, with the presence of BRAF V600E mutation. Computational approaches developed in this PhD project were demonstrated to be able to find novel therapeutic targets and prognostic biomarkers for a more effective treatment in melanoma and thyroid cancer.

## SOMMARIO

Le vie di segnalazione del cancro sono state oggetto di ampio studio. Tuttavia, il modo in cui eventuali cross-talk processano e integrano le risposte delle diverse vie di segnalazione nel cancro è ancora ben lungi dall'essere completamente chiarito. Le alterazioni genetiche ed epigenetiche possono contribuire ad un'aberrante proliferazione cellulare e all'elusione del meccanismo fisiologico che controlla la crescita, la sopravvivenza e la migrazione delle cellule. In questo contesto, mutazioni specifiche trasformano i proto-oncogeni cellulari in oncogeni, innescando l'iperattivazione delle vie di segnalazione, mentre l'inattivazione dei soppressori tumorali rimuove i regolatori negativi critici della segnalazione. Le cascate di segnalazione MAPK e PI3K/AKT presentano spesso geni mutati in diversi tipi di tumore e sono fortemente coinvolti in complessi cross-talk.

E' presente una sempre più crescente consapevolezza di come la modellizzazione e la simulazione computazionale risultino più che utili nel migliorare la comprensione a livello cellulare e molecolare dei fenomeni biologici, e contribuiscano all'accelerazione del processo di scoperta dei farmaci e l'identificazione di strategie alternative per superare la resistenza farmacologica presente in molte forme di cancro.

L'obiettivo principale di questa tesi è quello di rivelare, attraverso l'utilizzo di modelli computazionali basati su equazioni differenziali ordinarie accoppiate ad approcci algoritmici, i potenziali meccanismi biochimici e genetici alla base della resistenza dei farmaci nel melanoma e nel cancro della tiroide. Questi tumori condividono entrambe le vie di segnalazione MAPK e PI3K/AKT e la presenza della mutazione BRAFV600E. Gli approcci computazionali sviluppati in questo progetto di dottorato sono stati efficaci nell'identificazione di nuovi bersagli terapeutici (nonché di biomarcatori prognostici) per un trattamento più efficace del melanoma e del cancro della tiroide.

## ACKNOWLEDGEMENTS

Undertaking this PhD has been a truly life-changing experience for me and it would not have been possible to do without the support and guidance that I received from many people. Hence, I would like to extend thanks to who, so generously, contributed to the work presented in this thesis.

Special mention goes to my enthusiastic supervisor Prof. Francesco Pappalardo, for guiding and supporting me over the years. It has been a honor to be his first PhD student. He has taught me, both consciously and unconsciously, how a computational biologist should be. I appreciate all his contributions of time, ideas, feedbacks and opportunity to make my PhD experience productive and stimulating. I must confess that my PhD has been an amazing experience and I thank Francesco wholeheartedly, not only for his tremendous academic support, but also for giving me so many wonderful opportunities. Not many PhDs involve travelling a lot and through many countries, like to get to a conference in New Delhi! The joy and enthusiasm he owns for his research was contagious and intensively motivational for me. I am more than grateful for the excellent and invaluable example he has provided me as a researcher, mentor, instructor and go-to person. Without his guidance and constant feedback, this PhD would not have been achievable.

I am also hugely appreciative to Prof. Massimo Libra, especially for sharing his oncology expertise so willingly, and for being so dedicated to his role as my secondary supervisor.

The members of the COMBINE group have contributed immensely to my personal and professional time at University of Catania. The group has been a source of friendships as well as good advice and collaboration. I would like to acknowledge the senior group member Prof. Santo Motta for his insightful observations and precious suggestions he gave me since the beginning of my PhD I also would like to extend my special thanks to Marzio, for nurturing my enthusiasm for computational



modeling and to the junior part of the COMBINE group made of Giuseppe Sgroi and Giuseppe Parasiliti Palumbo. With all of them, I have had the pleasure to work with and alongside in a brilliantly and creatively way.

I would particularly like to acknowledge Guanglan Zhang, who has long been an inspiring research figure for me and a wonderful and generous friend. She constantly gave me enthusiasm, encouragement and suggestions during the thesis writing hell from the other part of the world. Nevertheless, unbelievably I feel her very close to me!

I would like to thank also the research group supervised by Prof. Massimo Libra and the one guided by Prof. Francesco Frasca that contributed to this research.

A special thank goes to my amazing family for the love, support, and constant encouragement I have gotten over the years. In particular, I would like to thank my parents, my brother (especially for his insights and suggestions about the state of the art of thyroid cancer), Andrea and my little niece Elena. You are the salt of the earth, and I undoubtedly could not have done this also without you.

And last but not the least, I would like to thank my passion for swimming and all the people around the swimming-pool center that allow me to feel constantly enthusiastic, encouraged, cheerful and full of life.

# 1 INTRODUCTION

## 1.1 The importance of signaling pathways and cross-talks in cancer

Biological cells communicate each other using physical signals but mostly through chemical signals. Within an organism, cells are immersed in an ocean of growth factors and hormones that represent the most important sources of chemical signals, secreted firstly from a cell and then released into the extracellular space<sup>1,2</sup>.

The chemical signal represents a real message with a specific biological meaning and is carried out by a ligand or a growth factor<sup>3</sup>. It is often communicated through a sequence of secondary messengers inside the cell and then it is propagated towards the neighboring cells<sup>4</sup>. After that, cell changes its status because of an alteration in the activity of a gene or when a whole process such as cell division has been initiated. Ultimately, the original intercellular signal is converted into a new signal that triggers a biological response<sup>5</sup>.

This complex and accurate function of communicating is guaranteed through a number of pathways that receive and process signals originating not only from the external environment and from other cells within the organism, but also from different regions within the cell, hence moving from a micro to a macroscale<sup>6</sup>. Furthermore, all of this cell machinery is strongly capable to adapt the function of an organism to environmental changes in a signal-directed way and to control all the cellular functions as well. The capability to coordinate and regulate cellular function results from the complex network of communications among cells, where signals are transduced into intracellular biochemical reactions that follow, on a case-by-case basis, different kinetic laws such as mass action equilibrium<sup>7</sup>, Michaelis-Menten kinetics<sup>8</sup>, constant flux equations<sup>9</sup> and so forth<sup>10</sup>. The two general categories of cell signaling include intercellular and intracellular signaling:

- *intercellular* signaling: it coordinates and regulates the physiological functions of a multicellular organism through the communication among cells<sup>11</sup>. In this case, a single cell

influences the behavior of other cells in a specific way. Signals propagated during intercellular signaling are delivered and processed in target cells with the aim to trigger biochemical reactions that absolve a specific cell function<sup>12</sup>. Intercellular communication uses messenger substances, such as hormones<sup>13</sup>, secreted by signal-producing cells and gathered by target cells. The extracellular signals are transduced into intracellular signaling sequences that control many of the biochemical activities of a cell and can trigger the formation of further extracellular signals<sup>14,15</sup>. Typical examples of signaling deal with physiological activities such as response to external signals<sup>16</sup>, intermediary metabolism<sup>17</sup>, cell growth<sup>18</sup>, cell division<sup>19</sup>, cell motility<sup>20</sup>, cell morphology<sup>21</sup>, cell differentiation<sup>22</sup> and cell development<sup>23</sup>. Cells communicate each other via messenger substances, gap junctions, surface proteins, electrical signals<sup>24-27</sup>. Communication steps between cells could be summarized as follows: *i*) formation of a signal in the signal-producing cell as a result of an external trigger; *ii*) transport of the signal to the target cell; *iii*) recording of the signal in the target cell<sup>28,29</sup>.

- *intracellular* signaling: it coordinates and regulates signals within the cell, in response to extracellular and intracellular stimuli<sup>5,30</sup>. Sensory signals or external growth factors are specifically recognized, processed and transduced by cell receptors that convert the external signal into an intracellular signaling chain. The intracellular signaling paths modulate intermediary metabolism<sup>17</sup>, cell division<sup>19</sup>, cell morphology<sup>4</sup>, and also the transcription process<sup>31</sup>.

Both intercellular and intracellular signaling are regulated by specific control mechanisms and mediators in a certain tissue<sup>32</sup>. Modulation of intercellular signaling is mainly regulated via external trigger signals, feedback loops, degradation and modification processes, and amount and activity of receptors<sup>33-35</sup>.

Typically, a large number of signaling components participate in the transduction of an extracellular signal into intracellular biochemical reactions that define the endpoint of signal transduction<sup>36</sup>. To characterize and describe a signal transduction pathway, the number and type of signaling

components involved, as well as their linkages, represent the essential features to consider. However, it is increasingly documented that the existence of subtypes of signaling proteins allow different signals to access and to be processed in the same type of signaling path, leading then to variable outcomes<sup>37</sup>. Besides, the features of branching and cross-talk of signaling in biology, in which one or more components of one signal transduction pathway affect other pathways, usually include a large number of possible linkages within a signaling path and between different signaling paths<sup>38,39</sup>. In these signal transduction pathways, there are often shared components that can interact with either pathway.

Commonly, signaling pathways are depicted through a sequential transmission of signals in a linear signaling chain. Linear pathway description is very useful to illustrate the main biochemical steps in a signaling cascade of events that help to outline the intrinsic biological and biochemical meaning of a signaling pathway. Each signal is listed by an upstream component of a signaling chain and is then transferred to the downstream constituent that will sequentially propagate the signal to the next protein<sup>40</sup>. This linear description of signaling comes out from *in vitro* experiments where signaling is originated by strong signals produced by overexpression or mutation of signaling proteins<sup>41</sup>. A component will activate the next component through intrinsic mechanisms of activation and deactivation by specific enzymes, commonly known as tyrosine and serine-threonine protein kinase<sup>42,43</sup>. They represent a complex system with elaborated internal and external interactions and are known to play a fundamental role in protein phosphorylation<sup>44</sup>, the main enzymatic process for the initiation of cellular processes such as cell division, metabolism, survival and apoptosis. The routing of signals depends on the amplitude, that is the signal intensity, and on the frequency that influences the duration of the signal. It is well known that many signaling proteins own multiple downstream reactions that can be activated for further signal transduction<sup>40</sup>. This feature leads to a degeneracy of signals and to a distribution of alternative reaction partners (or branching reactions)<sup>45</sup> that are not always been well defined experimentally.

Within the signaling pathways, different routes and alternative paths connect one pathway with another one, reinforcing each other and constantly receiving excessively signals simultaneously<sup>46</sup>. Basically, the multiple outputs that originate from the same type of signaling protein lead to an activation of alternative routes and to the biological phenomenon of cross-talk.

A cross-talk is a biological process that involve the signaling cascades of transduction pathways and it refers to the interdependence among signaling pathways<sup>37–39,47</sup>.

In specific occurrences, one or more components of one signal transduction pathway affect the other one, sharing the same components that can interact and be linked with either pathway. These phenomena process a large number of signals at the same time and the information flow does not run through a single conduit.

Moreover, in cross-talk dynamics, when a signal propagates through different branches and meet a common target, the signaling responses along these branches will influence, with an incremental effect, the overall target response. Furthermore, each intersection that connects one pathway with another could potentially represent a regulatory checkpoint for the signal flow itself. Noteworthy is the multivalency of signaling proteins, that determines several effects on the components of a signaling, and the plausible role of cross-talk in achieving robust activation of key downstream targets by low physiological doses of external stimuli<sup>48</sup>. In the light of this extraordinary complexity of signaling networks, it becomes more and more evident how sophisticated hypothesis and accurate predictions of cellular response and their intricate relationship represent a mandatory goal in signaling research.

## 1.2 MAPK and PI3K/AKT pathways: common target in cutaneous melanoma and thyroid cancer

Many examples of cross-talk were found in cell signaling<sup>38</sup>. In particular, multiple levels of cross-talk interactions between PI3K/AKT and MAPK signaling pathways have been discovered in the

modulation of cell fate<sup>47,49,50</sup>. In this view, specific feedforward and feedback loops, involving interacting pathways, coordinate both input and output response of both pathway<sup>34,47</sup>.

The mitogen-activated protein kinase (MAPK) and the phosphoinositide 3-kinase (PI3K/AKT) pathway are the most common signaling pathways downstream of cellular growth factor receptor<sup>51-54</sup>. These signaling pathways orchestrate the majority of cellular physiological processes, such as cell growth, differentiation, metabolism, survival and mitogenesis<sup>43,55-57</sup>. A graphical summary of both pathways is shown respectively in Figure 1 and Figure 2.

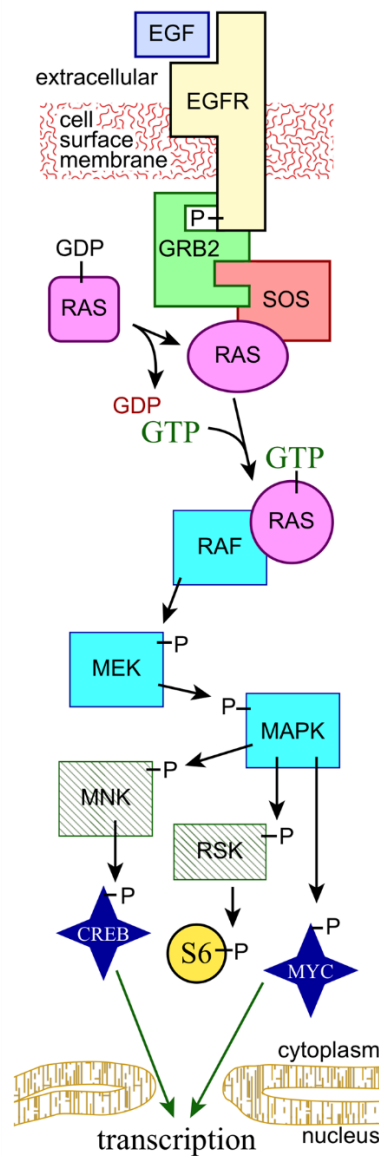


**Figure 1. Schematic illustration of MAPK signalling cascade.**

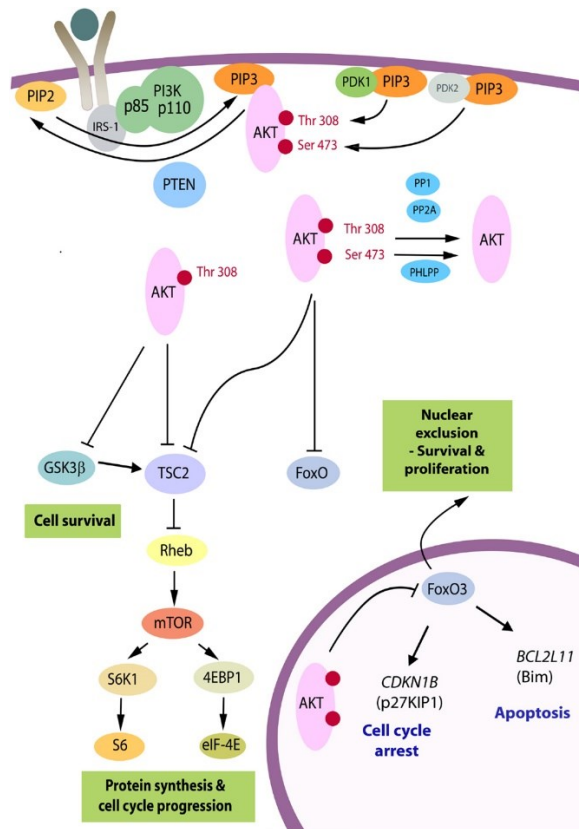


**Figure 2. Schematic illustration of PI3K/AKT signalling cascade.**

Robbins et al. *Frontiers in Endocrinology* 2016;6:188

MAPK cascade is a highly conserved pathway expressed in mammals<sup>58</sup> in at least four distinct regulated groups of MAPKs<sup>59</sup>, extracellular signal-related kinases (ERK)-1/2<sup>60</sup>, Jun amino-terminal kinases (JNK1/2/3)<sup>61,62</sup>, p38 proteins (p38alpha/beta/gamma/delta)<sup>63,64</sup> and ERK5<sup>65</sup>. All of these kinases are activated by specific MAPKKs: MEK1/2 for ERK1/2<sup>66</sup>, MKK3/6<sup>67,68</sup> for the p38, MKK4/7<sup>69</sup> (JNKK1/2) for the JNKs, and MEK5<sup>70</sup> for ERK5. Each MAPKK, however, can be activated by more than one MAPKKK<sup>71</sup>, increasing the complexity and diversity of MAPK signalling. Apparently, each MAPKKK confers responsiveness to distinct stimuli. For example, activation of ERK1/2 by growth factors depends on the MAPKKK C-RAF<sup>72</sup>, but other MAPKKKs

may activate ERK1/2 in response to pro-inflammatory stimuli<sup>59</sup>. The fundamental protein network involved in this signalling cascade is reported below in Table 1.

<b>Signaling pathway KEGG network</b>	<b>Cell function</b>	<b>Reference</b>
EGF-EGFR-RAS-ERK	Cell proliferation	73
PDGF-PDGFR-RAS-ERK	Cell migration, proliferation and survival	74
FGF-FGFR-RAS-ERK	Cellular proliferation, differentiation and migration	75
EGF-EGFR-PLCG-ERK	Cell motility	76
IL1-IL1R-p38	Pro-inflammatory activities, innate immune reactions	77
IL1-IL1R-JNK	Cellular apoptosis, response to stress stimuli	78
TGFA-EGFR-RAS-ERK	Cell proliferation, differentiation and development	79
IGF2-IGF1R-RAS-ERK	Pro-proliferative and anti-apoptotic effects	80
REG-EGFR-RAS-ERK	Tumorigenesis	81
AREG-EGFR-RAS-ERK	Immunity, inflammation and tissue repair	82

**Table 1. Signaling pathways involved in MAPK cascade**

In physiological conditions, the activation of the MAPK signalling pathway initiates through ligand activation of receptor tyrosine kinases (RTKs)<sup>83</sup> followed by guanosine triphosphate-bound RAS binding<sup>84</sup> to RAF kinase and its family members<sup>85</sup>, BRAF<sup>86</sup> and/or CRAF<sup>87</sup>. This interaction transposes the RAF kinase “activator” to the plasma membrane, where conformational changes and consequent phosphorylation lead to a heterodimerization or homodimerization of the activator RAF with a “receiver” RAF kinase<sup>88,89</sup>. In particular, BRAF, being the RAF activator, transactivates CRAF, the bound receiver, that will be able to phosphorylate MEK<sup>90</sup>. ARAF own a marginal role even though it is able also to dimerize itself; ARAF kinase activity is weak in comparison to the other family members BRAF and CRAF and it seems that it works more than scaffold molecule for stabilizing the interactions between BRAF and CRAF<sup>91</sup>. Participation of BRAF in this signalling cascade is fundamental<sup>92</sup>. Indeed, Freeman et al., have shown how a depletion of BRAF in HeLa cells



reduce CRAF kinase activity induced by epidermal growth factor, by 90%, while CRAF depletion reduces BRAF activity by only 50%, and ARAF depletion present no significant effect<sup>88</sup>.

For what concerns PI3K-AKT signaling pathway, several types of cellular stimuli or toxic insults this cascade<sup>93</sup>. The binding of growth factors to their RTK or G protein-coupled receptors (GPCR) stimulates respectively class Ia and Ib PI3K isoforms<sup>94</sup>. PI3K catalyzes the production of phosphatidylinositol-3,4,5-triphosphate (PIP3) at the cell membrane<sup>95</sup>. PIP3 in turn works as a second messenger that contributes to activate AKT<sup>53</sup>. Once active, AKT can regulate key cellular processes by phosphorylating substrates involved in cell cycle, protein synthesis, metabolism and apoptosis<sup>96,97</sup>.

The fundamental protein network involved in this signalling cascade is reported below in Table 2.

<b>Signaling pathway KEGG network</b>	<b>Cell function</b>	<b>Reference</b>
EGF-EGFR-RAS-PI3K	Cell proliferation	73
EGF-EGFR-PI3K	Survival, proliferation, migration, and differentiation	98
FGF-FGFR-PI3K	Proliferation, migration, angiogenesis and survival of cancer cells	99
PDGF-PDGFR-PI3K	Survival, proliferation, growth, and metabolism	100
HGF-MET-PI3K	Cell proliferation, migration, tumorigenesis, angiogenesis	101
KITLG-KIT-PI3K	Cell survival, proliferation, hematopoiesis, stem cell maintenance, gametogenesis, mast cell development, migration and function and in melanogenesis	102
CXCR-GNB/G-PI3K-AKT	Migration, intracellular signalling and intercellular communication in the microenvironment, transcription, translation, proliferation, growth, and survival	103
IGF-IGFR-PI3K-NFKB	Regulation of protein synthesis, glucose metabolism, cell development, inhibition of apoptosis and triggering of inflammatory responses	104

PTEN-PI3K-AKT	Survival, migration, cell cycle progression and arrest, metabolism, tumorigenesis	105
TGFA-EGFR-PI3K	Cell proliferation, differentiation and development	73
IGF2-IGF1R-PI3K	Growth, development, and maintenance tissue, anti-apoptotic effects, promoting glucose metabolism	106
EREG-EGFR-PI3K	Cellular growth, proliferation, tissue regeneration, pain processing	107
AREG-EGFR-PI3K	Cell proliferation, survival, cell growth	108

**Table 2. Signaling pathways involved in PI3K/AKT cascade**

PI3K phosphorylates the phosphatidylinositol-3,4,5-trisphosphate (PI(3,4,5)P<sub>3</sub>), a fundamental second-messenger of survival signaling<sup>109</sup>. PI3K kinases are heterodimers made of a catalytic subunit called P110 and a regulatory subunit named p85, which is activated by RTKs and by GPCR<sup>110–112</sup>.

The signaling downstream steps of RTK receptor include phosphorylation of the insulin receptor substrate (IRS)<sup>113</sup> with the concomitant binding of the SH2-containing phosphatase (SHP-2)<sup>114</sup> and the phosphorylation of p85 subunit of PI3K<sup>115</sup>. This determines PI3K activation and, via PI(3,4,5)P<sub>3</sub>, the stimulation of 3-phosphoinositide-dependent kinase-1 (PDK1) and the enhancement of the phosphorylation and, then, of the activity of AKT<sup>53,116–118</sup>.

Frequent genetic alterations, especially in cancer, were found in these signaling pathways: about 50% of melanoma patients present mutations in the serine/threonine kinase BRAF of melanocytes<sup>119</sup>, which are regulated by the RAS/RAF/MEK/ERK MAPK pathway<sup>120</sup>, while PI3K pathway is often dysregulated during melanomagenesis<sup>121</sup>. AKT itself is overexpressed during melanoma progression<sup>122</sup>.

In more than 70% of papillary thyroid carcinoma, genetic alterations such as point mutations of BRAF and RAS gene, lead to an activation of MAPK<sup>123,124</sup>. Moreover, several aberrant RTKs and genetic mutations result in a continuous activation of PI3K/AKT in its downstream effectors leading to a high cell proliferation in thyroid carcinomas<sup>125,126</sup>. Typical examples of genetic modifications are

represented by phosphatase and tensin homolog deleted on chromosome 10 (PTEN) encoding genes<sup>127</sup>, extra copies of phosphoinositide-3 kinase catalytic  $\alpha$  (PIK3CA)<sup>128</sup>, phosphoinositide-3 kinase catalytic  $\beta$  (PIK3CB) and PDK1 encoding genes<sup>129</sup>.

### 1.3 Target therapy with BRAF inhibitors

BRAF gene, also known as BRAF proto-oncogene or serine/threonine kinase, is a human gene that allows the transmission of chemical signals from outside the cell to the nucleus<sup>130</sup>. The cytogenetic location of BRAF gene is 7q34, which is the long (q) arm of chromosome 7 at position 34 and it encodes a protein belonging to the RAF family of serine/threonine protein kinases called BRAF. BRAF protein is a serine/threonine-specific protein kinase made of 766 amino acids and its mammalian RAF kinase family is composed by three RAF isoforms: A-RAF, BRAF and C-RAF<sup>131</sup>. Several findings suggest that BRAF is the family member the most strongly involved in mediating MAPK activation<sup>132</sup>. In particular, it consists of three conserved domains characteristic of RAF kinase family:

- i)* conserved region 1 (CR1), a Ras-GTP-binding self-regulatory domain;
- ii)* conserved region 2 (CR2), a serine-rich hinge region;
- iii)* conserved region 3 (CR3), a catalytic protein kinase domain that phosphorylates a sequence of protein substrates.

Before becoming active, BRAF must be initially bound to RAS-GTP. Then, BRAF changes its conformation leading to a dimerization via hydrogen-bonding and electrostatic interactions of the kinase domains. BRAF catalyzes the phosphorylation of serine and threonine residues in a sequence of cascade proteins through the energetic contribution of ATP, yielding ADP and specific substrates of phosphorylated proteins as products. It is not surprisingly that, due to the high BRAF kinase activity compared to the other family members, a high frequency of BRAF point mutations and a constitutively activation of BRAF is observed in human cancers<sup>133,134</sup>. Mutations in this gene, mostly

V600E alteration, represent the most frequently detected cancer-causing mutations in melanoma (V600E has been examined in 66% of malignant melanomas)<sup>135-137</sup> and in several other cancers including non-Hodgkin lymphoma<sup>138</sup>, colorectal cancer<sup>139</sup>, thyroid carcinoma<sup>140</sup>, non-small cell lung carcinoma<sup>141</sup>, hairy cell leukemia<sup>142</sup> and adenocarcinoma of lung<sup>143</sup>. Approximately 80–90% of V600 BRAF mutations regard V600E<sup>144-146</sup> and they deal with an amino acid substitution at position 600 in BRAF, from a valine (V) to a glutamic acid (E). This mutation is specifically localized to the serine/threonine kinase domain and occurs within the activation segment of the kinase domain, leading to a constitutive activation of the protein itself and insensitivity to negative feedback mechanisms<sup>147,148</sup>.

Among the BRAF mutations observed in melanoma, over 90 % are at codon 600 and, among these, over 90 % are single nucleotide mutations resulting in substitution of glutamic acid for valine<sup>149</sup>. BRAFV600E mutation has been implicated in melanoma progression, through the activation of the downstream MEK/ERK within MAPK signalling pathway, evasion of senescence and apoptosis, angiogenesis, tissue invasion and metastasis process, and evasion of immune response<sup>137,150</sup>.

Activating mutation in the BRAF serine/threonine kinase represents also the most common genetic alteration in thyroid cancer, occurring in approximately 45% of papillary thyroid cancer, and in a lower proportion of poorly differentiated thyroid cancer (PDTC) and anaplastic thyroid cancer (ATC)<sup>140,151,152</sup>.

Over 95% of all BRAF mutations detected in thyroid cancer is a thymine to adenine transversion at exon 15 nucleotide 1799 (T1799A) of the BRAF gene leading to substitution of valine by glutamic acid at residue 600 of the protein chain (V600E)<sup>153</sup>. This alteration results in a constitutively active BRAF molecule with sustained kinase activity that promotes chronic stimulation of MAPK pathway, thereby resulting in increased phosphorylation of downstream targets, including ERK kinase<sup>154</sup>. This altered signalling results in an increased cell proliferation, survival and tumor progression, in a growth factor independent manner<sup>155</sup>.

In comparison to wild-type BRAF, activating mutations in BRAF are constitutively active and there is some evidence that these changes lead to bypass the dimerization process<sup>156</sup>. In melanoma, BRAF V600E mutation permits BRAF to signal as a monomeric enzyme without the presence of activated RAS and upstream RTK inputs to amplify its dimerization<sup>157</sup>. In papillary thyroid cancer (PTC), the BRAF V600E gene mutation is associated with more rapid cancer growth and a higher death rate<sup>158</sup>. The discovery of genetic underpinnings in cancer has opened the way for targeted therapies consisting in drugs that directly target cells with specific gene changes, acting on specific cell processes and changing the way tumor cells signal to each other<sup>159–161</sup>. These drugs can stimulate the body to attack or control the growth of cancer cells. Given the crucial role both in melanoma and in thyroid cancer, BRAF V600E represents the most promising therapeutic target for treatment of patients with metastatic melanoma and advanced thyroid cancer refractory to standard approaches<sup>162,163</sup>. Several small molecule BRAF inhibitors have been developed during the last years, showing encouraging results in clinical trials both in melanoma and thyroid cancer<sup>164</sup>. These drugs work through a selective competitive mechanism of action for the modified adenosine triphosphate binding site of the active forms of BRAF V600E kinase; in this way, they inhibit its ability to participate in MAPK pathway activation. Vemurafenib and dabrafenib have been shown to be highly selective for BRAF V600E mutant cells that are respectively 100 and 500 fold higher than those for cells with wild-type BRAF<sup>165,166</sup>. Small molecules as vemurafenib, also known as PLX4032, and dabrafenib or GSK2118436 belong to BRAF inhibitors and reduce or slow tumor growth in people whose metastatic melanoma has a BRAF gene change<sup>167</sup>. Such drugs can help some patients to live longer, even though the melanoma typically starts increasing over again. Dabrafenib can be used after surgery in people with stage III melanoma (tumors that have spread to regional lymph nodes) and can contribute to decrease the risk of cancer recurrence.

MEK protein, which properties downstream from BRAF, represents an additional target in melanoma treatment because agents that block MEK proteins can indirectly help melanoma patients with BRAF mutation. MEK inhibitors as trametinib and cobimetinib have been shown to shrink BRAF-mutant

melanoma<sup>168</sup>. However, when used by themselves, these drugs do not seem to shrink the tumor as BRAF inhibitors usually do. Hence, a combination therapy with BRAF and MEK inhibitors represents a more successful therapeutic approach in decreasing tumors for longer periods than administering either type of drug alone. The combination of dabrafenib with vemurafenib or trametinib has significantly extended the progression free survival compared to dabrafenib alone in advanced BRAF V600E mutated melanoma<sup>169–171</sup> and in advanced BRAF V600E mutated anaplastic thyroid cancer<sup>172,173</sup>. Unfortunately, response to BRAF inhibition differs among cell types: in most patients who initially respond to these treatments, then resistance is inevitably acquired to BRAF inhibitors as cells develop alternative mechanisms to pathway activation. Up to now, several potential resistance mechanisms have been identified within the context of both cancers that lead to reactivation of the MAPK pathway<sup>171,174–176</sup>.

For what concerns melanoma, the resistance mechanisms include:

- i)* NRAS mutations<sup>177</sup>;
- ii)* activation of upstream RTKs (e.g., insulin-like growth factor 1 receptor, platelet-derived growth factor receptor  $\beta$  [PDGFR $\beta$ ], epidermal growth factor receptor [EGFR])<sup>178</sup>;
- iii)* BRAF V600E kinase splice variants unable to be inhibited by BRAF inhibitors<sup>179</sup>;
- iv)* transactivation of an uninhibited RAF dimer partner by the inhibited BRAF V600 mutant<sup>180</sup>;
- v)* acquisition of MEK-activating mutations<sup>181</sup>.

Thyroid cancer cells harboring BRAF V600E mutation show a not well-defined intrinsic resistance mechanism to BRAF kinase inhibitors (KIs). High levels of EGFR in thyroid cancer cells show a positive response to the combination of vemurafenib with an EGFR inhibitor, while poorly responses were observed when vemurafenib was administered alone<sup>172</sup>. In the light of this, EGFR expression level represents a sensitivity factor to BRAF V600E inhibitors<sup>182</sup> and its response mechanism seems

to be the deactivation of EGFR-negative feedback loops by vemurafenib and the following prompt activation of RTK<sup>183</sup>.

These mechanisms result in continuous signalling along the MAPK pathway or an alternative pro-survival pathway such as the PI3K pathway. Other alterations, both upstream and downstream of BRAF can alternatively activate other signalling pathways. Hence, growing concerns over drug resistance to molecular targeted therapies such as in melanoma and papillary thyroid cancer<sup>184</sup>, including BRAF and MEK inhibitors, have stimulated researchers to discover alternative molecular targets for the treatment of disorders linked to BRAF mutations.

Pathways have not only facilitated researchers to understand the theoretical complexity of cell molecular mechanisms, at the same time, supported by the interdisciplinary framework of systems biology, but they have constituted a bridge for the development of innovative tools for complex biological events<sup>185</sup>.

From a systems biology perspective, there are many tools and resources for pathway analysis<sup>186–188</sup>, an emergent discipline combining software tools, database models and computational algorithms with the aim to help biologists in converting protein interaction data into a set of computational models<sup>189</sup>. High-throughput technologies also contribute to a significant amount of protein interaction data, generated through deep sequencing and microarrays<sup>190</sup>. All of these data help to acquire an overall picture of cell regulatory processes.

An accurate classification of these methods remains discussable, according to the fact that pathway analysis methods evolve very fast. However, three main groups of methods in pathway analysis are available by now: *i*) Over-Representation Analysis or Enrichment Analysis (ORA); *ii*) Functional Class Scoring (FCS) and *iii*) Pathway Topology (PT).

ORA measures the percentage of genes in a specific pathway or any gene group (gene ontology (GO) groups, protein families and so on) that own differential expression. The main scope of ORA is to

provide a list of the most relevant pathways, sorted in accordance to a p-value. It is possible, hence, to identify relevant pathway, through the number of genes differently expressed in the experiment that pathways contain. The statistical significance of the correspondence among genes from a pathway and the list of differently expressed genes is determined by statistical tests as Fisher's test, hypergeometric distribution test and so forth<sup>191,192</sup>.

FCS analyzes the expression change of overall genes in the list (not ranking by statistical significance) of differently experimental expressed genes. FCS removes the ORA cut-off threshold limitation. The aim of FCS is to evaluate differently expressed genes enrichment scores using pathways as gene sets to execute their calculations<sup>193,194</sup>. One of the first and most popular methods using the FCS approach is the Gene Set Enrichment Analysis (GSEA), also known as functional enrichment analysis<sup>195</sup>. GSEA is useful to identify genes that display precise changes at the individual level and harmonious enrichment within a set<sup>196</sup>. It is worth mentioning that pathway enrichment methods can be distinguished by the use or the absence of an explicit gene-wise statistic to measure the gene's association with a specific treatment and evaluate the relevance of a specific pathway in a specific treatment. Conversely, Gene Set Analysis (GSA)<sup>197</sup> is able to rank genes applying the max-mean statistic in order to summarize gene sets and re-standardize them for more accurate inferences.

PT is similar to FCS, but PT uses gene-level statistics through different databases integration. The critical difference is that PT is able to re-score the implication of a pathway as the connections change by taking into account the information about the role, the position and the direction of a biochemical interaction directly from the pathway database<sup>198</sup>. Oppositely, FCS will always provide the same score. Signaling Pathway Impact Analysis (SPIA)<sup>199</sup>, EnrichNet<sup>200</sup>, Gene Graph Enrichment Analysis (GGEA)<sup>201</sup> and TopoGSA<sup>202</sup> are some examples of PT approaches.

Thomas et al. suggested a method to analyse the topology of genes in a pathway employing a genetic algorithm for the estimation of the contribution of each gene, coupled with a system biology-based approach for the identification of significant perturbed genes in a specific pathway<sup>203</sup>.



Additionally, Bayesian Network (BN) models have gained popularity for learning biological pathways from microarray gene expression data<sup>204,205</sup>. Biological pathways as BN were modeled in 2014 by Korucuoglu et al., pioneers in developing the Bayesian Pathway Analysis (BPA) helpful for the identification of cancer-related pathways<sup>206</sup>.

At the same time, other methods such as cluster analysis with depth of inference approach<sup>207</sup>, correlation statistics analysis<sup>208</sup>, weight matrices<sup>209</sup>, neural networks<sup>210</sup>, genetic algorithms<sup>211</sup> and supervised learning algorithms<sup>212</sup> represent a helpful set of resources for pathway analysis and discovery.

In this scenario, three major “actors” play a fundamental and necessary role in the game:

1. Databases: essential to storage molecular interaction network, collect pathways, molecular annotation and classifications (ontologies).
2. Algorithms: fundamental to allow the navigation of the network in the databases, the statistical analysis of the high - throughput data, the pathway inference and the network modeled.
3. Software client interface: useful for pathway and network layout and visualization.

## 1.4 Computational strategies for signaling networks

### 1.4.1 Database and tools for the visualization, simulation and analysis of signaling networks

A growing number of databases provides information and knowledge about function annotation, protein interactions and experimentally validated biological pathways. These databases represent excellent and essential resources to ease pathway predictions and models in general<sup>213,214</sup>. Most researches and scientists have focused on integrating function annotation and protein–protein networks with expression data to ameliorate the accuracy and precision of a pathway model construction.

Several public universities have taken a pioneering lead in the attempt to become a fundamental authority for pathway and molecular interaction databases. In particular, Kyoto University has developed the Kyoto Encyclopedia of Genes and Genomes (KEGG) database promptly curated by its own staff and containing a comprehensive collection of pathways curated by scientists considered to be the top experts in the field<sup>215</sup>.

KEGG classifies pathways into seven specific classes: metabolism, genetic information processing, environmental information processing, cellular processes, organismal systems, human diseases and drug development. KEGG utilizes a sort of “maplink” to represent an interaction between a protein belonging to one pathway and a protein within the linked pathway. Moreover, KEGG associates more pathways from different species into one framework.

There are other databases that is worth mentioning for the investigation of biological pathway and the improvement of research in general:

- A. WikiPathways: it is particularly useful to create manually electronic graphs of structured pathways both for cellular signaling and for metabolic processes<sup>216</sup>. Moreover, each pathway sheet includes a brief description, a curated bibliography, an updated pathway version history and a list of all the component genes and proteins linked to public resources.
- B. Gene Ontology (GO): it provides gene composition information of pathways pointing out the gene function and its relationships with three ontology categories, such as biological process, molecular function and cellular component<sup>217</sup>.
- C. Protein ANalysis THrough Evolutionary Relationships (PANTHER): it represents a large curated biological database of gene/protein families based on a classification system that identify gene function and classify them with their functionally related subfamilies. PANTHER takes part of the Gene Ontology Reference Genome Project aimed to categorize proteins and genes for high-throughput analysis<sup>218</sup>.

D. Reactome: it is an open source curated bioinformatics database of human pathways and biochemical enzymatic reactions in which the concept of “reaction” is generalized through the typical transformations of specific entities such as nucleic acids, proteins (with or without post-translational modifications) and macromolecular complexes<sup>219</sup>. These transformations include the transport of a specific entity from one compartment to another, the consequent interaction necessary to induce the protein complex formation and so on. This simple generalization allows to capture the range of biological processes that spans signaling, metabolism, transcriptional regulation, apoptosis and synaptic transmission in a single internally consistent, computationally navigable format.

#### 1.4.2 Algorithms for Pathway visualization, investigation and prediction

Several applications can be found in the literature about two dimensional graph layout for pathway analysis<sup>220</sup>. The most popular are force-based and energy-based algorithms able to exploit the N-body simulation method and helpful to reveal hubs and clusters in the signaling networks<sup>221</sup>.

Force-based algorithms are based on the ascription of definite physical properties to the nodes (treated as a set of interacting particles) and edges of the graph that will influence the equilibrium state of the entire system. This method uses both repulsive (i.e., electrostatic interaction between every pair of particles) and attractive forces (i.e., spring interaction along the graph edges) with the target to identify the stationary node position matching the equilibrium state of the entire system.

Energy-based algorithms are similar to force-based ones, as the equilibrium state of the system corresponds to a minimum of energy. These approaches offer a good basis for arbitrary graph placement but need huge computational resources<sup>222</sup>.

For every fixed node  $\bar{u}$  ( $\bar{u} \in V$ ) we have:

$$\sum_{v \in V} F_{rep}(r_{\bar{u}} - r_v) + \sum_{(\bar{u}, v) \in E} F_{attr}(r_{\bar{u}} - r_v) = 0$$

(1)

Zero net force corresponds to the result of force-based algorithms, while the result of energy-based algorithms matches with the state corresponding to the minimum energy

$$U_{min} = \min \left[ \sum_{\{u,v\} \in V} U_{rep} (r_u - r_v) - \sum_{(u,v) \in E} U_{attr} (r_u - r_v) \right] \quad (2)$$

where  $U_{rep}$  and  $U_{attr}$  are absolute values of the repulsion and attraction potentials.

In both the approaches, the main goal is to achieve the stationary equilibrium for each node position. The force-based algorithm implementation consists of a solution of a nonlinear set of algebraic equations from a mathematical point of view, while the energy-based algorithm performs functional minimization. Both of these properties can be derived from one another.

For what concerns pathway investigation and prediction, genetic algorithms (GAs)<sup>223</sup> and supervised learning algorithms represent a class of methods to search knowledge and targets within gene interaction networks and also to automatically identify functionally cooperative genes.

GAs originate from the studies of cellular automata conducted by Holland and collaborators in the early 1970s<sup>224</sup>. From that moment forward, GAs have been increasingly applied to several optimization problems in different fields, with a special attention in biomedicine. GAs consist on randomised, parallel search algorithms that model the principles of natural selection that leads to evolution. Like natural selection, GAs is a robust search method needing little information to explore effectively in large and poorly understood search spaces. In literature, several genetic algorithms were developed in order to take a data-driven approach to annotate and detect novel biological pathways, clusters in biological networks and to isolate functional and disease pathways.

Nguyen et al., described a method for orienting protein–protein interaction networks (PPIs) and discovering pathways, conducting multiple runs on the data of yeast PPI networks<sup>225</sup>. They tested the

best option for the problem through the design of a GA. Their GA is able to detect specific populations on a protein-protein interaction network and to evaluate their number and size against existing references.

Supervised learning algorithms are a class of machine learning algorithms that customise a known training dataset to make predictions. This dataset contains input data and response values from which the supervised learning algorithm tries to build a predictive model of the response values for a new dataset.

Dale and co-workers<sup>222</sup> applied this machine learning method to obtain a metabolic pathway prediction starting from a gold standard genome annotation dataset made of specific and well-known features, considered as input data. The final output was the estimation of the probability that a pathway is present or not in a specific organism.

### 1.4.3 Software for Pathway Analysis

Pathway analysis applications can be usually classified into: *i)* web-based applications; *ii)* desktop programs and, *iii)* programming packages.

Web-based applications for pathway analysis can offer both network visualization and simple analysis possibilities, such as STRING<sup>226</sup>, Cytoscape<sup>227</sup>, Ondex Web<sup>228</sup>, Visant<sup>229</sup>, CellMaps<sup>230</sup>.

Typical examples of desktop programs are *i)* GSEA-P, a Java desktop program application for Gene Set Enrichment Analysis with a user-friendly graphic interface<sup>231</sup>; *ii)* Genome Informatics Data Explorer (Guide), a desktop application designed to help biologists analyse RNA-seq and microarray gene expression data<sup>232</sup>.

Programming packages are principally written in R and Python languages, and are freely shared through the BioConductor<sup>233</sup> project and GitHub<sup>234</sup> service.

#### 1.4.4 Algorithms in finding alternative pathways and new drug targets

One of the first undirected pathway prediction algorithms used was NetSearch<sup>235</sup>. Its function consists on the enumeration of linear pathways and the generation of their ranking through a clustering of gene expression profile of each pathway entities. In parallel, NetSearch allows to generate a hypergeometric distribution-based score.

However, linear paths do not easily and fully capture the complexity of signaling networks. To this aim, researchers have been looking for other pathway prediction strategies. For example, Scott and colleagues<sup>236</sup>, employed a specific color-coding technique finalized to search paths and higher order structures, namely trees and parallel paths, in a weighted protein interaction graph. Similarly to the work done by Scott and collaborators, Lu and co-workers<sup>237</sup>, showed a randomized divide-and-conquer algorithm able to support complex non-linear pathway structures.

PathFinder, another tool commonly used for pathway analysis<sup>238</sup>, allows to: *i*) associate several data sources and extract combining rules that describe protein function in a well-known signaling pathway; *ii*) detect new pathways in the network of interest employing the extracted rules, along with annotation and expression data.

These methods essentially are capable to search potential target pathways in an individual way, but it is worth to mention that other approaches, such as the one formulated by Zhao et al,<sup>239</sup>, own the potentiality to recognize a single universal signaling subnetwork, using an unoriented edge selection algorithm<sup>240</sup>.

In this scenario, Yosef et al.<sup>241</sup> tried to combine these two different approaches using an algorithm able to recognize the trade-off between local and global search methods, and giving a preference to one or the other on a particular run of interest.

Even if these methods pointed out valuable outcomes, none of them is capable to generate directed pathways and specific targets. To overcome the orientation problem for length-bounded pathways in

weighted interaction networks, Gitter and collaborators<sup>242</sup> implemented several algorithms based on probabilistic selection and alternative methods to solve specific issues about weighted Boolean satisfiability (SAT)<sup>243</sup>. They applied these algorithms to PPI networks using simulated and biologically derived sources and targets. These algorithms can recover many well-known pathways and improve upon previous approaches for pathway discovery, using real signaling networks. These algorithms are able to discover and analyzed pathways that do not appear in existing signaling databases and successfully they match notorious knowledge about the directionality of the interactions within pathways. Moreover, these algorithms rely on a number of reasonable biological assumptions including limiting the path length, using the confidence in the interaction edges and allowing for parallel pathways between sources and targets.

A very common need in pathway analysis is represented by the research of nodes that make significant contribution to a specific target. This is required, for example, in the identification of potential targets that may elicit an effect at cellular level through the controlling cascade of a specific biological function. These nodes, however, could not belong to the neighborhood of the biological target under investigation. It is also possible that effective targets could be hidden within pathways that are only connected to the analyzed one by only one or few nodes.

## 2 AIM OF THE THESIS

Computational modeling of signal transduction is currently attracting much attention as it promotes the understanding of complex signal transduction mechanisms. Although several computational models have been used to examine signaling pathways, little attention has been given to crosstalk mechanisms. In this PhD research project, we developed a computational model that automatically explores and detects the most relevant nodes within the MAPK and PI3K/AKT pathways, attributing a specific weight and simulating the dynamics of MAPK and PI3K/AKT signaling cascades involved in melanoma and thyroid cancer. Moreover, the dynamics of the protein activities were analyzed based on a set of kinetic equations fostered with data coming from both literature and experimental sources. In silico analysis revealed that the RAF and AKT pathways act independently in both diseases and that novel prognostic biomarkers and therapeutic targets could be identified for obtaining benefits and a more effective treatment in thyroid cancer and melanoma.

This PhD project has as the main goal the advancement of the state of the art in the development of computational strategies able to simulate both PI3K/AKT and MAPK pathways and their interactions, in order to deeper examine and investigate the cascade reactions involved in melanoma and thyroid cancer development and progression with a special attention to unresponsivity to conventional treatments.



## 3 COMPUTATIONAL MODELING IN MELANOMA

### 3.1 Melanoma background

Skin is the largest organ of the body and represents the first line of defense from external factors. To this aim, integumentary system protects body against pathogens and excessive water loss and is fundamental for vitamin D production, sensory stimuli and temperature regulation. Melanocytes are responsible for the production of melanin, a pigment that defends skin from damage effects of sunrays. In physiological conditions, melanocytes lead to dark agglomerations formation, visible on the skin, known as nevi<sup>244</sup>.

A tumor transformation of melanocytes could lead to cutaneous melanoma that represents a small percentage (about 5%) of all skin cancers<sup>245</sup>. It is estimated that one American dies of melanoma every hour, and according to the American Cancer Society 3.5 million cases of basal and squamous cell skin cancer and about 73,000 cases of melanoma are diagnosed each year in the U.S., more than all other cancers combined, and 50 million people are treated for it annually<sup>246</sup>.

Epidemiological data coming from Italian Association of Tumor Registers (AIRTUM) report about 13 cases per 100000 people of melanoma in Italy, and a growing and doubled incidence in the last ten years. Cutaneous melanoma affects men and women around 40-50 years old and is quite rare in children. It originates from skin or pre-existing nevi that could be congenital, if present from birth, or acquired, if they appear during the course of life<sup>247</sup>. Cutaneous melanoma is classified into:

- I. superficial spreading melanoma (the most common);
- II. lentigo malignant melanoma;
- III. acral lentiginous melanoma;
- IV. nodular melanoma.

The main symptom of cutaneous melanoma is the change of a nevi shape or the formation of a new one. The characteristics of a nevi, that may indicate the onset of melanoma, are summarized in the acronym ABCDE<sup>248</sup>:

A= asymmetry form (a benign nevus has a circular form, while melanoma is more irregular);

B= border (irregular and indistinct);

C= color variable (with different shades within the same nevus);

D= dimensions (a clear increase in melanoma);

E= evolution of nevus (which also shows changes in a short time).

Other symptoms could be represented by a nevus that bleeds, surrounded by reddened area or itches.

Cutaneous melanomas are generally classified into four stages, I to IV, in which zero represents the melanoma in situ, restricted to the surface layer of the skin. These four stages are defined on the basis of the TNM system, which takes into account the characteristics of the tumor as the thickness, the rate of replication of cancer cells, the presence of ulcerations (T), the involvement of lymph nodes (N) and the possible presence of metastases (M)<sup>249</sup>. The prognosis is different according to the thickness of the lesion.

The main risk factor for melanoma is an excessive exposure to ultraviolet light (UVA and UVB), mainly in the form of sun's rays, but also of tanning beds that should be used with caution, without abuse. Prolonged exposure to UV radiation is potentially dangerous because it can damage the DNA of skin cells and trigger tumor transformation<sup>250</sup>. Other risk factors are the failure of the immune system (due to previous chemotherapy treatments or transplant) and some genetic diseases such as xeroderma pigmentosum (in which patients DNA is not able to repair the damage caused by radiation). The risk increases in people with freckles, nevi, fair skin and eyes, in those who have a family history of melanoma and in those who was already affected from melanoma<sup>251</sup>.

To prevent the risk of development of skin cancer there are several good manners and recommendations that dermatologists suggest for a healthy skin. The European Society for Medical Oncology clinical practice guidelines for cutaneous melanoma highlight the importance of a detailed diagnosis for the establishment of the tumor stage and, in some tumors, a mutation test is also required<sup>252</sup>. A periodic skin self-examination usually allows to identify changes or suspicious nevi and to consult a dermatologist in time. The dermatologist will assess a family history and the presence of typical signs and symptoms of cutaneous melanoma. The visual examination of the skin is more accurate when digital epiluminescence dermatoscope is used, in parallel to a magnifying glass and light illumination technique. However, the established clinical diagnosis of cutaneous melanoma requires a biopsy. Hence, early diagnosis is essential. Thanks to specific test analysis on tissue samples, it is possible to identify typical molecular mutations of different forms of cutaneous melanoma and establish relative prognosis and treatment. Diagnostic imaging tests such as x-rays of the chest, Computed Axial Tomography (CAT), Positron Emission Tomography (PET) and Magnetic Resonance Imaging (MRI) are useful to determine if and where the disease is spreading<sup>253</sup>.

Currently, the US Food and Drug Administration (FDA) have approved several options for treatment of cutaneous melanoma over the past years<sup>254</sup>. Current therapeutic approaches include surgical resection, chemotherapy, photodynamic therapy, immunotherapy, biochemotherapy, and targeted therapy<sup>255</sup>. The therapeutic strategy can include single agents or combined therapies, depending on the patient's health, stage, and location of the tumor. The efficiency of these treatments can be decreased due to the development of diverse resistance mechanisms. New therapeutic targets have emerged from studies of the genetic profile of melanocytes and from the identification of molecular factors involved in the pathogenesis of the malignant transformation. The main approach is represented by surgery intervention that generally can permanently treat the disease at an early stage for patients with stage I-IIIb melanoma. Other following interventions depend on melanoma stage, as the removal of a portion of healthy tissue around the sick one. In some cases, the "sentinel" lymph nodes are also removed and radiotherapy is used as an adjuvant therapy after surgery or to treat cases

of recurrence. If melanoma has metastasized from the skin to other organs, the cancer is very unlikely to be treated by surgery. Even though resistance to apoptosis is probably the major cause of chemotherapy drug resistance in melanoma<sup>256</sup>, chemotherapy remains the most important palliative treatment of refractory, progressive, and relapsed melanomas<sup>257</sup>. In Table 3, the most important and conventional approaches in melanoma treatment<sup>258</sup> are summarized and described in brief. Unfortunately, for most of them, melanoma in its advanced stages, is generally considered to be resistant.

<b>TREATMENT</b>	<b>DESCRIPTION</b>	<b>REFERENCE</b>
<b>Dacarbazine (DTIC)</b>	For decades and until 2010, DTIC, a cell cycle-nonspecific antineoplastic, was the current standard treatment for patients with inoperable metastatic melanoma. Nevertheless, it has never shown beneficial effects on survival of patients in phase III trials. DTIC acts both as a cytotoxic agent and as an immunostimulatory drug because it is able to induce local activation of natural killer (NK) and T cells.	<sup>259,260</sup>
<b>Temoxolomide (TMZ)</b>	TMZ is the first-choice treatment for patients with malignant melanoma who are not able to receive an intravenous chemotherapy intervention. TMZ owns the same mechanism of DTIC, being the prodrug of DTIC and acting as an alkylating agent. TMZ demonstrates equal activity of DTIC with the advantage to be administered orally and to easily penetrate the blood-brain barrier.	<sup>261,262</sup>
<b>Electrochemotherapy (ECT)</b>	ECT may be considered as an alternative strategy for local tumor control or as an additional treatment to the systemic ones. It uses a combination of physical properties of electroporation (through electric current) and chemical properties of chemotherapeutics with the aim to treat locally melanoma metastases.	<sup>263</sup>
<b>Photodynamic therapy (PDT)</b>	PDT plays a possible role as an adjuvant therapy in the management of advanced melanoma (stage III and IV). It involves a systemic or a local administration of a photosensitizer that, after its activation by irradiation, will take place within the tumor. The effects of PDT may be summarized as follows: induction of high levels of DNA damage, cytoskeleton alterations and enhanced pigmentogenesis.	<sup>264</sup>
<b>Immunotherapy</b>	Since 2011, FDA has approved four new drugs for melanoma treatment. These drugs are ipilimumab, pembrolizumab, nivolumab, and talimogene laherparepvec (T-VEC). The last one is an oncolytic virus drug that stimulates stronger anti-tumor immune responses, while the other ones are checkpoint inhibitors that take the “brakes” off the immune system and enable it to fight cancer.	<sup>265–267</sup>

<b>Oncolytic virus therapy</b>	This group includes viruses genetically modified as well as the ones found in nature to reproduce efficiently themselves in cancer cells without harming healthy cells. T-VEC (also known as OncoVEXGM-CSF) is approved from FDA for melanoma patients with injectable but non-resectable lesions in the skin and lymph nodes. It represents the first oncolytic virus approved for cancer therapy in the US.	268,269
<b>IFN-<math>\alpha</math>-2b</b>	FDA has approved high-dose of IFN- $\alpha$ -2b in patients after resection of high-risk melanoma (stage IIB and stage III). IFN- $\alpha$ -2b may interfere with the growth of tumor cells and slow the growth of melanoma. Even though IFN is approved as adjuvant treatment in melanoma, in clinic its use is restricted due to the high toxicity and dubious effectiveness.	259,270
<b>Peg-IFN</b>	On March 2011, pegylated-IFN- $\alpha$ -2b (Peg-IFN) has been approved for the treatment of melanoma patients with a high risk of recurrence after radical surgery and for adjuvant treatment of lymph node-positive melanoma. Peg-IFN owns a persistent absorption and a prolonged half-life; this means a better effectiveness compared with the non-pegylated form.	271
<b>Biochemotherapy</b>	Biochemotherapy is defined as a therapeutic regimen that consists, at least, of a chemotherapy (in single or combination formulation) and IL-2. This strategy may provide better relapse-free survival (RFS) than high-dose interferon (HDI) in patients with high-risk melanoma.	272
<b>IL-2</b>	Immunotherapy based on IL-2 has been the mainstay of systemic therapy for advanced melanoma. When administered at high-doses, IL-2 produces a small number of durable remissions in patients with metastatic melanoma, and due to this fact, it was approved in the US in 1998 for metastatic melanoma. Unfortunately, IL-2 shows a significant toxicity and low-doses of IL-2 display low response rates and ineffectiveness. IL-2 effects consist on: <i>i)</i> blockage of the reproduction and spread of cancer cells; <i>ii)</i> stimulation of white blood cells helpful to attack cancer cells; <i>iii)</i> release of chemicals by cancer cells that attract cancer-killing immune system cells.	273,274
<b>Treg inhibitors</b>	According to the major role of Tregs in promoting tumor progression, targeting Tregs seems to be promising approach in cancer immunotherapy. Several approaches have been developed for targeting Tregs, for example the depletion of Tregs, the suppression of Treg function, the disruption of Treg recruitment to the tumour microenvironment (TME) and inhibition of pTreg generation. Some examples of these therapeutic strategies are low-dose chemotherapy drugs and immune checkpoint inhibitors (ICIs). The main idea is to target Tregs specifically in the TME rather than peripheral depletion to minimize the risk of autoimmune diseases.	275,276
<b>CTLA-4 blockade</b>	Monoclonal antibodies directed against cytotoxic T lymphocyte-associated antigen-4 (CTLA-4), such as ipilimumab, harvests overall survival in patients with metastatic melanoma both in monotherapy and in combination with other checkpoint inhibitors.	277,278
<b>PD-1/PD-1 ligand (PD-L1) blockade</b>	To maintain the discrepancy between immune surveillance and cancer cell proliferation, checkpoint antibody inhibitors, such as anti-PD-1/PD-L1, are a novel class of inhibitors that act as a tumor suppressing factor through the modulation of immune cell-tumor cell interaction. These checkpoint blockers are increasingly becoming a sophisticated and promising cancer therapeutic	279,280

	strategy that produces significant antitumor responses with limited adverse reactions.	
<b>Gp100 Peptide vaccine</b>	In a phase 2 study, patients with metastatic melanoma that received high-dose of IL-2 plus gp100 peptide vaccine have shown a higher rate of response than the rate expected among patients treated with IL-2 alone. This study demonstrates that the injection of gp100 produces very high levels of circulating T cells, able to recognize and kill melanoma cancer cells in vitro.	281
<b>Toll like receptor (TLR) agonists</b>	Toll like receptor (TLR) agonists seem to be an interesting strategy to enhance the vaccination or the immune system itself at the tumor microenvironment level. The trial conducted by Royal et al. evaluates the biologic and clinical effects of resiquimod, a TL3 7/8 agonist capable to trigger myeloid (mDC, TLR 8) and plasmacytoid (pDC, TLR 7) dendritic cells in advanced melanoma patients. Resiquimod, in vaccinated hosts with type-1 IFN and IFN- $\gamma$ , leads to a regression of metastases, through an antitumor response, independently of previous vaccinations.	282
<b>Adoptive T-cell therapy (ACT)</b>	ACT is a type of immunotherapy based on the administration of autologous tumor-infiltrating lymphocytes (TILs). A high percentage of CD4 + CD25 + CD127lowFoxp3+ T cells among the infused TIL population was associated with a significant overall survival in pretreated advanced melanoma patients. The combination of ACT with checkpoint inhibitors could enhance the TIL effect by opposing the local immunodeficiency.	283
<b>Cyclin-dependent kinases (CDKs) inhibitors</b>	CDKs are protein kinases involved in <i>i</i> )progression of cell cycle, <i>ii</i> )control of transcription and <i>iii</i> )regulation of cell proliferation. Each CDK regulates a specific stage of cell cycle and acts as a checkpoint to stop cell cycle progression in response to specific alterations in the mitotic spindle or DNA damage process. Recently, a novel multi-CDK inhibitor called P1446A-05, is able to limit melanoma growth and synergistically is showing positive effects in combination with MAPK pathway inhibitors.	284,285
<b>Erythroblastic leukemia viral oncogene homolog 4 (ErbB4) inhibitors</b>	ErbB4 is a member of the EGFR family and activating mutations in ERBB4 have been reported in multiple studies dealing with melanoma. Recently, several clinical trials are evaluating ibrutinib, a covalent inhibitor of Bruton's tyrosine kinase (BTK) in cutaneous melanoma (NCT02581930).	286
<b>Targeted therapy</b>	Targeted drugs act in a different way from conventional chemotherapy drugs, which basically attack any rapidly dividing cells. These treatment options selectively block activity of key driving mutations identified in melanoma growth such as BRAF, NRAS, C-KIT and so forth.	164
<b>BRAF, MEK, c-KIT, VEGF, PI3K/AKT-mTOR inhibitors</b>	The development of selective inhibitors of phosphokinases has considerably extended the therapeutic prospect and drastically enriched the therapeutic outcome for melanoma. BRAF-mutated melanoma patients significantly benefit of kinase inhibitor therapies, especially through the combination of BRAF and MEK inhibitors that provide a good long-term disease control. Moreover, such regimens have been shown to achieve a progression-free survival of more than ten months and an overall survival of more than two years, along with good quality of life. Despite this, the majority of patients develop secondary resistance during long-term kinase inhibitor therapy. To this aim, current clinical	287,288

	<p>trials are oriented towards the investigation of alternative drug combinations including inhibitors of other signaling pathways as well as immune checkpoint inhibitors.</p>	
--	---	--

**Table 3. Treatment strategies for advanced melanoma**

In this perspective, computational model could contribute to discover and understand any mechanisms of acquired resistance, including reactivation of the MAPK pathway, constitutive activation of RTKs, activation of PI3K or overexpression of EGFR.

## 3.2 Methods

### 3.2.1 Pathway model

The behavior of malignant melanoma A375 cell line, harboring BRAFV600E mutation, was modeled through an in silico platform to study the effects of a commercial selective BRAF inhibitor (e.g., Dabrafenib) that usually improves the response to standard treatments at an early stage but also shows an intrinsic resistance in several treated patients<sup>289</sup>.

A software for simulation and analysis of biochemical networks and their dynamics, named COPASI (COmplex PATHway SIMulator), was used to develop the model for the analysis of the effects of BRAF alterations on both MAPK and PI3K/AKT pathways<sup>290</sup>. COPASI platform includes a specific standard methodology helpful to understand complex biochemical processes. In particular, it uses deterministic integration of ordinary differential equations (ODEs)<sup>291</sup> and stochastic simulation of reaction networks through using Gillespie's algorithm<sup>292</sup>. Moreover, it allows the computation of steady states<sup>293</sup>, stoichiometric network analysis<sup>294</sup>, sensitivity analysis<sup>295</sup>, optimization and parameter estimation<sup>296</sup>.

All model entities and their relative interactions were retrieved from KEGG (Kyoto Encyclopedia of Genes and Genomes) PATHWAY Database<sup>215</sup>. The model consists of 48 species and 48 biochemical

reactions. In Figure 3, one can see the overall representation diagram of MAPK and PI3K/AKT model in melanoma.

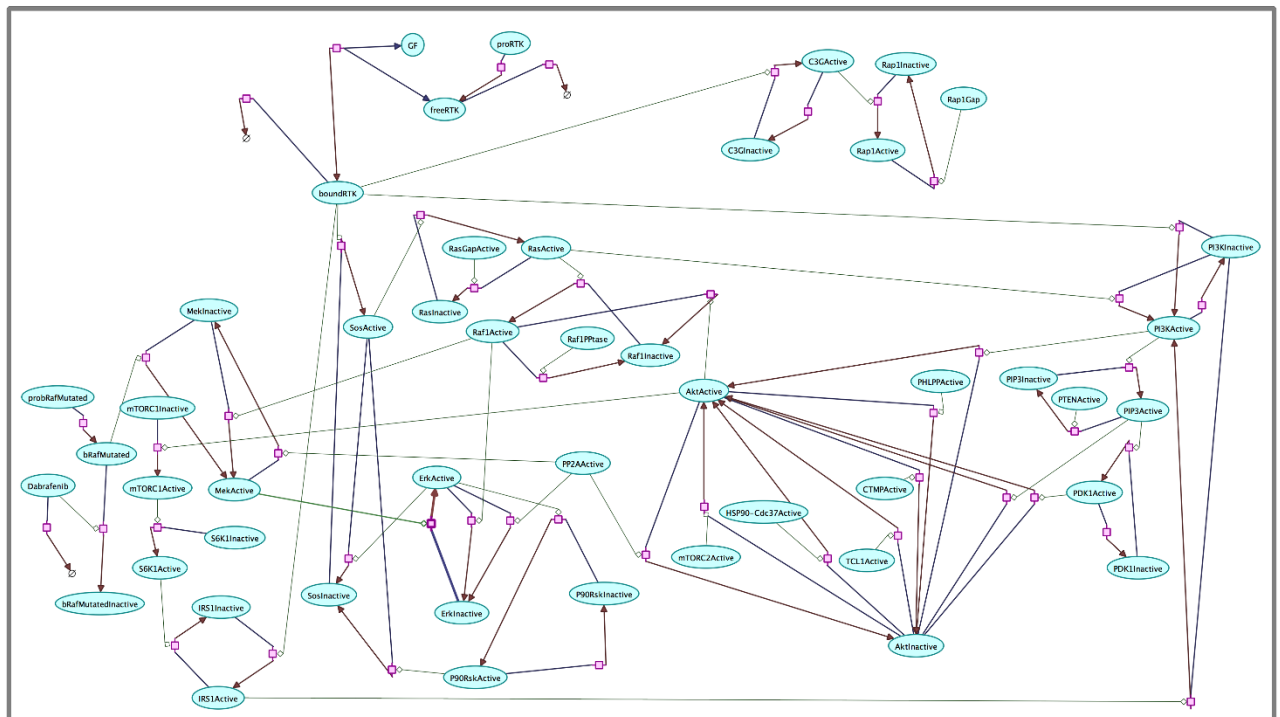


**Figure 3. Representation diagram of MAPK and PI3K/AKT model in melanoma.**

Pappalardo et al. PLOS ONE 2016;11: e0152104

To model the interactions between the two specific pathways, “Kegg reference map ko04010” was considered for MAPK signaling pathway, while “Kegg reference map hsa04151” for PI3K/AKT. Other protein kinase cascades such as the ones involved in EGFR activation, PIK3CA function, AKT modulation and RAF1 signaling were modeled.

Moreover, RAS signalling pathway (Kegg reference: ko04014) and mTOR signalling pathway (Kegg reference: ko041150) were included within the model to investigate any possible mechanisms not observed before in terms of possible escapement of apoptosis and alternative mechanisms that may induce Dabrafenib resistance phenomena through the activation of additional signalling pathways.



The values for the initial concentration of entities were gathered from GSE22301 available on GEO (Gene Expression Omnibus) dataset<sup>297</sup>.

Typically, Henri-Michaelis-Menten kinetics rules and modulates activation and deactivation of the majority of the biochemical reactions that take place inside the cell<sup>8</sup> and its formula is given by:

$$\frac{V \times S}{K_m + S}$$

Where S is the substrate, “V” is the maximum rate gained by the system and “K<sub>m</sub>” (Henri-Michaelis-Menten constant) is the substrate concentration at which the reaction rate is half of V.

For modeling purposes, a new modified version of the well-known Henri-Michaelis-Menten law was adopted in order to consider both substrate and modifier function in those activation or deactivation reactions of specific proteins.

The modified Henri-Michaelis-Menten equation may be represented schematically as:

$$\frac{K_{cat} \times S_1 \times S_2}{(K_m + S_2)}$$

Contrarily to the classical one, the new equation includes two types of substrates: S<sub>1</sub> represents the modifier of the reaction and S<sub>2</sub> is the generic substrate. Moreover, the kinetic law includes an additional parameter, described as “K<sub>cat</sub>”, that symbolizes the number of enzymatic reactions catalyzed per second. While Henri-Michaelis-Menten law refers to the rate of enzymatic reactions, the modified Henri-Michaelis-Menten equation inspects the ratio between the reactions of the biochemical system and their affinity for the substrate, on the basis of how efficient the modifier involved is.

Within the model, one can see a specific kinetic law for a specific class of biochemical reaction. In particular, a modified version of Henri-Michaelis-Menten law was employed to model the activation and deactivation reactions; mass action law were inserted to model two specific biochemical

reactions, in particular the physiological deactivation reactions of model species and protein degradation reactions; an irreversible constant flux law was considered to model proteins production reactions.

A375 melanoma cell line harboring B-RAFV600E mutation was modeled to analyze and investigate the dynamics of critical nodes within the main pathways involved in melanoma development and progression. To obtain this a “bRafMutated” species was modeled similarly to a “bRafInactive” species, especially in terms of initial concentration, while its behavior regarding the activation of MEK was modeled such as a “bRafActive” species.

To better investigate, the dynamics and the effects of a specific therapeutic protocol for melanoma, and eventually its possible mechanisms of resistance, a selective B-RAF inhibitor was modeled within the in silico lab to reproduce the potential drug effects in the multifaceted dynamics of PI3K/AKT and MAPK signalling pathways. To this aim, a “Dabrafenib” species was inserted within the model at different concentrations (2, 1, 0.5, 0.25 and 0.125 nM) along with all its biochemical machinery, in particular the physiological drug degradation and its main actions in the inhibition of “bRafMutated” species.

To simulate the physiological drug degradation, the half-life of Dabrafenib is about 10 hours, according to the data available on European Medicines Agency web site, and represents the main parameter used to set the related mass action law and able to reproduce the drug decay.

Moreover, the central role of AKT protein kinase in the crosstalk between PI3K/AKT and MAPK pathways was modeled taking into account the activation of mTORC1 pathway and the activation/deactivation machinery of several proteins on AKT signaling such as (PDK1 and HSP90/Cdc37). The relative set and list of ODEs representing the species and their relative reactions of the model can be found looking at Figure 4. The entire MAPK and PI3K/AKT model is hosted in SBML (L2V4) format on BioModels Database<sup>298</sup> and is identified by the following code: “BIOMD0000000666”.

$$\begin{aligned}
\frac{d[\text{boundRTK}]}{dt} &= V_{\text{total}} \left( k_{11} [\text{RTK}] - k_{12} [\text{boundRTK}] \right) - V_{\text{total}} k_{13} [\text{boundRTK}] \\
\frac{d[\text{freeRTK}]}{dt} &= V_{\text{total}} \left( k_{11} [\text{RTK}] - k_{12} [\text{boundRTK}] - k_{13} [\text{boundRTK}] \right) \\
\frac{d[\text{SocActive}]}{dt} &= V_{\text{total}} \left( \frac{k_{21} [\text{boundRTK}][\text{SocInactive}]}{k_{22} + [\text{SocInactive}]} - \frac{k_{23} [\text{SocActive}][\text{SocInactive}]}{k_{24} + [\text{SocActive}]} \right) \\
\frac{d[\text{SocInactive}]}{dt} &= V_{\text{total}} \left( \frac{k_{23} [\text{SocActive}][\text{SocInactive}]}{k_{24} + [\text{SocActive}]} - \frac{k_{21} [\text{boundRTK}][\text{SocInactive}]}{k_{22} + [\text{SocInactive}]} \right) \\
\frac{d[\text{RasActive}]}{dt} &= V_{\text{total}} \left( \frac{k_{31} [\text{SocActive}][\text{RasInactive}]}{k_{32} + [\text{RasInactive}]} - \frac{k_{33} [\text{RasActive}][\text{RasInactive}]}{k_{34} + [\text{RasActive}]} \right) \\
\frac{d[\text{RasInactive}]}{dt} &= V_{\text{total}} \left( \frac{k_{33} [\text{RasActive}][\text{RasInactive}]}{k_{34} + [\text{RasActive}]} - \frac{k_{31} [\text{SocActive}][\text{RasInactive}]}{k_{32} + [\text{RasInactive}]} \right) \\
\frac{d[\text{RafActive}]}{dt} &= V_{\text{total}} \left( \frac{k_{41} [\text{RasActive}][\text{RafInactive}]}{k_{42} + [\text{RafInactive}]} - \frac{k_{43} [\text{RafActive}][\text{RafInactive}]}{k_{44} + [\text{RafActive}]} \right) \\
\frac{d[\text{RafInactive}]}{dt} &= V_{\text{total}} \left( \frac{k_{43} [\text{RafActive}][\text{RafInactive}]}{k_{44} + [\text{RafActive}]} - \frac{k_{41} [\text{RasActive}][\text{RafInactive}]}{k_{42} + [\text{RafInactive}]} \right) \\
\frac{d[\text{MEKActive}]}{dt} &= V_{\text{total}} \left( \frac{k_{51} [\text{RafActive}][\text{MEKInactive}]}{k_{52} + [\text{MEKInactive}]} - \frac{k_{53} [\text{MEKActive}][\text{MEKInactive}]}{k_{54} + [\text{MEKActive}]} \right) \\
\frac{d[\text{MEKInactive}]}{dt} &= V_{\text{total}} \left( \frac{k_{53} [\text{MEKActive}][\text{MEKInactive}]}{k_{54} + [\text{MEKActive}]} - \frac{k_{51} [\text{RafActive}][\text{MEKInactive}]}{k_{52} + [\text{MEKInactive}]} \right) \\
\frac{d[\text{ERKActive}]}{dt} &= V_{\text{total}} \left( \frac{k_{61} [\text{MEKActive}][\text{ERKInactive}]}{k_{62} + [\text{ERKInactive}]} - \frac{k_{63} [\text{ERKActive}][\text{ERKInactive}]}{k_{64} + [\text{ERKActive}]} \right) \\
\frac{d[\text{ERKInactive}]}{dt} &= V_{\text{total}} \left( \frac{k_{63} [\text{ERKActive}][\text{ERKInactive}]}{k_{64} + [\text{ERKActive}]} - \frac{k_{61} [\text{MEKActive}][\text{ERKInactive}]}{k_{62} + [\text{ERKInactive}]} \right) \\
\frac{d[\text{PIP3Active}]}{dt} &= V_{\text{total}} \left( \frac{k_{71} [\text{RasActive}][\text{PIP3Inactive}]}{k_{72} + [\text{PIP3Inactive}]} - \frac{k_{73} [\text{PIP3Active}][\text{PIP3Inactive}]}{k_{74} + [\text{PIP3Active}]} \right) \\
\frac{d[\text{PIP3Inactive}]}{dt} &= V_{\text{total}} \left( \frac{k_{73} [\text{PIP3Active}][\text{PIP3Inactive}]}{k_{74} + [\text{PIP3Active}]} - \frac{k_{71} [\text{RasActive}][\text{PIP3Inactive}]}{k_{72} + [\text{PIP3Inactive}]} \right) \\
\frac{d[\text{PDK1Active}]}{dt} &= V_{\text{total}} \left( \frac{k_{81} [\text{PIP3Active}][\text{PDK1Inactive}]}{k_{82} + [\text{PDK1Inactive}]} - \frac{k_{83} [\text{PDK1Active}][\text{PDK1Inactive}]}{k_{84} + [\text{PDK1Active}]} \right) \\
\frac{d[\text{PDK1Inactive}]}{dt} &= V_{\text{total}} \left( \frac{k_{83} [\text{PDK1Active}][\text{PDK1Inactive}]}{k_{84} + [\text{PDK1Active}]} - \frac{k_{81} [\text{PIP3Active}][\text{PDK1Inactive}]}{k_{82} + [\text{PDK1Inactive}]} \right) \\
\frac{d[\text{mTORC1Active}]}{dt} &= V_{\text{total}} \left( \frac{k_{91} [\text{PDK1Active}][\text{mTORC1Inactive}]}{k_{92} + [\text{mTORC1Inactive}]} - \frac{k_{93} [\text{mTORC1Active}][\text{mTORC1Inactive}]}{k_{94} + [\text{mTORC1Active}]} \right) \\
\frac{d[\text{mTORC1Inactive}]}{dt} &= V_{\text{total}} \left( \frac{k_{93} [\text{mTORC1Active}][\text{mTORC1Inactive}]}{k_{94} + [\text{mTORC1Active}]} - \frac{k_{91} [\text{PDK1Active}][\text{mTORC1Inactive}]}{k_{92} + [\text{mTORC1Inactive}]} \right) \\
\frac{d[\text{S6K1Active}]}{dt} &= V_{\text{total}} \left( \frac{k_{101} [\text{mTORC1Active}][\text{S6K1Inactive}]}{k_{102} + [\text{S6K1Inactive}]} - \frac{k_{103} [\text{S6K1Active}][\text{S6K1Inactive}]}{k_{104} + [\text{S6K1Active}]} \right) \\
\frac{d[\text{S6K1Inactive}]}{dt} &= V_{\text{total}} \left( \frac{k_{103} [\text{S6K1Active}][\text{S6K1Inactive}]}{k_{104} + [\text{S6K1Active}]} - \frac{k_{101} [\text{mTORC1Active}][\text{S6K1Inactive}]}{k_{102} + [\text{S6K1Inactive}]} \right) \\
\frac{d[\text{bRafMutated}]}{dt} &= V_{\text{total}} \left( \frac{k_{111} [\text{Dabrafenib}][\text{bRafMutated}]}{k_{112} + [\text{bRafMutated}]} - \frac{k_{113} [\text{bRafMutated}]}{k_{114} + [\text{bRafMutated}]} \right) \\
\frac{d[\text{Dabrafenib}]}{dt} &= V_{\text{total}} \left( k_{111} [\text{Dabrafenib}][\text{bRafMutated}] - k_{113} [\text{bRafMutated}] \right) \\
\frac{d[\text{bRafMutatedInactive}]}{dt} &= V_{\text{total}} \left( \frac{k_{121} [\text{Dabrafenib}][\text{bRafMutated}]}{k_{122} + [\text{bRafMutated}]} - \frac{k_{123} [\text{bRafMutatedInactive}]}{k_{124} + [\text{bRafMutatedInactive}]} \right) \\
\frac{d[\text{PI3KInactive}]}{dt} &= V_{\text{total}} \left( \frac{k_{131} [\text{boundRTK}][\text{PI3KInactive}]}{k_{132} + [\text{PI3KInactive}]} - \frac{k_{133} [\text{PI3KActive}][\text{PI3KInactive}]}{k_{134} + [\text{PI3KActive}]} \right) \\
\frac{d[\text{PI3KActive}]}{dt} &= V_{\text{total}} \left( \frac{k_{133} [\text{PI3KActive}][\text{PI3KInactive}]}{k_{134} + [\text{PI3KActive}]} - \frac{k_{131} [\text{boundRTK}][\text{PI3KInactive}]}{k_{132} + [\text{PI3KInactive}]} \right)
\end{aligned}$$

**Figure 4. List of the ODEs of MAPK and PI3K/AKT model.**

Pappalardo et al. PLOS ONE 2016;11:e0152104

The A375 cell line employed for this study derives from a 54 years old female affected by malignant melanoma and was obtained from ATCC (LGC Standards, Italy). This cell line was very useful to study the role of MAPK and AKT pathways because of the presence of the single alteration exhibited in BRAFV600E.

Western blot analysis was performed to validate the *in silico* results using the Anti-MAP Kinase ERK1/ERK2 (pThr202/ pThr204) rabbit Ab and Anti-MAP Kinase ERK1/ERK2 rabbit Ab in order to detect respectively phosphorylated and total ERK 1/2 proteins. The Anti-beta Tubulin Ab was used as housekeeping gene. Moreover, student's t-test was used for statistical analysis.

### 3.2.2 DNA methylation

Pathway analysis could benefit of different forms of enrichment to better elucidate the biological function of each node. This is particularly true when this strategy is applied to novel therapeutic targets discovery in melanoma (in particular) and in cancer (in general). Among the existing strategy to enrich signaling pathways, DNA mutations occurring in driver genes such as B-RAF mutation could represent an important aspect to consider. However, DNA mutations are not the only reasons of tumor heterogeneity<sup>299</sup>. Also, epigenetic modifications can influence gene function and alter signaling pathways involved in cell physiological process and cell homeostatic balance<sup>300</sup>. Within the possible epigenetic mechanism, DNA methylation represents a greatly stable marker of gene regulation and other epigenetic mechanisms such as histone modifications<sup>301,302</sup>. In particular, it deals with a process by which DNA methyltransferases (DNMTs) enzyme transfers a methyl group to cytosine of palindromic CpG dinucleotides of a DNA sequence. This mechanism has been widely recognized to be correlated with transcriptional activity and in particular dealing with the inverse correlation between promoter methylation and gene expression. However, the functional role of global methylation patterns in gene regulation is still understood and an increased knowledge of these mechanisms that modulate gene expression through DNA methylation can lead to several advances. In particular, high-throughput technology and bioinformatics analysis can contribute to the development of alternative strategies to overcome methylome modification in cancer and the identification of new diagnostic and prognostic biomarkers associated to methylation hotspots and hence, to cancer proliferation<sup>303-305</sup>.

With the goal to enhance pathway analysis with an effective enrichment strategy, we developed an R package named Epigenetic Methylation and Expression (EpiMethEx) to investigate the functional role of global methylation patterns in gene regulation, useful to identify any methylation hotspots as well as extended genomic regions involved in regulation of relative genes<sup>306</sup>.

EpiMethEx is able to identify methylation modifications of wide genomic regions that affect gene expression modulation. In particular, it detects:

- E. single methylation hotspots (CG probeset);
- F. extended methylation regions (methylation groups) by combining the CG probesets accordingly to specific genomic regions (TSS1500, TSS200, 3'UTR, body and so on...);
- G. CpG islands necessary for the modulation of the equivalent methylated gene.

This R package executes cyclic correlation analysis between gene expression and methylation levels of each gene analyzed. EpiMethEx has been tested on a large series of data including both DNA methylation and gene expression profiling of melanoma samples achieved from “The Cancer Genome Atlas” (TCGA)<sup>307</sup>.

The data in input are represented by 3 datasets:

- a) expression levels of all genes according to RNAseq analysis;
- b) relative methylation data;
- c) data about CG dinucleotides probesets

Melanoma data for the execution of beta-test study were obtained from:

- a) the SKCM gene expression (Pancan Normalized) [ <https://genome-cancer.ucsc.edu/>];
- b) the SKCM DNA methylation Methylation450k [ <https://genome-cancer.ucsc.edu/>]
- c) probeset annotation [ <https://www.ncbi.nlm.nih.gov/>]

The analysis was performed on a total of 20,530 genes and 485,577 CG probesets, all referring to 473 different TCGA samples. The main steps of the analysis are reported in Figure 5.

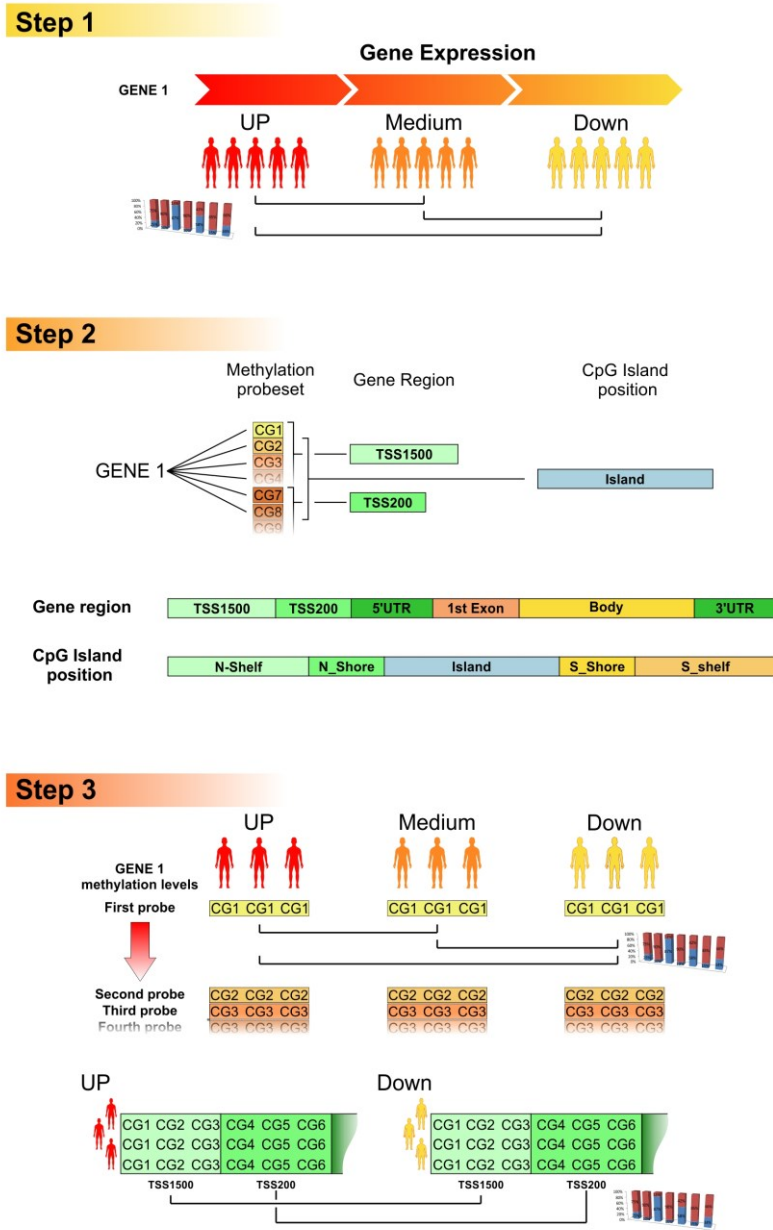


**Figure 5. EpiMethEx workflow**

Candido et al. BMC Bioinformatics 2018; to appear

Each step is described as follows:

- Step 1: Gene expression analysis

This phase consist on the analysis of the gene expression datasets of tumor samples that report the expression levels of genes. Then, a preprocessing and cleaning phase was achieved in order to remove from the analysis all the genes having null values across all samples. Furthermore, gene expression dataset was put in a descending order according to the TCGA sample gene expression value. In conclusion, a division in three equally spaced groups was executed, according to the sample gene expression, in order to create, for each gene, Up, Medium and Down expression groups.

- Step 2: CG probeset pre-processing

The main phases of step 2 includes:

- a) a pre-processing analysis performed to assign to each CG probeset: *i)* the corresponding gene; *ii)* the position within the region of the assigned gene (TSS1500, TSS200, 3'UTR, 1stExon, Body and 5'UTR); *iii)* the relative position within CpG islands, including proximal regions (Shore, Shelf);
  - b) mapping of several CG probesets on different regions of the same gene, due to several transcript isoforms;
  - c) pre-processing of dataset to obtain a one-to-one relation and in order to have a unique “cg-gene-ID-position” correspondence;
  - d) use of the resulting CG probeset annotation matrix to extrapolate from SKCM DNA methylation dataset the methylation levels of CG probesets relative to each gene analyzed in step 1;
  - e) ordering and grouping of CG methylation values through the same TCGA expression order obtained from the sorting of the first dataset (step 1).
- Step 3: CG probesets grouping and analysis:
    - a) median of CG methylation levels stratified according Up, Medium and Down gene expression groups;

- b) beta-difference and p-value of each methylation level of CG probesets among gene expression groups;
- c) pearson correlation and p-value among gene expression levels and relative CG methylation levels;
- d) grouping of CG probesets within gene regions (all CG probesets belonging to the same gene region that are TSS1500, TSS200, 3'UTR, 1stExon, Body and 5'UTR);
- e) grouping of CG probesets within Island positions and adjacent Shore and Shelf regions of each gene;
- f) grouping of all CG probesets within the same gene.

The final step consists on data filtering script for the Beta-test study. In particular, external script on EpiMethEx output data files was executed to: *i)* filter methylation data according to the median values among stratification levels; *ii)* filter methylation data according to  $\beta$ -difference and according to the methylation stratification level p value; *iii)* filter gene data according to FC and p-value; *iv)* filter data according to Pearson correlation p value.

The R scripts along with a detailed documentation including the user manual and how to utilize the software are available in the GITHUB repository at the following url:

<https://github.com/giupardeb/EpiMethEx>.

### 3.3 Results and discussion

#### 3.3.1 Pathway model results

Two simulations of our model were performed under different conditions that are shown in Figure 6. Panel A depicts the pathway model simulated under normal EGF stimulation conditions in order to obtain a high transient activation of ERK. Panel B shows A375 cell line scenario under B-RAF mutation condition, hence, a strong ERK activity is pointed out, typical of B-RAFFV600E mutated melanomas.



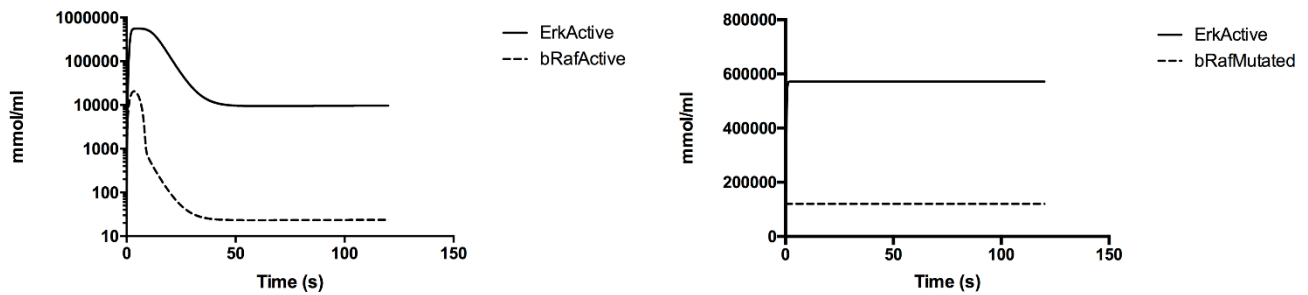


**Fig 6. pERK (ErkActive) and BRAF dynamics**

Pappalardo et al. PLOS ONE 2016;11: e0152104

As a final point, the simulation correctly predicts the expected behavior of an elevated ERK activity. In other words, the species pERK owns a constant preeminent activity. It is worth mentioning that higher levels of pERK are not observed possibly due to the fact that pERK is already nearby to its threshold points and/or due to the involvement of alternative nodes within the entire pathway that may impact on the final outcome.

Furthermore, we performed 48 hours of simulation to analyze the specific behavior and response of A375 cell lines at different concentrations of Dabrafenib inhibitor (0.125 nM, 0.250 nM, 0.500 nM, 1.0 nM and 2.0 nM). The dynamics of pERK, BRAF mutated and Dabrafenib at different Dabrafenib dosage are reported in Figure 7. BRAF inhibition leads to an ERK phosphorylation reduction and consequently also to a reduction of its activity. This reduction of pERK concentrations is in agreement with the behavior observed in vitro.

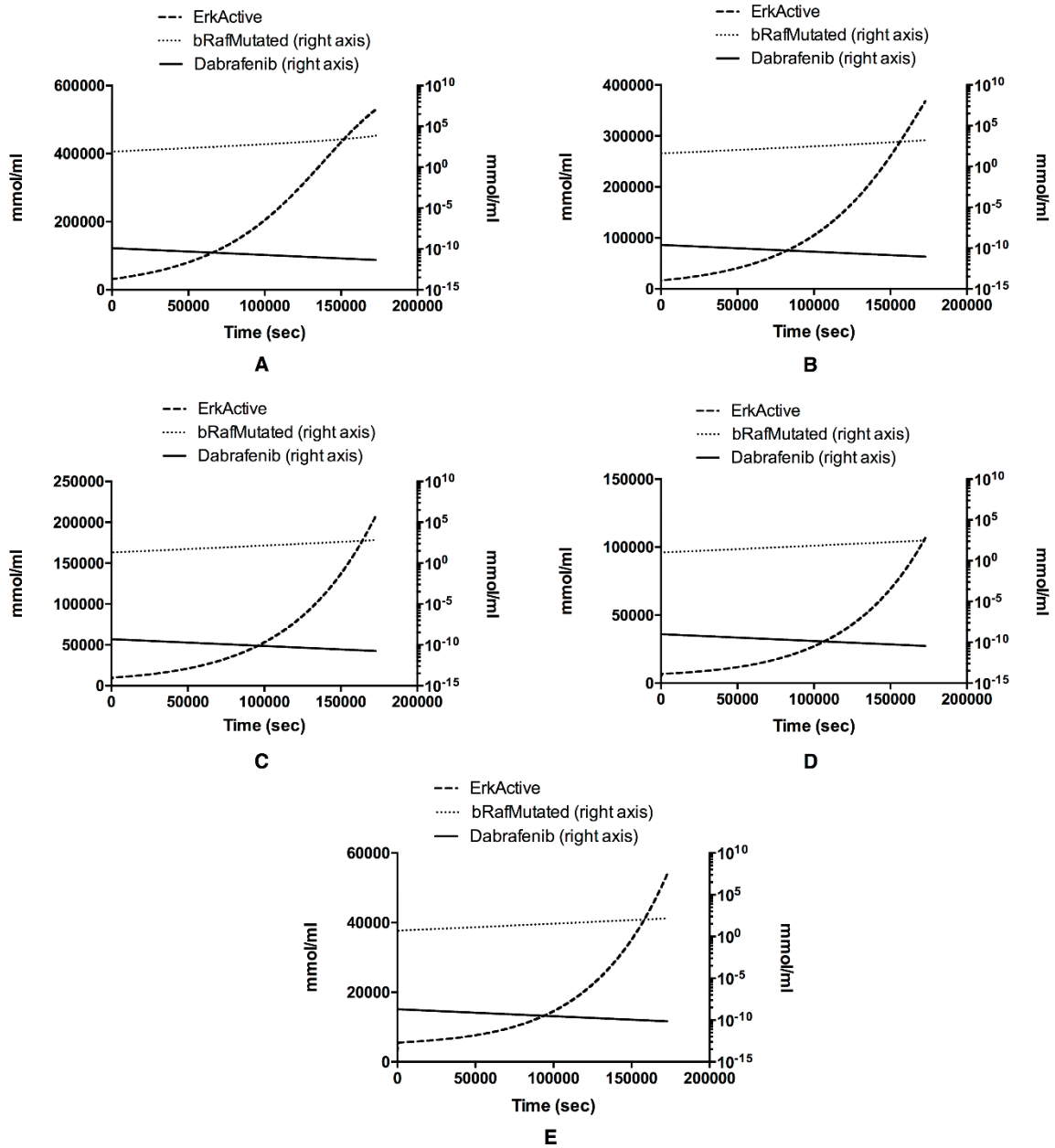


**Figure 7. In silico dynamics of pERK (ErkActive), BRAF (bRafMutated) and Dabrafenib.**

Pappalardo et al. PLOS ONE 2016;11: e0152104

In silico results were confirmed through western blot analysis as reported in Figure 8. One can notice that pERK levels decrease due to Dabrafenib inhibitor activity against BRAFV600E protein.

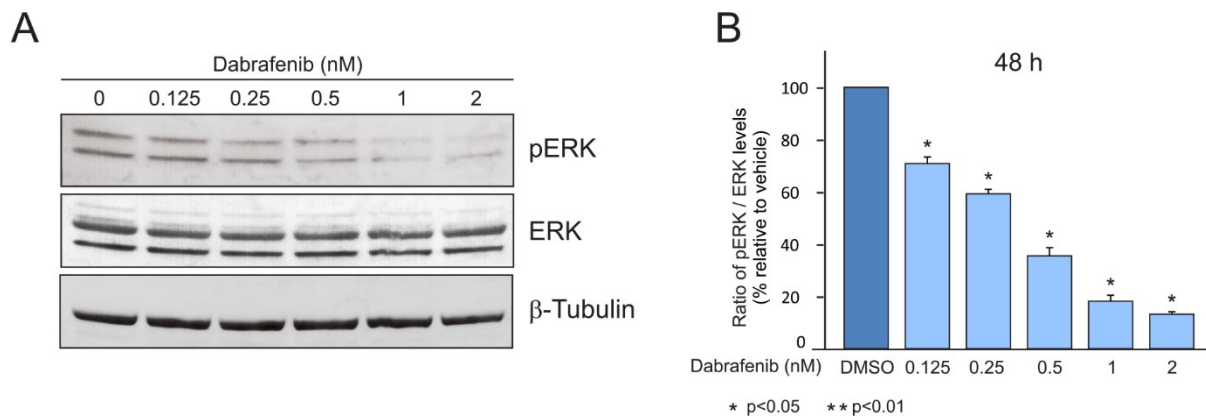


**Figure 8. In vitro validation of in silico results.**

Pappalardo et al. PLOS ONE 2016;11: e0152104

At this stage, we can assert that this in silico model could be used as starting point for the investigation and the simulation of any drug resistance phenomena, unresponsivity mechanism to selective inhibition treatment protocols and target discovery in specific and detailed cancer scenario.

Moreover, this in silico analysis has confirmed the crucial role of AKT kinase in the crosstalk between PI3K/AKT and MAPK pathways due to the fact that in parallel, pathways such as mTORC1 and specific proteins such as PDK1, could affect and interfere with AKT signalling, leading to an enhanced phosphorylation profile of ERK.

The in silico model of MAPK and PI3K/AKT developed for melanoma was then implemented with specific modeling features to generate a predictive model for target discovery of possible resistance mechanisms typical in advance thyroid cancer (See Chapter 4).

### 3.3.2 DNA Methylation results

In order to evaluate the biological significance of EpiMethEx selected genes and probesets, output data derived from the analysis of SKCM TGCA dataset were analyzed by using the filtering script mentioned above.

In Figure 2, one can see the percentage of CG probesets positively (light gray boxes) and negatively (dark gray boxes) correlated to gene expression grouped, according to their relative position in gene

regions. The most CG probesets positively correlated are mapped in 3'UTR (88%) and Body (79%) regions, conversely negative correlations were observed in TSS1500 (71%), TSS200 (90%), 1stExon (84%).

Moderate differences were obtained comparing the CG probesets of 5'UTR region, while low difference were observed between all positive and negative correlated CG probesets, as shown in panel A of Figure 9. These results were in agreement with the literature concerning both the well-described link between promoter hypermethylation and gene downregulation and the emerging role of intragenic methylation in regulation of gene expression.

The additional stratification for island position of the CG probesets revealed a sensible increase of CG probesets belonging to Island (21% vs 7%) and N Shore (29% vs 17%) in negative correlated CG of both TSS1500 and TSS200 regions. Among 3'UTR CG probesets, increment of CG percentages was observed in N Shore and S Shore region of negative correlated probesets. Moderate increase was observed for S Shelf probesets (9% vs 0%) of positive correlated in 1st Exon CG and similar trend was observed for Island of negative correlated CG in 5'UTR region (12% vs 27%).

Finally, negatively correlated CG probeset in Body region showed increment of N Shore, Island and S Shore groups compared to relative regions of positive correlated CGs. These results are reported in panel B of Figure 2. These stratification criteria showed that hypomethylation of promoter regions was mainly associated to demethylation of the CG probesets belonging to Islands and S Shore of promoter. Moreover, these findings highlight the importance of the high frequency of CpG in promoter region to induce down regulation as a result of the methylation of these CpG sites.

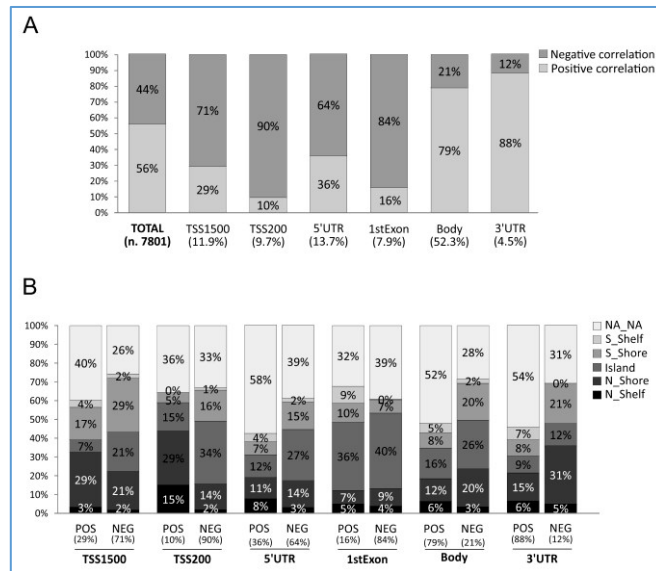


**Figure 9. Methylation CG probesets vs gene expression.**

Candido et al. BMC Bioinformatics 2018; to appear

For what concerns the stratification of CG probesets according to Island position showed a moderate increment of negative correlated CG within Island region (60%) and adjacent N and S Shore regions (49% and 62%). On the contrary, Shelf regions showed a sensitive reduction of negative correlated CG (26% and 22%) as shown in panel A of Figure 10. Body-associated CG probesets mapped in Island and Shore regions showed a decrease of about 15 % compared to Shelf regions. As consequence, an increase of CG probesets included in TSS1500, TSS200, 3'UTR and 1stExon regions was observed among Island and adjacent Shore regions. No variation was observed for 5'UTR CG probesets as reported in panel B of Figure 10. A further analysis performed stratifying the Island positions CG probesets and according to gene regions showed a similar behavior for each Island positions with significant increase of negative correlated CG probesets included between TSS500 and 1stExon region (as reported in panel A and B of Figure 10). The same CG probesets were decreased within Body regions as one can see on panel C of Figure 10). Overall, Island position analysis suggested that hypomethylation observed in Island and Shore regions mainly affects CG probesets

included in TSS1500, TSS200, 3'UTR, 1stExon, and 5'UTR. As consequence, the gene overexpression was mostly related to hypomethylation of Island of body regions.

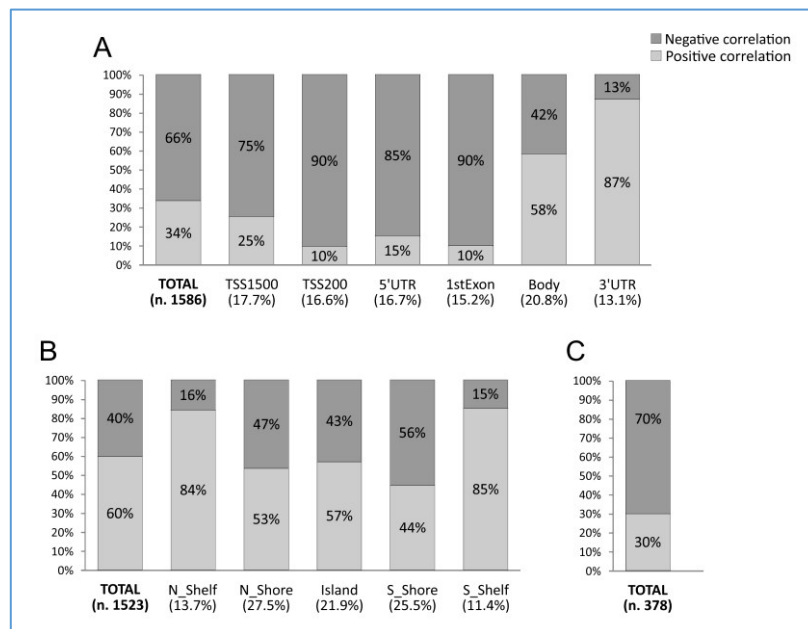


**Figure 10. Correlation of CGs grouped by position in gene regions.**

Candido et al. BMC Bioinformatics 2018; to appear

To summarize, EpiMethEx tool, through the cyclic correlation analysis between gene expression and methylation levels for each gene, is able to identify methylation hotspots and extended genomic regions involved in the regulation of their relative genes. Overall, the beta-test analysis showed a negative association between methylation and gene expression for the most modulated genes in melanoma; then, positive correlation was observed in some overexpressed genes that showed intragenic hypermethylated hotspots. New information gained through the application of EpiMethEx allow to explore signaling pathways related to genes that, without this enrichment strategy, would have not be considered.

## 4 COMPUTATIONAL MODELING IN THYROID CANCER

### 4.1 Thyroid cancer background

Thyroid cancer (TC) is the most common malignancy of the endocrine system and in the past three decades, there has been a dramatic increase in the number of people diagnosed with thyroid cancer<sup>308</sup>

Based on reports from the National Cancer Institute (NCI) and the American Cancer Society, the incidence of TC has risen over the past 10 years by an average of 5.5% annually, and the death rate rose by 0.8% annually from 2002 to 2011<sup>1</sup>.

TC represents 3.8% of all new cancer cases in the United States and is the ninth most common cancer overall. The American Cancer Society has estimated that 62,450 people in the United States would have been diagnosed with thyroid cancer in 2015, and 1950 deaths would have been result from the disease<sup>2</sup>.

Recently, the number of new cases of thyroid cancer is estimated to be 12.9 per 100,000 men and women annually, and the number of associated deaths is estimated to be 0.5 per 100,000 men and women annually<sup>309</sup>.

Thyroid cancer occurs more frequently in women than in men, along with an approximate ratio of 3:1 and can occur in any age group but more so in adults aged 45 to 54 years, with a mean age of 50 years at diagnosis<sup>310</sup>.

The rise in the incidence of thyroid cancers may be attributable to the widespread use of imaging studies, such as computed tomography, ultrasounds, magnetic resonance imaging, and positron emission tomography (PET) scans that incidentally detect thyroid nodules<sup>311</sup>.

---

<sup>1</sup> National Cancer Institute. SEER stat fact sheets: thyroid cancer. <http://seer.cancer.gov/statfacts/html/thyro.html>. Accessed January 12, 2015

<sup>2</sup> American Cancer Society. Thyroid cancer: what are the key statistics about thyroid cancer? Revised January 12, 2015. [www.cancer.org/cancer/thyroidcancer/detailedguide/thyroid-cancer-key-statistics](http://www.cancer.org/cancer/thyroidcancer/detailedguide/thyroid-cancer-key-statistics). Accessed January 12, 2015

Moreover, the effect of environmental factors cannot be excluded such as a volcanic environment and several chemicals with potential carcinogenic properties<sup>312,313</sup>.

TC is categorized into four main types: *i*) papillary thyroid carcinoma (PTC); *ii*) follicular thyroid carcinoma (FTC); *iii*) medullary thyroid carcinoma (MTC) and *iv*) anaplastic thyroid carcinoma (ATC)<sup>314</sup>.

PTC is the most common thyroid malignancy (it represents approximately 70% to 80% of thyroid cancers) and is also the least aggressive type of cancer, because it has the tendency to grow and metastasize slowly<sup>315</sup>.

FTC accounts for around 14% of thyroid cancers. It is more aggressive than papillary thyroid carcinoma and may be associated with iodine deficiency<sup>316</sup>. A variant of follicular carcinoma is represented by the Hürthle-cell carcinoma that is treated at the same way as follicular carcinoma<sup>317</sup>.

PTC and FTC are considered well-differentiated thyroid cancer. The lifetime risk for PTC and FTC is approximately 1.1%, and the 5-year survival rate has risen to 97.8%, because almost 70% of cases are now diagnosed at an early stage, when the cancer is localized at the gland<sup>318</sup>.

MTC is a cancer of parafollicular cells that are physiologically present in thyroid gland and it represents approximately 3% of thyroid cancers. Moreover, it is often associated with multiple endocrine neoplasia. Furthermore, medullary carcinoma is capable to produce calcitonin in excess, which makes it a valuable tumor biomarker<sup>319</sup>.

ATC represents around 2% of thyroid cancers and is the most dangerous type of TC, due to the fact that it metastasizes early both to the neighboring lymph nodes and both to distant sites<sup>320</sup>.

Other thyroid malignancies, such as lymphoma and other variants of the four TC types listed above, represent the remaining segment of thyroid cancers.



For what concerns the treatment options for TC, they consist of surgery, radioactive iodine (<sup>131</sup>I) therapy and thyroid hormone replacement aimed at maintaining thyroid-stimulating hormone (TSH) levels at the very low or low-to-normal range<sup>321</sup>.

In patients whose cancer no longer takes up iodine, the employment of tyrosine kinase inhibitors represent a valuable treatment alternative to radioactive iodine therapy for recurrent or metastatic thyroid cancers<sup>322</sup>. An emerging therapeutic strategy for these cancers is target therapy with small molecule kinase inhibitors (KIs). The major drugs are represented by vandetanib, cabozantinib, sorafenib.

Vandetanib was approved in 2011 by FDA for the treatment of patients with symptomatic or progressive, unresectable, locally advanced or metastatic medullary TC. It targets RTK, EGFR and VEGF receptor<sup>323</sup>. The approval was based on data coming from the phase 3 Zactima Efficacy in Thyroid Cancer Assessment (ZETA) study<sup>324</sup>.

Cabozantinib was the second TKI approved by FDA for the same indication as vandetanib<sup>325</sup>, on the basis of the EXAM (Efficacy of XL184 in Advanced Medullary Thyroid Cancer) trial<sup>3</sup>. Cabozantinib targets three pathways in MTC: MET, VEGF receptor 2, and RTK. Vandetanib and cabozantinib have shown significant prolongation of progression-free survival, and calcitonin and carcinoembryonic antigen levels decrease dramatically with these agents. However, no overall survival benefit was seen in these trials so far. These kinase inhibitors need to be personalized to patients due to their several side effects; then, a great deal of clinical judgment is mandatory before treating patients with them.

Sorafenib is a multikinase inhibitor of RET, wild-type and BRAFV600E mutation, VEGF receptors 2 and 3 approved in 2013 by FDA for the treatment of <sup>131</sup>I-refractory, locally recurrent or metastatic, progressive, differentiated thyroid cancer<sup>326</sup>. The study, which led to the FDA's approval of sorafenib,

---

<sup>3</sup> Exelixis. FDA approves Cometriq (cabozantinib) for treatment of progressive, metastatic medullary thyroid cancer. November 29, 2012. <http://exelixis.com/investors-media/press-releases>. Accessed January 21, 2015

was a phase 3, multicenter, randomized, double-blind, placebo-controlled clinical trial that included patients with locally recurrent or metastatic, progressive differentiated thyroid cancer<sup>327</sup>.

In conclusion, several KIs have been explored for the treatment of advanced thyroid tumors, but just some of them have been approved for the use in clinical practice. To date, sorafenib and lenvatinib were approved by FDA for the treatment of advanced differentiated thyroid carcinoma. In contrast, kinase inhibitors did not exhibit any significant effect in patients with poorly differentiated and ATC. Among them, also a BRAFV600E inhibitor, named vemurafenib (or PLX4032), was approved by FDA for treatment of metastatic melanoma<sup>328</sup>. Unfortunately, it did not provide any satisfactory result as a single agent in patients with poorly differentiated and ATC. In a small cohort of seven patients with ATC, only two patients achieved long-lasting responses to vemurafenib therapy while for four patients a progression of disease was registered<sup>329</sup>. This result suggests that poorly differentiated and anaplastic thyroid cancer cells show mechanisms tumor relapse due to an intrinsic or acquired resistance to vemurafenib.

To this aim, computational modeling and in silico simulations represent nowadays essential resources for the analysis and the investigation of controversial and unknown mechanisms of resistance to conventional drug therapy and are able to predict possible new interventions to overcome this issue still unresolved.

## 4.2 Methods

Starting from a previous evidence that the so-called cancer stem cells (CSCs)<sup>330</sup> own the ability to:

- i)* grow as non-adherent spheroids (thyrospheres)<sup>331</sup>;
- ii)* to sustain self-renewal in vitro and also tumor growth<sup>332–334</sup>;
- iii)* to promote metastasis and to confer resistance to chemotherapeutic agents<sup>335–339</sup>

we developed an in silico model including MAPK and PI3K/AKT pathways and their associated protein networks, with the molecular entities and interactions involved in CSCs resistance to vemurafenib.

In this view, we tailored resistance to vemurafenib by focusing on the mechanisms underlying the enhanced ERK/AKT phosphorylation in response to the drug. The model is built on a system of ODEs able to simulate both the expected and the emergent behavior within the protein network.

To instantiate the model, we used KEGG<sup>215</sup> as main source to import data into the model. In particular, this database was used to: *i)* obtain all the entities that participate in the biochemical reactions involved in tumorigenesis of thyroid cancer (to this aim we considered the protein kinase cascades that sequentially contain EGF-Sos-Ras-Raf1-Mek1-ERK and EGFR-PI3K-PIP3-AKT); *ii)* display how a specific node shares one or more signaling pathways of our interest; *iii)* obtain the entire network and localization of molecules needed to simulate the biological scenario obtained in vitro.

Serine/threonine-protein kinase BRAF represents the main step in the transduction of mitogenic signals from the cell membrane to the nucleus. BRAF protein is strongly linked both to MAPK and PI3K/AKT pathways that are mainly involved in tumor progression. Hence, we focused on BRAF protein and its role in regulating the signaling pathways involved in cell proliferation, differentiation and apoptosis. Moreover, we performed a comparative modeling how wild type BRAF gene and its V600E mutant variant may influence the entire biochemical system.

To reproduce the experimental conditions of cell environment, we assumed that all the molecular entities examined had a homogenous concentration overall the cell volume, ranging from  $\approx 10$  nM/l to  $\approx 10$   $\mu$ M/l<sup>340</sup>. For mutated species, in particular BRAF, we set the concentration to 100 nM/l, because this protein is constitutively activated and overexpressed during the entire time course of the simulation; for growth factors entities that occupy the culture medium (i.e., Fibroblast growth factor (FGF)) the concentration was set to  $1 \times 10^6$  nM/l; for all the remaining molecules to 10 nM/l.

The model tailored for 8505C CSCs was built with 74 entities, including protein kinases (i.e., AKT), growth factors (i.e., EGF), membrane receptors in their different status of activation (i.e., pEGFR in

its activated form), small molecules, including protein kinase inhibitors at different concentrations (i.e., vemurafenib) and 85 biochemical reactions. The number of enzymatic reactions catalyzed per second and the Henri-Michaelis-Menten constant were set to the same value i.e., 0.1. This because experimental data do not indicate any predominant velocity in the considered biochemical reactions. To simulate the dynamics of the system, we used the COPASI pathway software tool <sup>341</sup>. The model is available in GitHub repository visiting the following URL: <https://github.com/francescopappalardo/MAP3K8-Thyroid-Spheres-V-3.0>.

Besides the classic Henri-Michaelis Menten law, we used a slightly modified version of this law as mentioned for melanoma modeling (See Chapter 3, paragraph 3.2.1).

To reproduce drug resistance phenomenon, we introduced the Mutated-BRAF species at the concentration of 100 nM/l that is the same concentration of the initial Inactive-BRAF. We then removed all the biochemical pathways not influencing Mutated-BRAF species (i.e., the activation of BRAF by Rap1) and replaced Active-BRAF with Mutated-BRAF species in the switch of Mek activation. Moreover, new elements were subsequently inserted to reproduce the inhibitory effect of vemurafenib. To this purpose, we introduced vemurafenib species at a concentration of 1000 nmol/l that corresponds to the same one used in vitro in 8505C-CSCs.

To better define the reaction framework of vemurafenib, we also included its degradation rate and its inhibitory effect against BRAF Mutated-species. Indeed, vemurafenib half-life in vivo is about 57 hours<sup>342</sup> and this parameter was used to rate the associated mass action law and simulate its decay.

With the aim to simulate the resistance mechanism, we applied a further modified version of the Henri-Michaelis-Menten (HMM2) law that simulates how the inhibition of a modifier could lead to a counter-regulatory mechanism, which may invert the typical response to the inhibitor. In particular, we defined a piecewise equation that reads as follows:

$$(1) \quad HMM2(Kcat, Km, s_1, s_2) = \begin{cases} \frac{Kcat * s_1 * s_2}{km + s_2} & \text{if } s_1 \leq 1, \\ 0 & \text{Otherwise} \end{cases}$$

As shown in the equation (1), this rule develops towards an “inverted” direction: if the modifier  $S_1$  is absent or at low concentration, the reaction could take place. Otherwise, if the modifier is in a normal or constitutive activated status, the biochemical reaction will not take place.

In order to find ever long-distance crosstalk in the graph defined by the signaling network under study, we identified (through a depth first approach<sup>343</sup>) both forward edges and back edges.

Forward edges are directed from one node of the graph to one of its descendants (for example TNF for ERK and TRAF complex for AKT). Back edges are directed from one node to one of its ancestors (inverted effect). By this search, we found that MAP3K8 contributes to ERK activation, suggesting that this kinase may be targeted to overcome drug resistance.

To facilitate the discovery of these potentially effective nodes, a further computational strategy was developed. Specifically, we developed a *mapreduce* approach based algorithm able to scan and detect nodes that are far from the target taken into account. The project is divided into three main sections:

1. "mapReduce.py"
2. "launchScript.sh"
3. A web interface that allows the user to perform the analysis in an interactive way.

The interface gives the user the option to select different parameters in order to launch the search. It includes:

- a) “Gene (hsa)”: the starting gene from which the detection of neighbors commences.
- b) “Pathway (hsa)”: the starting pathway for the neighbors gene search.
- c) “Hop”: the distance from the gene target i.e., how many “hops” are needed to reach and discover linked nodes.

Once all the parameters have been set, the bash script "launchScript.sh" is launched. At the end of the analysis the web interface provides to the user a graph containing all the nodes and links generated on the basis of the starting gene.

Then "launchScript.sh" script takes as input the parameters selected from the web interface and executes the "mapReduce.py" script, as many times as necessary to analyze all the pathways that are gradually discovered during the depth analysis within the nodes. This analysis provides all the useful information to determine which is the least recurrent pathway and the results can be visualized through a specific graph produced by the web interface.

"MapReduce.py" script receives in input, through the "launchScript.sh", the pathway of interest. If the input gene does not exist, the program itself will download the "xml" file through the KEGG API machinery and will convert it into the ".txt" format. In order to obtain this, several functions have been implemented within the Python script and they include:

- a. `download_html (gene)`: the function takes as input the gene and downloads the corresponding html page. Then, it gets and returns the list of pathways in which the gene is present;
- b. `download_xml (hsa)`: this function takes as input the hsa pathway downloading it in ".xml" format through the API of KEGG.
- c. `create_txt (hsa)`: this function uses the downloaded pathway in ".xml" format, and converts it to a ".txt" format. It contains, for each line: *i*)starting gene ID; *ii*)arrival gene ID; *iii*)type of relationship that connects these genes (e.g., 34; 30 # PPrel # phosphorylation #).
- d. `id_to_hsa (hsa)`: this function takes as input the file produced by the "create\_txt" utility. Then, through the "read" function of the "Bio.KEGG.KGML.KGML\_parser" library, the IDs of the genes are converted with their corresponding hsa memberships. This is particularly useful due to the fact that for each pathway considered, the same gene has different ID (e.g., hsa: 5594 + hsa: 5595; hsa: 5604 # PPrel # phosphorylation #).

- e. `hsa_to_name ()`: this function transforms the hsa of genes into their corresponding names using an ad hoc constantly updated dictionary through the "read" function of the library "Bio.KEGG.KGML.KGML\_parser" (e.g., `hsa: 5594 + hsa: 5595` ---> MAPK1).

Once the pathway is downloaded, the "ReducePathway.run ()" function is executed and performs the following functions:

- 1) "mapper1" takes the ".txt" format pathway generated by the "create\_txt" function and gives two elements to "reducer1" that consist of *i*) a first string corresponding to the gene selected by the user and *ii*) a second string that corresponds to the direct neighbors of gene.
- 2) "reducer1" transforms the second string received by "mapper1" into a list-type object in order to associate the gene with the list of the respective neighbors. Consequently, it will return this result to "mapper2".
- 3) "mapper2" takes in input the reference gene and the list returned by the reducer1. Afterwards, two operations are performed:
  - for each element the function "download\_html" is run; this function generates a new list and for each element of this list "download\_xml", "create\_txt" and "id\_to\_hsa" are run.
  - Each element in the list returned by "reducer1" is concatenated to the string of the gene received as input from the reducer1. This operation allows a step by step final pathway building.

After "mapper2" ends, a file with the maps of all the neighbors of the gene analyzed is created. Then, on the newly created file, the function "hsa\_to\_name ()" is called.

This final file is useful for the creation of a "Json file" which in turn is used to create the final graph.

For what concerns the biological setting, anaplastic thyroid cancer cells HTH74 (BRAF wild-type) and SW1736 (BRAF V600E positive) were provided by Dr N. E. Heldin (Uppsala, Sweden). 8505-

C (BRAF V600E positive) cell line was purchased from European Animal Cell Culture (Salisbury, United Kingdom). The follicular cancer cell line WRO was provided by A. Fusco (Naples, Italy). BRAF V600E mutation in thyroid cancer cell lines was confirmed by PCR amplification and sequencing.

### 4.3 Results and discussion

The developed model allows to investigate alternative signaling pathways and we identified other pathways that do not directly influence ERK dynamics. In particular, we found that TNF signaling pathway, that is divided in two branches, stimulates both ERK and AKT protein kinases; ERK pathway is activated by TNFR1, while AKT by TNFR2. This bifurcation contains fundamental nodes, not considered before, to stimulate ERK and AKT phosphorylation. ERK activation is allowed through MAP3K8 contribution. AKT activation is triggered through the intervention of the TRAF complex and then, at a second stage, through PI3K activation.

At this stage, the depth first search carried on our *in silico* model of 8505C-CSCs allowed to predict that the concomitant inhibition of both MAP3K8 and BRAF V600E is able to consistently reduce ERK phosphorylation. This prediction was confirmed by *in vitro* experiments with selective inhibitors.

*In silico* predictions about the inhibitor combination protocol are shown in Figure 11 where the computational framework was applied to simulate and predict two different cases.



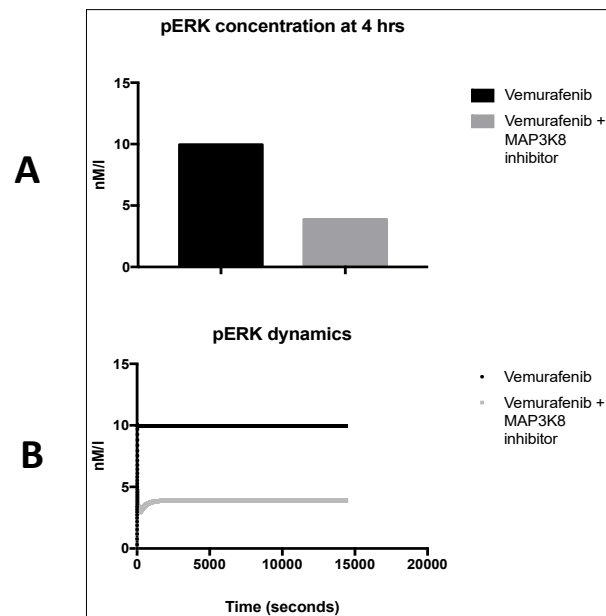


**Figure 11. In silico prediction of Vemurafenib plus MAP3K8 inhibitor combination protocol.**

Adapted from Gianì et al., Bioinformatics 2018; to appear

Panel A shows pERK concentration at time 4 hours while panel B depicts its dynamics over time. ERK behaviour under BRAF knock-out condition when vemurafenib is administered at 1  $\mu$ M concentration is simulated setting the PLX4032 species value to 1000 nM in the in silico model. These results show an initial p-ERK deactivation after BRAF arm knock-out and then a significant increase of the resistance mechanism against vemurafenib and the ineffectiveness of the treatment with conventional kinase inhibitors. When MAP3K8 inhibitor is administered at 10  $\mu$ M concentration along with vemurafenib (at 1  $\mu$ M concentration) the in silico model predicts a significant decrease of pERK (more than half of reduction, in comparison with the vemurafenib only administration). Inhibition of MAP3K8 was simulated setting MAP3K8:NF-kB\_Inactive species value to 0 in the in silico model.

The *mapreduce* paradigm was able to automatically scan and detect nodes that are far from our specific target taken into account (pErk). As one can see on Figure 12, MAPK1 gene that corresponds to ERK gene, according to KEGG nomenclature, is modulated by two arms that are respectively MAP2K1 and MAP2K2. For MAPK1 gene, the “hop” selected was equal to “2” and after the launch

of the script, we obtained a generation of nine neighbor genes for MAPK1 and a generation of six neighbor genes for MAPK2. In both isoforms of the same gene, the output graph pointed out the presence of MAP3K8 gene as one of the possible neighbor gene involved in the modulation and in the phosphorylation of ERK.

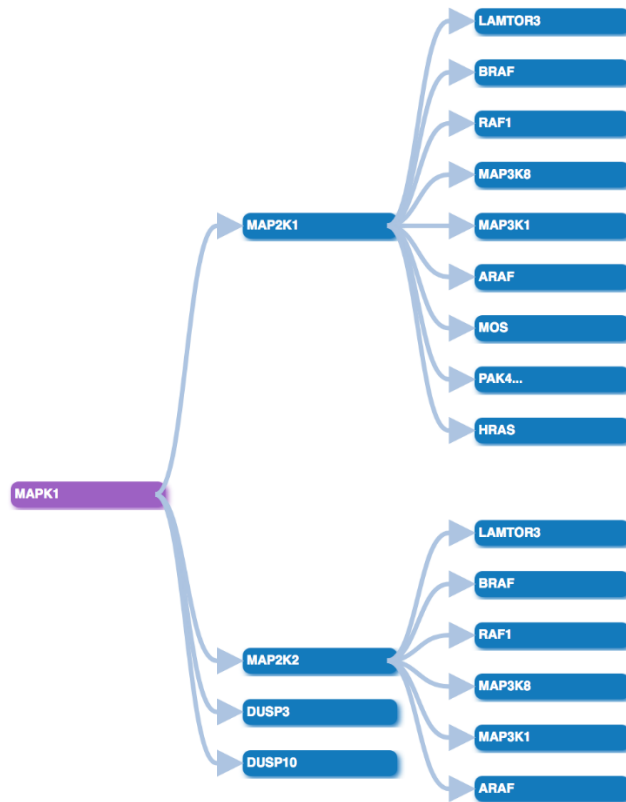


**Figure 12. A screenshot of *mapreduce* paradigm based algorithm.**

Adapted from Biondi et al., Euromicro Conference on Parallel and Distributed Processing 2019; submitted

To validate in silico prediction, we compared the expression levels of MAP3K8 between the 8505C-CSCs and monolayer 8505C cancer cells counterpart by qRT-PCR. These results are shown in Figure 13.

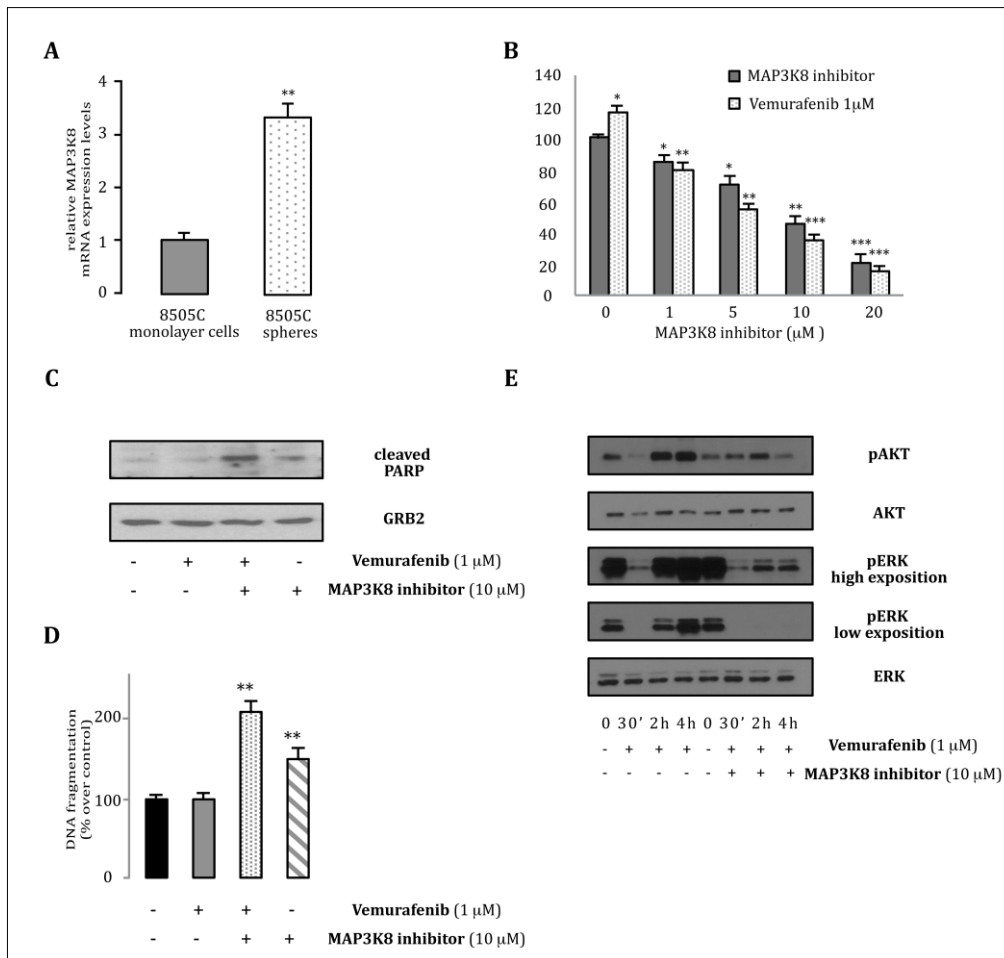


**Figure 13. MAP3K8 kinase expression and function in 8505C-Spheres.**

Adapted from Gianì et al. Bioinformatics 2018; to appear

Interestingly, 8505C-CSCs showed higher levels of MAP3K8 expression than 8505C monolayer parental cells (Figure 13A).

Next, we evaluated the effect of a selective inhibitor of MAP3K8 on 8505C-CSCs response to vemurafenib in terms of cell growth and apoptosis by measuring both the cleavage of poly (ADP-ribose) polymerase (PARP) and DNA fragmentation analysis.

To this end, we exposed 8505C-CSCs to increasing doses of the MAP3K8 inhibitor with or without 1 μM vemurafenib for 7 days. MAP3K8 inhibitor significantly restored in a dose-dependent manner the effect of vemurafenib on sphere formation in 8505C-CSCs harbouring the BRAF V600E mutation (Figure 13B).

According to growth inhibition, western blot analysis revealed a substantial PARP cleavage in 8505C-CSCs upon combined treatment, indicative of apoptosis induction (Figure 13C). More specifically, treatment of MAP3K8 inhibitor used as single agent did induce PARP cleavage; however, it was less marked as compared to combined treatment. As expected, vemurafenib alone failed to induce cleavage of PARP. Similar results were observed in DNA fragmentation assay (Figure 13D).

Finally, combined treatment of vemurafenib and MAP3K8 inhibitor resulted in effective suppression of ERK rebound and AKT overactivation compared to vemurafenib alone, providing a rationale for the observed synergy in both growth and apoptotic assays (Figure 13E). We also confirmed our results using an additional thyroid cancer cell lines harboring BRAF mutation, SV1736 (data not shown).

To summarizing, these results indicate that a small subpopulation of cancer cells, cancer stem cells (CSCs), may be involved in the failure of therapies targeting BRAF V600E in advanced thyroid cancer. These data have been obtained in CSCs derived from a panel of well-established thyroid cancer cell lines by a sphere-formation assay. This cell system provided a reliable model for further experiments on KI resistance. The stem cell identity of these cancer spheres is supported by their extensive self-renewal in vitro and overexpression of several stemness-related genes, such as OCT-4, ABCG-2, HES-1 and HEY-1, compared to monolayer parental cells.

Here we find a paradoxical stimulatory effect of BRAF-inhibitor vemurafenib on mutant BRAF V600E spheres (8505C-spheres) at variance with their parental monolayer cultures (8505C-monolayers). Indeed, same drug dose, while inhibiting cell growth and ERK activation in mutant BRAF V600E monolayer cultures, it stimulated sphere proliferation with a markedly different effect on kinetics of both ERK and AKT activation. In 8505C-spheres vemurafenib induced only a transient inhibition of ERK phosphorylation with a rapid and paradoxical re-activation starting at 30 minutes. In the same experimental context, a progressive increase in AKT activation was also observed. In accordance with the theory of the role of CSCs in chemoresistance, these data suggest a resistance phenomenon to vemurafenib in a subpopulation of these thyroid cancer cells.

Importantly, the *in silico* approach allowed us to identify MAP3K8 protein, a serine/threonine kinase expressed in 8505C-CSCs, as possible mechanism of resistance. Here, we developed a computational model with the aim to investigate alternative signaling transduction pathways over long distances that can affect possible crosstalk links between MAPK and PI3K/AKT.

Applying depth first search strategy, we tracked alternative pathways able to explain the escapement from ERK activation. Under BRAF inhibition, the depth first search identified long distance entities that, in turn, may affect the dynamics of ERK activation. By a computational view, this method identifies forward edges, which point from a node of the graph to one of its descendants (for example TNF for ERK and TRAF complex for AKT), and back edges, which point from a node to one of its ancestors (inverted effect). By this search, we found that MAP3K8 (MAP3K8) contributes to ERK activation, suggesting that this kinase may be targeted to overcome drug resistance.

*In vitro* experiments indicated that in mutant BRAF V600E 8505C-CSCs the inhibitory activity of vemurafenib is restored by the addition of the selective MAP3K8 inhibitor. Hence, these data were in agreement with and confirmed our prediction obtained by simulation modeling.

MAP3K8 kinase was shown to be an important mediator in inflammation during both innate and adaptive immune response<sup>43,344,345</sup>. Activation of MAP3K8 involves downstream signaling pathways such as MEK/ERK, JNK, p38 MAPK, and NF- $\kappa$ B not only involved in inflammatory response but also in the production of pro-inflammatory cytokines such as TN $\alpha$ , IL-1 $\beta$  and IFN- $\gamma$ <sup>346-349</sup>. Recently, accumulating evidences suggest that MAP3K8 may play a role in cell transformation, tumor growth and metastatic progression in several human cancers<sup>350-354</sup>. In this view, a recent report indicates that that higher expression of MAP3K8 correlates with both the BRAF V600E mutation and tumor recurrence in papillary thyroid cancer (PTC)<sup>355</sup>.

Our data indicate for the first time that MAP3K8 is up-regulated in 8505C-CSCs compared to 8505C cell monolayer. Moreover, treatment with MAP3K8 inhibitor alone induced both marked DNA fragmentation and PARP cleavage, indicative of apoptosis induction in 8505C-CSCs.

Taken together, MAP3K8 appears not only drive vemurafenib resistance in CSCs but might represent a potential novel prognostic marker and therapeutic targets for advanced thyroid cancer treatment. Indeed, MAP3K8 expression levels may be a clinically useful biomarker to predict the response to vemurafenib monotherapy in BRAF mutant tumors as well as may also help guide the selection of MAP3K8 combination therapy in these cancers.

Moreover, these data are suggestive that MAP3K8 may support the development of stem cell capabilities in the thyroid cancer cells and, and also be associated with tumor progression and metastasis. Thus, future study will be directed to investigate the role of MAP3K8 in thyroid cancer.

In conclusion, our data highlight a distinct mechanism by which mutant BRAF V600E thyroid cancer escape from vemurafenib inhibitory activity. Our current data reveal that MAP3K8 contributes to vemurafenib resistance of mutant BRAF V600E thyroid CSCs.

The further role of MAP3K8 as biomarker in predicting response in thyroid cancer under vemurafenib treatment could be better assessed through in vivo experiments that will be performed in due course. Moreover, with a limited effort, the in silico model can be adapted to other diseases that share the same signaling pathway.

## 5 CONCLUSIONS

Nowadays, computational modeling and simulation are more than useful in finding novel therapeutic targets and prognostic biomarkers for a more effective treatment in cancer. In particular, these strategies are able to better understand controversial mechanisms both at cellular and molecular level, to speed-up the drug discovery process and to help in overcoming specific drug resistance phenomena.

In this PhD project, we applied ordinary differential equations based models coupled with algorithmic approaches to reveal biochemical and genetic mechanisms underlying drug resistance phenomena in melanoma and thyroid cancer treatments.

For what concerns melanoma, we developed a computational model able to simulate PI3K/AKT and MAPK pathways and their interactions, both in physiological conditions and in melanoma A375 cell line harboring B-RAF mutation. The physiological model correctly reproduces the strong transient activation of ERK, while the melanoma A375 model reproduces pERK behavior when Dabrafenib intervention is administered. Its behavior is correlated to Dabrafenib concentration and p-ERK levels drop down due to the inhibitor activity of Dabrafenib over BRAFV600E protein.

This model represents a good starting point for further investigations of other fundamental signalling pathways of specific diseases that show genetic alterations and constitutive activation of particular nodes within the pathways.

In parallel, EpiMethEx, a computational tool for the correlation analysis between gene expression and methylation levels, was developed to identify methylation hotspots and extended genomic regions involved in gene regulation. The beta-test analysis showed a negative association between methylation and gene expression for the most modulated genes in melanoma. At the same time, a positive correlation was observed in some overexpressed genes that showed intragenic hypermethylated hotspots. The information gained through the application of EpiMethEx facilitates

the exploration of signaling pathways for a specific gene that, without this enrichment strategy, would have not be considered.

To investigate particular types of thyroid cancer that are refractory to kinase inhibitors treatment (e.g. vemurafenib), the developed computational strategy simulates MAPK and PI3K/AKT pathways and their associated protein networks. Moreover, the application of a depth first search strategy carried on the in silico model of 8505C-CSCs was able to identify alternative signaling pathways that do not directly influence ERK dynamics. In particular, we found that TNF signaling pathway stimulates both ERK and AKT protein kinases and the model was able to predict that the concomitant inhibition of both MAP3K8 and BRAF V600E is able to drastically reduce ERK phosphorylation. The prediction was then confirmed in vitro with a selective inhibition protocol.

The novel insights revealed by these innovative computational approaches allowed researchers to simplify the challenge of identifying novel targets and circumventing the need for costly and time-consuming experiments. The results achieved in this project, also pave the way for a wide variety of future research, including design of new drugs that inhibit, in a more effective way, specific functional sites and a better understanding of evolutionary biology.

Prospectively speaking, these results provide the opportunity to look further into possible applications. According to the new findings able to overcome drug resistance in thyroid cancer, a gene expression study of MAP3K8 in malignant melanoma A375 cell line, harboring BRAFV600E mutation, will be investigated to evaluate potential activity in ERK modulation. Methylation analysis through EpiMethEx will be performed in other cancer datasets (e.g., thyroid cancer) to establish further combination roles of gene expression and methylation levels. The very interesting result coming from the in vitro validation of MAP3K8 as an efficient inhibitor of ERK activity in 8505C-CSCs deserves an in vivo trial in order to confirm its biological function.



## 6 BIBLIOGRAPHY

1. Reece, J. & Urry, L. *Campbell biology*. *Campbell Biology* (2011). doi:10.1039/c3ra44507k
2. Scott, J. D. & Pawson, T. Cell signaling in space and time: Where proteins come together and when they're apart. *Science* (2009). doi:10.1126/science.1175668
3. Smock, R. G. & Gierasch, L. M. Sending signals dynamically. *Science* (2009). doi:10.1126/science.1169377
4. Svoboda, K. K. H. & Reenstra, W. R. Approaches to studying cellular signaling: A primer for morphologists. *Anat. Rec.* (2002). doi:10.1002/ar.10074
5. Signalling, C., Michael, B., Pathways, C. S. & Berridge, M. J. Cell Signalling Pathways. *Biochem. J.* (2009). doi:10.1042/csb0001002
6. Purvis, J. E. & Lahav, G. Encoding and decoding cellular information through signaling dynamics. *Cell* (2013). doi:10.1016/j.cell.2013.02.005
7. Trachtman, H. The law of mass action. *American Journal of Bioethics* (2006). doi:10.1080/15265160600755730
8. Bajzer, Ž. & Strehler, E. E. About and beyond the Henri-Michaelis–Menten rate equation for single-substrate enzyme kinetics. *Biochem. Biophys. Res. Commun.* **417**, 982–985 (2012).
9. Beard, D. A., Babson, E., Curtis, E. & Qian, H. Thermodynamic constraints for biochemical networks. *J. Theor. Biol.* (2004). doi:10.1016/j.jtbi.2004.01.008
10. Liebermeister, W., Uhlendorf, J. & Klipp, E. Modular rate laws for enzymatic reactions: Thermodynamics, elasticities and implementation. *Bioinformatics* (2010). doi:10.1093/bioinformatics/btq141
11. Antebi, Y. E., Nandagopal, N. & Elowitz, M. B. An operational view of intercellular signaling pathways. *Current Opinion in Systems Biology* (2017).

doi:10.1016/j.coisb.2016.12.003

12. Dobrescu, G. [Intercellular communication]. *Rev Med Chir Soc Med Nat Iasi* (1998).
13. Nakanishi, S. Molecular mechanisms of intercellular communication in the hormonal and neural systems. in *IUBMB Life* (2006). doi:10.1080/15216540600746385
14. Kramer, Ij. M. in *Signal Transduction* (2016). doi:10.1016/B978-0-12-394803-8.00002-4
15. Dragovich, T., Rudin, C. M. & Thompson, C. B. Signal transduction pathways that regulate cell survival and cell death. *Oncogene* (1998). doi:10.1038/sj.onc.1202587
16. Levy, E. D., Landry, C. R. & Michnick, S. W. Signaling through cooperation. *Science* (2010). doi:10.1126/science.1190993
17. Braeckman, B. P., Houthoofd, K. & Vanfleteren, J. R. Intermediary metabolism. *WormBook* (2009). doi:10.1895/wormbook.1.146.1
18. Tyson, J. J. & Novak, B. Control of cell growth, division and death: Information processing in living cells. *Interface Focus* (2014). doi:10.1098/rsfs.2013.0070
19. Rhind, N. & Russell, P. Signaling pathways that regulate cell division. *Cold Spring Harb. Perspect. Biol.* (2012). doi:10.1101/cshperspect.a005942
20. Hanna, S. & El-Sibai, M. Signaling networks of Rho GTPases in cell motility. *Cellular Signalling* (2013). doi:10.1016/j.cellsig.2013.04.009
21. Yeh, B. J., Rutigliano, R. J., Deb, A., Bar-Sagi, D. & Lim, W. A. Rewiring cellular morphology pathways with synthetic guanine nucleotide exchange factors. *Nature* (2007). doi:10.1038/nature05851
22. Albert Basson, M. Signaling in cell differentiation and morphogenesis. *Cold Spring Harb. Perspect. Biol.* (2012). doi:10.1101/cshperspect.a008151

23. Pieper, K., Grimbacher, B. & Eibel, H. B-cell biology and development. *Journal of Allergy and Clinical Immunology* (2013). doi:10.1016/j.jaci.2013.01.046
24. Fujita, T., Kanno, T. & Kobayashi, S. in *The Paraneuron* 78–84 (Springer Japan, 1988). doi:10.1007/978-4-431-68066-6\_7
25. Batra, N., Kar, R. & Jiang, J. X. Gap junctions and hemichannels in signal transmission, function and development of bone. *Biochim Biophys Acta* (2012). doi:10.1016/j.bbamem.2011.09.018
26. Alberts, B., Johnson, A. & Lewis, J. Signaling through G-Protein-Linked Cell-Surface Receptors. *Molecular Biology of the Cell. 4th edition* (2002).
27. Constantin, C. E. *et al.* Identification of Cav2–PKC $\beta$  and Cav2–NOS1 complexes as entities for ultrafast electrochemical coupling. *Proc. Natl. Acad. Sci.* (2017). doi:10.1073/pnas.1616394114
28. Wilson, M. R., Close, T. W. & Trosko, J. E. Cell population dynamics (apoptosis, mitosis, and cell-cell communication) during disruption of homeostasis. *Exp. Cell Res.* (2000). doi:10.1006/excr.1999.4771
29. Perbal, B. Cell Communication and Signaling Communication is the key. *Cell Commun. Signal.* (2003).
30. Derynck, R. & Zhang, Y. Intracellular signalling: The mad way to do it. *Current Biology* (1996). doi:10.1016/S0960-9822(96)00702-6
31. Poveda, A. M., Le Clech, M. & Pasero, P. Transcription and replication. *Transcription* (2010). doi:10.4161/trns.1.2.12665
32. Lodish, H. *et al.* *Molecular Cell Biology. 4th edition.* New York: W. H. Freeman (2000). doi:10.1017/CBO9781107415324.004

33. Mitrophanov, A. Y. & Groisman, E. A. Positive feedback in cellular control systems. *BioEssays* (2008). doi:10.1002/bies.20769
34. Brandman, O. & Meyer, T. Feedback loops shape cellular signals in space and time. *Science* (2008). doi:10.1126/science.1160617
35. Freeman, M. Feedback control of intercellular signalling in development. *Nature* (2000). doi:10.1038/35042500
36. Lukas, T. J. A signal transduction pathway model prototype I: From agonist to cellular endpoint. *Biophys. J.* (2004). doi:10.1529/biophysj.103.035253
37. Vert, G. & Chory, J. Crosstalk in Cellular Signaling: Background Noise or the Real Thing? *Developmental Cell* (2011). doi:10.1016/j.devcel.2011.11.006
38. Nishi, H., Demir, E. & Panchenko, A. R. Crosstalk between signaling pathways provided by single and multiple protein phosphorylation sites. *J. Mol. Biol.* (2015). doi:10.1016/j.jmb.2014.11.001
39. Saxena, M., Williams, S., Taskén, K. & Mustelin, T. Crosstalk between cAMP-dependent kinase and MAP kinase through a protein tyrosine phosphatase. *Nat. Cell Biol.* (1999). doi:10.1038/13024
40. Gomperts, B. D., Kramer, Ij. M. & Tatham, P. E. R. *Signal Transduction. Signal Transduction* (2009). doi:10.1016/B978-0-12-369441-6.00024-6
41. Prelich, G. Gene overexpression: Uses, mechanisms, and interpretation. *Genetics* (2012). doi:10.1534/genetics.111.136911
42. Manning, G. Genomic overview of protein kinases. *WormBook* (2005). doi:10.1895/wormbook.1.60.1
43. Arthur, J. S. C. & Ley, S. C. Mitogen-activated protein kinases in innate immunity. *Nat. Rev.*

*Immunol.* **13**, 679–692 (2013).

44. Sefton, B. M. & Shenolikar, S. Overview of protein phosphorylation. *Curr. Protoc. Mol. Biol.* (2001). doi:10.1002/0471140864.ps1301s00
45. Kholodenko, B. Cell-signalling dynamics in time and space. *Nat. Rev. Mol. Cell Biol.* (2006). doi:doi: 10.1038/nrm1838
46. Gong, Y. & Zhang, Z. Alternative signaling pathways: When, where and why? *FEBS Lett.* **579**, 5265–5274 (2005).
47. Aksamitiene, E., Kiyatkin, A. & Kholodenko, B. N. Cross-talk between mitogenic Ras/MAPK and survival PI3K/Akt pathways: a fine balance. *Biochem. Soc. Trans.* **40**, 139–146 (2012).
48. Sriram, S. M., Banerjee, R., Kane, R. S. & Kwon, Y. T. Multivalency-Assisted Control of Intracellular Signaling Pathways: Application for Ubiquitin- Dependent N-End Rule Pathway. *Chemistry and Biology* (2009). doi:10.1016/j.chembiol.2009.01.012
49. Mendoza, M. C., Er, E. E. & Blenis, J. The Ras-ERK and PI3K-mTOR pathways: Cross-talk and compensation. *Trends in Biochemical Sciences* (2011). doi:10.1016/j.tibs.2011.03.006
50. Zhou, J. *et al.* Crosstalk between MAPK/ERK and PI3K/AKT signal pathways during brain ischemia/reperfusion. *ASN Neuro* (2015). doi:10.1177/1759091415602463
51. Plotnikov, A., Zehorai, E., Procaccia, S. & Seger, R. The MAPK cascades: Signaling components, nuclear roles and mechanisms of nuclear translocation. *Biochimica et Biophysica Acta - Molecular Cell Research* (2011). doi:10.1016/j.bbamcr.2010.12.012
52. Seger, R. & Krebs, E. G. The MAPK signaling cascade. *FASEB J.* (1995). doi:10.1096/FASEBJ.9.9.7601337
53. Hemmings, B. A. & Restuccia, D. F. The PI3k-PKB/Akt pathway. *Cold Spring Harbor*

*Perspectives in Biology* (2015). doi:10.1101/cshperspect.a026609

54. Vanhaesebroeck, B., Stephens, L. & Hawkins, P. PI3K signalling: The path to discovery and understanding. *Nature Reviews Molecular Cell Biology* (2012). doi:10.1038/nrm3290
55. Geary, L. & Labonne, C. FGF mediated mapk and pi3k/akt signals make distinct contributions to pluripotency and the establishment of neural crest. *Elife* (2018). doi:10.7554/eLife.33845
56. Schultze, S. M., Hemmings, B. A., Niessen, M. & Tschopp, O. PI3K/AKT, MAPK and AMPK signalling: Protein kinases in glucose homeostasis. *Expert Reviews in Molecular Medicine* (2012). doi:10.1017/S1462399411002109
57. Lee, E. R. *et al.* Interplay between PI3K/Akt and MAPK signaling pathways in DNA-damaging drug-induced apoptosis. *Biochim. Biophys. Acta - Mol. Cell Res.* (2006). doi:10.1016/j.bbamcr.2006.06.006
58. ZHANG, W. & LIU, H. T. MAPK signal pathways in the regulation of cell proliferation in mammalian cells. *Cell Res.* (2002). doi:10.1038/sj.cr.7290105
59. Cargnello, M. & Roux, P. P. Activation and Function of the MAPKs and Their Substrates, the MAPK-Activated Protein Kinases. *Microbiol. Mol. Biol. Rev.* (2011). doi:10.1128/MMBR.00031-10
60. Roskoski, R. ERK1/2 MAP kinases: Structure, function, and regulation. *Pharmacological Research* (2012). doi:10.1016/j.phrs.2012.04.005
61. Liu, J., Minemoto, Y. & Lin, A. c-Jun N-Terminal Protein Kinase 1 (JNK1), but Not JNK2, Is Essential for Tumor Necrosis Factor Alpha-Induced c-Jun Kinase Activation and Apoptosis. *Mol. Cell. Biol.* (2004). doi:10.1128/MCB.24.24.10844-10856.2004
62. Coffey, E. T. *et al.* c-Jun N-terminal protein kinase (JNK) 2/3 is specifically activated by

stress, mediating c-Jun activation, in the presence of constitutive JNK1 activity in cerebellar neurons. *J. Neurosci.* (2002). doi:20026401

63. Ono, K. & Han, J. The p38 signal transduction pathway: activation and function. *Cell Signal* (2000). doi:S0898-6568(99)00071-6 [pii]
64. Roux, P. P. & Blenis, J. ERK and p38 MAPK-activated protein kinases: a family of protein kinases with diverse biological functions. *Microbiol. Mol. Biol. Rev.* (2004). doi:10.1128/MMBR.68.2.320-344.2004
65. Nishimoto, S. & Nishida, E. MAPK signalling: ERK5 versus ERK1/2. *EMBO Reports* (2006). doi:10.1038/sj.embor.7400755
66. Roskoski, R. MEK1/2 dual-specificity protein kinases: Structure and regulation. *Biochemical and Biophysical Research Communications* (2012). doi:10.1016/j.bbrc.2011.11.145
67. Gelmedin, V., Spiliotis, M. & Brehm, K. Molecular characterisation of MEK1/2- and MKK3/6-like mitogen-activated protein kinase kinases (MAPKK) from the fox tapeworm *Echinococcus multilocularis*. *Int. J. Parasitol.* (2010). doi:10.1016/j.ijpara.2009.10.009
68. Baldari, S., Ubertini, V., Garufi, A., D'Orazi, G. & Bossi, G. Targeting MKK3 as a novel anticancer strategy: Molecular mechanisms and therapeutical implications. *Cell Death Dis.* (2015). doi:10.1038/cddis.2014.591
69. Zou, J. *et al.* The genome-wide identification of mitogen-activated protein kinase kinase (MKK) genes in Yesso scallop *Patinopecten yessoensis* and their expression responses to bacteria challenges. *Fish Shellfish Immunol.* (2015). doi:10.1016/j.fsi.2015.06.006
70. Drew, B. A., Burow, M. E. & Beckman, B. S. MEK5/ERK5 pathway: The first fifteen years. *Biochimica et Biophysica Acta - Reviews on Cancer* (2012). doi:10.1016/j.bbcan.2011.10.002

71. Li, L. *et al.* Mitogen-activated protein kinase kinase kinase (MAPKKK) 4 from rapeseed (*Brassica napus* L.) is a novel member inducing ROS accumulation and cell death. *Biochem. Biophys. Res. Commun.* (2015). doi:10.1016/j.bbrc.2015.10.063
72. Chang, L. & Karin, M. Mammalian MAP kinase signalling cascades. *Nature* (2001). doi:10.1038/35065000
73. Wee, P. & Wang, Z. Epidermal growth factor receptor cell proliferation signaling pathways. *Cancers* (2017). doi:10.3390/cancers9050052
74. Wu, E. *et al.* Comprehensive dissection of PDGF-PDGFR signaling pathways in PDGFR genetically defined cells. *PLoS One* (2008). doi:10.1371/journal.pone.0003794
75. Maehara, O. *et al.* Fibroblast growth factor-2-mediated FGFR/Erk signaling supports maintenance of cancer stem-like cells in esophageal squamous cell carcinoma. *Carcinogenesis* (2017). doi:10.1093/carcin/bgx095
76. Sekar, M. C., Shahiwala, K., Leloup, L. & Wells, A. Modulation of Epidermal Growth Factor Stimulated ERK Phosphorylation and Cell Motility by Inositol Trisphosphate Kinase. *J. Pharm. Sci. Pharmacol.* (2014).
77. Weber, A., Wasiliew, P. & Kracht, M. Interleukin-1 (IL-1) pathway. *Science Signaling* (2010). doi:10.1126/scisignal.3105cm1
78. Ip, Y. T. & Davis, R. J. Signal transduction by the c-Jun N-terminal kinase (JNK)--from inflammation to development. *Curr. Opin. Cell Biol.* (1998). doi:S0955-0674(98)80143-9 [pii]
79. Arkun, Y. & Yasemi, M. Dynamics and control of the ERK signaling pathway: Sensitivity, bistability, and oscillations. *PLoS One* (2018). doi:10.1371/journal.pone.0195513
80. Li, R., Pourpak, A. & Morris, S. W. Inhibition of the insulin-like growth factor-1 receptor



- (IGF1R) tyrosine kinase as a novel cancer therapy approach. *Journal of Medicinal Chemistry* (2009). doi:10.1021/jm9002395
81. Iijima, M., Anai, M., Kodama, T. & Shibasaki, Y. Epiregulin-blocking antibody inhibits epiregulin-dependent EGFR signaling. *Biochem. Biophys. Res. Commun.* (2017). doi:10.1016/j.bbrc.2017.03.006
  82. Zaiss, D. M. W., Gause, W. C., Osborne, L. C. & Artis, D. Emerging functions of amphiregulin in orchestrating immunity, inflammation, and tissue repair. *Immunity* (2015). doi:10.1016/j.immuni.2015.01.020
  83. Hubbard, S. R. & Miller, W. T. Receptor tyrosine kinases: mechanisms of activation and signaling. *Current Opinion in Cell Biology* (2007). doi:10.1016/j.ceb.2007.02.010
  84. Shima, F. *et al.* Structural basis for conformational dynamics of GTP-bound ras protein. *J. Biol. Chem.* (2010). doi:10.1074/jbc.M110.125161
  85. Roskoski, R. RAF protein-serine/threonine kinases: Structure and regulation. *Biochemical and Biophysical Research Communications* (2010). doi:10.1016/j.bbrc.2010.07.092
  86. Sithanandam, G., Kolch, W., Duh, F. M. & Rapp, U. R. Complete coding sequence of a human B-raf cDNA and detection of B-raf protein kinase with isozyme specific antibodies. *Oncogene* (1990).
  87. Leicht, D. T. *et al.* Raf kinases: Function, regulation and role in human cancer. *Biochimica et Biophysica Acta - Molecular Cell Research* (2007). doi:10.1016/j.bbamcr.2007.05.001
  88. Freeman, A. K., Ritt, D. A. & Morrison, D. K. Effects of Raf Dimerization and Its Inhibition on Normal and Disease-Associated Raf Signaling. *Mol. Cell* (2013). doi:10.1016/j.molcel.2012.12.018
  89. Rushworth, L. K., Hindley, A. D., O'Neill, E. & Kolch, W. Regulation and Role of Raf-1/B-

- Raf Heterodimerization. *Mol. Cell. Biol.* (2006). doi:10.1128/MCB.26.6.2262-2272.2006
90. Gardner, a M., Vaillancourt, R. R., Lange-Carter, C. a & Johnson, G. L. MEK-1 phosphorylation by MEK kinase, Raf, and mitogen-activated protein kinase: analysis of phosphopeptides and regulation of activity. *Mol. Biol. Cell* (1994). doi:10.1091/mbc.5.2.193
  91. Mooz, J. *et al.* Dimerization of the kinase ARAF promotes MAPK pathway activation and cell migration. *Sci. Signal.* (2014). doi:10.1126/scisignal.2005484
  92. McCain, J. The MAPK (ERK) Pathway: Investigational Combinations for the Treatment Of BRAF-Mutated Metastatic Melanoma. *P T* (2013).
  93. Manning, B. D. & Toker, A. AKT/PKB Signaling: Navigating the Network. *Cell* (2017). doi:10.1016/j.cell.2017.04.001
  94. Thorpe, L. M., Yuzugullu, H. & Zhao, J. J. PI3K in cancer: Divergent roles of isoforms, modes of activation and therapeutic targeting. *Nature Reviews Cancer* (2015). doi:10.1038/nrc3860
  95. Czech, M. P. PIP<sub>2</sub> and PIP<sub>3</sub>: complex roles at the cell surface. *Cell* (2000). doi:10.1016/S0092-8674(00)80696-0
  96. Chin, Y. R. & Toker, A. Function of Akt/PKB signaling to cell motility, invasion and the tumor stroma in cancer. *Cellular Signalling* (2009). doi:10.1016/j.cellsig.2008.11.015
  97. Song, G., Ouyang, G. & Bao, S. The activation of Akt/PKB signaling pathway and cell survival. *J Cell Mol Med* (2005). doi:10.1111/j.1582-4934.2005.tb00337.x
  98. Liu, W. *et al.* The Role of EGFR/PI3K/Akt/cyclinD1 Signaling Pathway in Acquired Middle Ear Cholesteatoma. *Mediators Inflamm.* **2013**, 651207 (2013).
  99. Wheler, J. J. *et al.* Presence of both alterations in FGFR/FGF and PI3K/AKT/mTOR confer improved outcomes for patients with metastatic breast cancer treated with PI3K/AKT/mTOR

inhibitors. *Oncoscience* **3**, 164–172 (2016).

100. Fantauzzo, K. A. & Soriano, P. PI3K-mediated PDGFR?? signaling regulates survival and proliferation in skeletal development through p53-dependent intracellular pathways. *Genes Dev.* (2014). doi:10.1101/gad.238709.114
101. Usatyuk, P. V *et al.* Role of c-Met/Phosphatidylinositol 3-Kinase (PI3k)/Akt Signaling in Hepatocyte Growth Factor (HGF)-mediated Lamellipodia Formation, Reactive Oxygen Species (ROS) Generation, and Motility of Lung Endothelial Cells. *J. Biol. Chem.* **289**, 13476–13491 (2014).
102. Jhun, B. H., Rivnay, B., Price, D. & Avraham, H. The MATK tyrosine kinase interacts in a specific and SH2-dependent manner with c-Kit. *J. Biol. Chem.* (1995). doi:10.1074/jbc.270.16.9661
103. O'Hayre, M., Degese, M. S. & Gutkind, J. S. Novel insights into G protein and G protein-coupled receptor signaling in cancer. *Current Opinion in Cell Biology* (2014). doi:10.1016/j.ceb.2014.01.005
104. Salminen, A. & Kaarniranta, K. Insulin/IGF-1 paradox of aging: Regulation via AKT/IKK/NF-??B signaling. *Cellular Signalling* (2010). doi:10.1016/j.cellsig.2009.10.006
105. Carnero, A., Blanco-Aparicio, C., Renner, O., Link, W. & Leal, J. The PTEN/PI3K/AKT Signalling Pathway in Cancer, Therapeutic Implications. *Curr. Cancer Drug Targets* (2008). doi:10.2174/156800908784293659
106. Denduluri, S. K. *et al.* Insulin-like growth factor (IGF) signaling in tumorigenesis and the development of cancer drug resistance. *Genes Dis.* (2015). doi:10.1016/j.gendis.2014.10.004
107. Martin, L. J. *et al.* Epiregulin and EGFR interactions are involved in pain processing. *J. Clin. Invest.* (2017). doi:10.1172/JCI87406

108. Toulany, M., Baumann, M. & Rodemann, H. P. Stimulated PI3K-AKT Signaling Mediated through Ligand or Radiation-Induced EGFR Depends Indirectly, but not Directly, on Constitutive K-Ras Activity. *Mol. Cancer Res.* (2007). doi:10.1158/1541-7786.MCR-06-0297
109. in *Inositol Phospholipid Metabolism and Phosphatidyl Inositol Kinases* (ed. Kuksis, A. B. T.-L. T. in B. and M. B.) **30**, 403–462 (Elsevier, 2003).
110. Jean, S. & Kiger, A. A. Classes of phosphoinositide 3-kinases at a glance. *J. Cell Sci.* (2014). doi:10.1242/jcs.093773
111. Hiles, I. D. *et al.* Phosphatidylinositol 3-kinase: Structure and expression of the 110 kd catalytic subunit. *Cell* (1992). doi:10.1016/0092-8674(92)90166-A
112. Yu, J. *et al.* Regulation of the p85/p110 Phosphatidylinositol 3'-Kinase: Stabilization and Inhibition of the p110 $\alpha$  Catalytic Subunit by the p85 Regulatory Subunit. *Mol. Cell. Biol.* (1998). doi:10.1128/MCB.18.3.1379
113. Boura-Halfon, S. & Zick, Y. Phosphorylation of IRS proteins, insulin action, and insulin resistance. *AJP Endocrinol. Metab.* (2009). doi:10.1152/ajpendo.90437.2008
114. Neel, B. G., Gu, H. & Pao, L. The 'Shp'ing news: SH2 domain-containing tyrosine phosphatases in cell signaling. *Trends in Biochemical Sciences* (2003). doi:10.1016/S0968-0004(03)00091-4
115. Geltz, N. R. & Augustine, J. a. The p85 and p110 subunits of phosphatidylinositol 3-kinase-alpha are substrates, in vitro, for a constitutively associated protein tyrosine kinase in platelets. *Blood* (1998).
116. Storz, P. & Toker, A. 3'-phosphoinositide-dependent kinase-1 (PDK-1) in PI 3-kinase signaling. *Front Biosci* (2002). doi:10.2741/storz

117. Liao, Y. & Hung, M. C. Physiological regulation of Akt activity and stability. *American Journal of Translational Research* (2010). doi:20182580
118. Cantley, L. C. The phosphoinositide 3-kinase pathway. *Science* (2002). doi:10.1126/science.296.5573.1655
119. Cheng, L., Lopez-Beltran, A., Massari, F., MacLennan, G. T. & Montironi, R. Molecular testing for BRAF mutations to inform melanoma treatment decisions: A move toward precision medicine. *Modern Pathology* (2018). doi:10.1038/modpathol.2017.104
120. Wellbrock, C. & Arozarena, I. The Complexity of the ERK/MAP-Kinase Pathway and the Treatment of Melanoma Skin Cancer. *Front. Cell Dev. Biol.* (2016). doi:10.3389/fcell.2016.00033
121. Silva, J. M., Bulman, C. & McMahon, M. BRAFV600E Cooperates with PI3K Signaling, Independent of AKT, to Regulate Melanoma Cell Proliferation. *Mol. Cancer Res.* (2014). doi:10.1158/1541-7786.MCR-13-0224-T
122. Cho, J. H. *et al.* AKT1 Activation Promotes Development of Melanoma Metastases. *Cell Rep.* (2015). doi:10.1016/j.celrep.2015.09.057
123. Jin, S., Borkhuu, O., Bao, W. & Yang, Y.-T. Signaling Pathways in Thyroid Cancer and Their Therapeutic Implications. *J. Clin. Med. Res.* (2016). doi:10.14740/jocmr2480w
124. Mondragón-Terán, P. *et al.* Intracellular signalling mechanisms in thyroid cancer. *Cirugía y Cir. (English Ed.* **84**, 434–443 (2016).
125. Robbins, H. L. & Hague, A. The PI3K/Akt Pathway in Tumors of Endocrine Tissues. *Front. Endocrinol. (Lausanne)*. **6**, 188 (2015).
126. Nozhat, Z. & Hedayati, M. PI3K/AKT Pathway and Its Mediators in Thyroid Carcinomas. *Mol. Diagnosis Ther.* (2016). doi:10.1007/s40291-015-0175-y

127. Stiles, B. L. Phosphatase and Tensin Homologue deleted on Chromosome 10: Extending its PTENacles. *Int. J. Biochem. Cell Biol.* **41**, 757–761 (2009).
128. Karakas, B., Bachman, K. E. & Park, B. H. Mutation of the PIK3CA oncogene in human cancers. *Br. J. Cancer* **94**, 455 (2006).
129. Nakanishi, Y. *et al.* Activating mutations in PIK3CB confer resistance to PI3K inhibition and define a novel oncogenic role for p110 $\beta$ . *Cancer Res.* (2016). doi:10.1158/0008-5472.CAN-15-2201
130. Marranci, A. *et al.* The landscape of BRAF transcript and protein variants in human cancer. *Mol. Cancer* (2017). doi:10.1186/s12943-017-0645-4
131. Matallanas, D. *et al.* Raf family kinases: Old dogs have learned new tricks. *Genes and Cancer* (2011). doi:10.1177/1947601911407323
132. Wan, P. T. C. *et al.* Mechanism of activation of the RAF-ERK signaling pathway by oncogenic mutations of B-RAF. *Cell* (2004). doi:10.1016/S0092-8674(04)00215-6
133. Davies, H. *et al.* Mutations of the BRAF gene in human cancer. *Nature* (2002). doi:10.1038/nature00766
134. Parrales, A. & Iwakuma, T. Targeting Oncogenic Mutant p53 for Cancer Therapy. *Front. Oncol.* (2015). doi:10.3389/fonc.2015.00288
135. Rajagopalan, H. *et al.* RAF/RAS oncogenes and mismatch-repair status. *Nature* (2002). doi:10.1038/418934a
136. Ibrahim, N. & Haluska, F. G. Molecular Pathogenesis of Cutaneous Melanocytic Neoplasms. *Annu. Rev. Pathol. Mech. Dis.* (2009). doi:10.1146/annurev.pathol.3.121806.151541
137. Ascierto, P. A. *et al.* The role of BRAF V600 mutation in melanoma. *Journal of Translational Medicine* (2012). doi:10.1186/1479-5876-10-85

138. Lee, J. W. *et al.* BRAF mutations in non-Hodgkin's lymphoma. *Br J Cancer* (2003). doi:10.1038/sj.bjc.6601371
139. Safae Ardekani, G., Jafarnejad, S. M., Tan, L., Saedi, A. & Li, G. The Prognostic Value of BRAF Mutation in Colorectal Cancer and Melanoma: A Systematic Review and Meta-Analysis. *PLoS One* (2012). doi:10.1371/journal.pone.0047054
140. Nikiforova, M. N. *et al.* BRAF Mutations in Thyroid Tumors Are Restricted to Papillary Carcinomas and Anaplastic or Poorly Differentiated Carcinomas Arising from Papillary Carcinomas. *J. Clin. Endocrinol. Metab.* **88**, 5399–5404 (2003).
141. Leonetti, A. *et al.* BRAF in non-small cell lung cancer (NSCLC): Pickaxing another brick in the wall. *Cancer Treat. Rev.* **66**, 82–94 (2018).
142. Falini, B., Martelli, M. P. & Tiacci, E. BRAF-V600E mutation in hairy cell leukemia: from bench to bedside. *Blood* (2016). doi:10.1182/blood-2016-07-418434
143. Robinson, S. D., O'Shaughnessy, J. A., Lance Cowey, C. & Konduri, K. BRAF V600E-mutated lung adenocarcinoma with metastases to the brain responding to treatment with vemurafenib. *Lung Cancer* (2014). doi:10.1016/j.lungcan.2014.05.009
144. Forbes, S. A. *et al.* The Catalogue of Somatic Mutations in Cancer (COSMIC). *Curr. Protoc. Hum. Genet.* **CHAPTER**, Unit-10.11 (2008).
145. Lovly, C. M. *et al.* Routine multiplex mutational profiling of melanomas enables enrollment in genotype-driven therapeutic trials. *PLoS One* (2012). doi:10.1371/journal.pone.0035309
146. Rubinstein, J. C. *et al.* Incidence of the V600K mutation among melanoma patients with BRAF mutations, and potential therapeutic response to the specific BRAF inhibitor PLX4032. *Journal of Translational Medicine* (2010). doi:10.1186/1479-5876-8-67
147. Yao, Z. *et al.* BRAF mutants evade ERK dependent feedback by different mechanisms that

- determine their sensitivity to pharmacologic inhibition. *Cancer Cell* **28**, 370–383 (2015).
148. Lake, D., Corrêa, S. A. L. & Müller, J. Negative feedback regulation of the ERK1/2 MAPK pathway. *Cell. Mol. Life Sci.* **73**, 4397–4413 (2016).
149. Libra, M. *et al.* Analysis of BRAF Mutation in Primary and Metastatic Melanoma. *Cell Cycle* **4**, 1382–1384 (2005).
150. Maurer, G., Tarkowski, B. & Baccarini, M. Raf kinases in cancer-roles and therapeutic opportunities. *Oncogene* (2011). doi:10.1038/onc.2011.160
151. Xing, M. BRAF mutation in thyroid cancer. *Endocrine-Related Cancer* (2005). doi:10.1677/erc.1.0978
152. Begum, S. *et al.* BRAF mutations in anaplastic thyroid carcinoma: implications for tumor origin, diagnosis and treatment. *Mod. Pathol.* **17**, 1359–1363 (2004).
153. Trovisco, V., Soares, P. & Sobrinho-Simões, M. B-RAF mutations in the etiopathogenesis, diagnosis, and prognosis of thyroid carcinomas. *Hum. Pathol.* **37**, 781–786 (2006).
154. Nikiforov, Y. E. & Nikiforova, M. N. Molecular genetics and diagnosis of thyroid cancer. *Nat. Rev. Endocrinol.* **7**, 569–580 (2011).
155. Knauf, J. A. & Fagin, J. A. Role of MAPK pathway oncoproteins in thyroid cancer pathogenesis and as drug targets. *Curr. Opin. Cell Biol.* **21**, 296–303 (2009).
156. Haling, J. R. *et al.* Structure of the BRAF-MEK Complex Reveals a Kinase Activity Independent Role for BRAF in MAPK Signaling. *Cancer Cell* (2014). doi:10.1016/j.ccr.2014.07.007
157. Tsao, H., Chin, L., Garraway, L. A. & Fisher, D. E. Melanoma: From mutations to medicine. *Genes and Development* (2012). doi:10.1101/gad.191999.112
158. Nikiforova, M. N. *et al.* BRAF Mutations in Thyroid Tumors Are Restricted to Papillary



Carcinomas and Anaplastic or Poorly Differentiated Carcinomas Arising from Papillary Carcinomas. *J. Clin. Endocrinol. Metab.* (2003). doi:10.1210/jc.2003-030838

159. Gautschi, O. *et al.* Targeted therapy for patients with BRAF-mutant lung cancer: results from the European EURAF cohort. *J Thorac Oncol* **10**, (2015).
160. American Cancer Society. Targeted Therapy. *Am. Cancer Soc.* (2013). doi:10.1007/978-3-540-47648-1\_5677
161. Sawyers, C. Targeted cancer therapy. *Nature* (2004). doi:10.1038/nature03095
162. Flaherty, K. T. *et al.* Inhibition of Mutated, Activated BRAF in Metastatic Melanoma. *N. Engl. J. Med.* (2010). doi:10.1056/NEJMoa1002011
163. Vultur, A., Villanueva, J. & Herlyn, M. Targeting BRAF in advanced melanoma: A first step toward manageable disease. *Clin. Cancer Res.* (2011). doi:10.1158/1078-0432.CCR-10-0174
164. Mackiewicz, J. & Mackiewicz, A. BRAF and MEK inhibitors in the era of immunotherapy in melanoma patients. *Contemp. Oncol.* **22**, 68–72 (2018).
165. Sharma, A., Shah, S. R., Illum, H. & Dowell, J. Vemurafenib. *Drugs* **72**, 2207–2222 (2012).
166. Menzies, A. M., Long, G. V & Murali, R. Dabrafenib and its potential for the treatment of metastatic melanoma. *Drug Des. Devel. Ther.* **6**, 391–405 (2012).
167. Holderfield, M., Deuker, M. M., McCormick, F. & McMahon, M. Targeting RAF kinases for cancer therapy: BRAF-mutated melanoma and beyond. *Nat Rev Cancer* **14**, (2014).
168. Grimaldi, A. M. *et al.* MEK Inhibitors in the Treatment of Metastatic Melanoma and Solid Tumors. *Am. J. Clin. Dermatol.* **18**, 745–754 (2017).
169. Eroglu, Z. & Ribas, A. Combination therapy with BRAF and MEK inhibitors for melanoma: latest evidence and place in therapy. *Ther. Adv. Med. Oncol.* **8**, 48–56 (2016).

170. Kim, S., Kim, H. T. & Suh, H. S. Combination therapy of BRAF inhibitors for advanced melanoma with *BRAF* V600 mutation: a systematic review and meta-analysis. *J. Dermatolog. Treat.* **29**, 314–321 (2018).
171. Griffin, M. *et al.* BRAF inhibitors: resistance and the promise of combination treatments for melanoma. *Oncotarget* **8**, 78174–78192 (2017).
172. Cabanillas, M. E. *et al.* BRAF inhibitors: experience in thyroid cancer and general review of toxicity. *Horm. Cancer* **6**, 21–36 (2015).
173. Subbiah, V. *et al.* Dabrafenib and Trametinib Treatment in Patients With Locally Advanced or Metastatic *BRAF* V600–Mutant Anaplastic Thyroid Cancer. *J. Clin. Oncol.* **36**, 7–13 (2018).
174. Welsh, S. J. *et al.* Resistance to combination BRAF and MEK inhibition in metastatic melanoma: Where to next? *Eur. J. Cancer* (2016). doi:10.1016/j.ejca.2016.04.005
175. Long, G. V *et al.* Increased MAPK reactivation in early resistance to dabrafenib/trametinib combination therapy of BRAF-mutant metastatic melanoma. *Nat Commun* **5**, (2014).
176. Villanueva, J., Vultur, A. & Herlyn, M. Resistance to BRAF inhibitors: unraveling mechanisms and future treatment options. *Cancer Res.* **71**, 7137–40 (2011).
177. Devitt, B. *et al.* Clinical outcome and pathological features associated with NRAS mutation in cutaneous melanoma. *Pigment Cell Melanoma Res.* **24**, 666–672 (2011).
178. Deng, W. *et al.* Role and therapeutic potential of PI3K-mTOR signaling in de novo resistance to BRAF inhibition. *Pigment Cell Melanoma Res.* **25**, 248–258 (2012).
179. Poulikakos, P. I. *et al.* RAF inhibitor resistance is mediated by dimerization of aberrantly spliced BRAF(V600E). *Nature* **480**, (2011).
180. Gibney, G. T., Messina, J. L., Fedorenko, I. V., Sondak, V. K. & Smalley, K. S. M.

Paradoxical oncogenesis-the long-term effects of BRAF inhibition in melanoma. *Nature Reviews Clinical Oncology* (2013). doi:10.1038/nrclinonc.2013.83

181. Emery, C. M. *et al.* MEK1 mutations confer resistance to MEK and B-RAF inhibition. *Proc. Natl. Acad. Sci. U. S. A.* **106**, 20411–20416 (2009).
182. Jia, Y. *et al.* EGFR inhibition enhances the antitumor efficacy of a selective BRAF V600E inhibitor in thyroid cancer cell lines. *Oncol. Lett.* **15**, 6763–6769 (2018).
183. Obaid, N. M., Bedard, K. & Huang, W. Y. Strategies for overcoming resistance in tumours harboring BRAF mutations. *International Journal of Molecular Sciences* (2017). doi:10.3390/ijms18030585
184. Chakraborty, R., Wieland, C. N. & Comfere, N. I. Molecular targeted therapies in metastatic melanoma. *Pharmgenomics. Pers. Med.* **6**, 49–56 (2013).
185. Bartocci, E. & Lió, P. Computational Modeling, Formal Analysis, and Tools for Systems Biology. *PLoS Computational Biology* (2016). doi:10.1371/journal.pcbi.1004591
186. Yuryev, A. *Pathway Analysis for Drug Discovery. Pathway Analysis for Drug Discovery: Computational Infrastructure and Applications* (John Wiley & Sons, Inc., 2008). doi:10.1002/9780470399279
187. Jin, L. *et al.* Pathway-based Analysis Tools for Complex Diseases: A Review. *Genomics. Proteomics Bioinformatics* (2014). doi:10.1016/j.gpb.2014.10.002
188. Cirillo, E., Parnell, L. D. & Evelo, C. T. A review of pathway-based analysis tools that visualize genetic variants. *Frontiers in Genetics* (2017). doi:10.3389/fgene.2017.00174
189. McGillivray, P. *et al.* Network Analysis as a Grand Unifier in Biomedical Data Science. *Annu. Rev. Biomed. Data Sci.* (2018). doi:10.1146/annurev-biodatasci-080917-013444
190. Soon, W. W., Hariharan, M. & Snyder, M. P. High-throughput sequencing for biology and

medicine. *Mol. Syst. Biol.* (2014). doi:10.1038/msb.2012.61

191. Huang, D. W., Sherman, B. T. & Lempicki, R. A. Bioinformatics enrichment tools: Paths toward the comprehensive functional analysis of large gene lists. *Nucleic Acids Res.* (2009). doi:10.1093/nar/gkn923
192. Leong, H. S. & Kipling, D. Text-based over-representation analysis of microarray gene lists with annotation bias. *Nucleic Acids Res.* **37**, e79–e79 (2009).
193. Pavlidis, P., Qin, J., Arango, V., Mann, J. J. & Sibille, E. Using the gene ontology for microarray data mining: A comparison of methods and application to age effects in human prefrontal cortex. *Neurochemical Research* (2004). doi:10.1023/B:NERE.0000023608.29741.45
194. Khatri, P., Sirota, M. & Butte, A. J. Ten Years of Pathway Analysis: Current Approaches and Outstanding Challenges. *PLoS Comput. Biol.* **8**, e1002375 (2012).
195. Nam, D. & Kim, S. Y. Gene-set approach for expression pattern analysis. *Briefings in Bioinformatics* (2008). doi:10.1093/bib/bbn001
196. Subramanian, A. *et al.* Gene set enrichment analysis: A knowledge-based approach for interpreting genome-wide expression profiles. *Proc. Natl. Acad. Sci.* (2005). doi:10.1073/pnas.0506580102
197. Efron, B. & Tibshirani, R. On testing the significance of sets of genes. *Ann. Appl. Stat.* (2007). doi:10.1214/07-AOAS101
198. Rahnenführer, J., Domingues, F. S., Maydt, J. & Lengauer, T. Calculating the Statistical Significance of Changes in Pathway Activity From Gene Expression Data. *Stat. Appl. Genet. Mol. Biol.* (2004). doi:10.2202/1544-6115.1055
199. Tarca, A. L. *et al.* A novel signaling pathway impact analysis. *Bioinformatics* **25**, 75–82

(2009).

200. Glaab, E., Baudot, A., Krasnogor, N., Schneider, R. & Valencia, A. EnrichNet: Network-based gene set enrichment analysis. *Bioinformatics* (2012).  
doi:10.1093/bioinformatics/bts389
201. Geistlinger, L., Csaba, G., Küffner, R., Mulder, N. & Zimmer, R. From sets to graphs: Towards a realistic enrichment analysis of transcriptomic systems. *Bioinformatics* (2011).  
doi:10.1093/bioinformatics/btr228
202. Glaab, E., Baudot, A., Krasnogor, N. & Valencia, A. TopoGSA: Network topological gene set analysis. *Bioinformatics* (2010). doi:10.1093/bioinformatics/btq131
203. Thomas, R. K. *et al.* High-throughput oncogene mutation profiling in human cancer. *Nat. Genet.* (2007). doi:10.1038/ng1975
204. Friedman, N., Linial, M., Nachman, I. & Pe'er, D. Using Bayesian networks to analyze expression data. *J. Comput. Biol.* (2000). doi:10.1089/106652700750050961
205. Imoto, S. *et al.* Bayesian network and nonparametric heteroscedastic regression for nonlinear modeling of genetic network. in *Proceedings - IEEE Computer Society Bioinformatics Conference, CSB 2002* (2002). doi:10.1109/CSB.2002.1039344
206. Korucuoglu, M., Isci, S., Ozgur, A. & Otu, H. H. Bayesian pathway analysis of cancer microarray data. *PLoS One* (2014). doi:10.1371/journal.pone.0102803
207. Tritchler, D., Parkhomenko, E. & Beyene, J. Filtering Genes for Cluster and Network Analysis. *BMC Bioinformatics* **10**, 193 (2009).
208. Tegge, A. N., Caldwell, C. W. & Xu, D. Pathway Correlation Profile of Gene-Gene Co-Expression for Identifying Pathway Perturbation. *PLoS One* **7**, e52127 (2012).
209. Siddharthan, R. Dinucleotide weight matrices for predicting transcription factor binding sites:

Generalizing the position weight matrix. *PLoS One* (2010).

doi:10.1371/journal.pone.0009722

210. Ghanat Bari, M., Ung, C. Y., Zhang, C., Zhu, S. & Li, H. Machine Learning-Assisted Network Inference Approach to Identify a New Class of Genes that Coordinate the Functionality of Cancer Networks. *Sci. Rep.* (2017). doi:10.1038/s41598-017-07481-5
211. Luque-Baena, R. M., Urda, D., Gonzalo Claros, M., Franco, L. & Jerez, J. M. Robust gene signatures from microarray data using genetic algorithms enriched with biological pathway keywords. *J. Biomed. Inform.* (2014). doi:10.1016/j.jbi.2014.01.006
212. Cuperlovic-Culf, M. Machine learning methods for analysis of metabolic data and metabolic pathway modeling. *Metabolites* (2018). doi:10.3390/metabo8010004
213. Karp, P. D., Latendresse, M. & Caspi, R. The Pathway Tools Pathway Prediction Algorithm. *Stand. Genomic Sci.* **5**, 424–429 (2011).
214. Pireddu, L., Szafron, D., Lu, P. & Greiner, R. The Path-A metabolic pathway prediction web server. *Nucleic Acids Res.* **34**, W714–W719 (2006).
215. Kanehisa, M., Goto, S., Kawashima, S., Okuno, Y. & Hattori, M. The KEGG resource for deciphering the genome. *Nucleic Acids Res.* **32**, D277-80 (2004).
216. Slenter, D. N. *et al.* WikiPathways: A multifaceted pathway database bridging metabolomics to other omics research. *Nucleic Acids Res.* (2018). doi:10.1093/nar/gkx1064
217. Gene Ontology Consortium. The Gene Ontology (GO) database and informatics resource. *Nucleic Acids Res.* (2004). doi:10.1093/nar/gkh036
218. Thomas, P. D. *et al.* PANTHER: a browsable database of gene products organized by biological function, using curated protein family and subfamily classification. *Nucleic Acids Res.* **31**, 334–341 (2003).

219. Croft, D. *et al.* Reactome: a database of reactions, pathways and biological processes. *Nucleic Acids Res.* **39**, D691–D697 (2011).
220. Gibson, H., Faith, J. & Vickers, P. A survey of two-dimensional graph layout techniques for information visualisation. *Information Visualization* (2013). doi:10.1177/1473871612455749
221. Schreiber, F., Dwyer, T., Marriott, K. & Wybrow, M. A generic algorithm for layout of biological networks. *BMC Bioinformatics* **10**, 375 (2009).
222. Dale, J. M., Popescu, L. & Karp, P. D. Machine learning methods for metabolic pathway prediction. *BMC Bioinformatics* (2010). doi:10.1186/1471-2105-11-15
223. Koo, C. L., Liew, M. J., Mohamad, M. S. & Mohamed Salleh, A. H. A Review for Detecting Gene-Gene Interactions Using Machine Learning Methods in Genetic Epidemiology. *Biomed Res. Int.* **2013**, 432375 (2013).
224. Holland, J. H. Adaptation in Natural and Artificial Systems. *Ann Arbor MI Univ. Michigan Press* (1975). doi:10.1137/1018105
225. Jordán, F., Nguyen, T.-P. & Liu, W.-C. Studying protein-protein interaction networks: a systems view on diseases. *Brief. Funct. Genomics* (2012). doi:10.1093/bfpg/els035
226. Szklarczyk, D. *et al.* STRING v10: Protein-protein interaction networks, integrated over the tree of life. *Nucleic Acids Res.* (2015). doi:10.1093/nar/gku1003
227. Franz, M. *et al.* Cytoscape.js: A graph theory library for visualisation and analysis. *Bioinformatics* (2015). doi:10.1093/bioinformatics/btv557
228. Taubert, J., Hassani-Pak, K., Castells-Brooke, N. & Rawlings, C. J. Ondex Web: Web-based visualization and exploration of heterogeneous biological networks. *Bioinformatics* (2014). doi:10.1093/bioinformatics/btt740
229. Hu, Z., Snitkin, E. S. & Delisi, C. VisANT: An integrative framework for networks in

- systems biology. *Brief. Bioinform.* (2008). doi:10.1093/bib/bbn020
230. Salavert, F. *et al.* Web-based network analysis and visualization using CellMaps. *Bioinformatics* (2016). doi:10.1093/bioinformatics/btw332
231. Subramanian, A., Kuehn, H., Gould, J., Tamayo, P. & Mesirov, J. P. GSEA-P: a desktop application for Gene Set Enrichment Analysis. *Bioinformatics* (2007). doi:10.1093/bioinformatics/btm369
232. Choi, J. Guide: A desktop application for analysing gene expression data. *BMC Genomics* (2013). doi:10.1186/1471-2164-14-688
233. Gentleman, R. *et al.* Bioconductor: open software development for computational biology and bioinformatics. *Genome Biol.* (2004). doi:10.1186/gb-2004-5-10-r80
234. Pipinellis, A. *GitHub Essentials. Packt Publishing Ltd.* (2015).
235. Steffen, M., Petti, A., Aach, J., D'haeseleer, P. & Church, G. Automated modelling of signal transduction networks. *BMC Bioinformatics* (2002). doi:10.1186/1471-2105-3-34
236. Scott, J., Ideker, T., Karp, R. M. & Sharan, R. Efficient algorithms for detecting signaling pathways in protein interaction networks. *J. Comput. Biol.* (2006). doi:10.1089/cmb.2006.13.133
237. Lu, S., Zhang, F., Chen, J. & Sze, S. H. Finding pathway structures in protein interaction networks. *Algorithmica (New York)* (2007). doi:10.1007/s00453-007-0155-7
238. Samal, B. B. & Eiden, L. E. pathFinder: A static network analysis tool for pharmacological analysis of signal transduction pathways. *Sci. Signal.* (2008). doi:10.1126/scisignal.131pt4
239. Zhao, X.-M., Wang, R.-S., Chen, L. & Aihara, K. Uncovering signal transduction networks from high-throughput data by integer linear programming. *Nucleic Acids Res.* **36**, e48–e48 (2008).



240. Gabow, H. N., Galil, Z., Spencer, T. & Tarjan, R. E. Efficient algorithms for finding minimum spanning trees in undirected and directed graphs. *Combinatorica* (1986). doi:10.1007/BF02579168
241. Yosef, N. *et al.* Toward accurate reconstruction of functional protein networks. *Mol. Syst. Biol.* (2009). doi:10.1038/msb.2009.3
242. Gitter, A., Klein-Seetharaman, J., Gupta, A. & Bar-Joseph, Z. Discovering pathways by orienting edges in protein interaction networks. *Nucleic Acids Res.* (2011). doi:10.1093/nar/gkq1207
243. Xing, Z. & Zhang, W. MaxSolver: An efficient exact algorithm for (weighted) maximum satisfiability. *Artif. Intell.* **164**, 47–80 (2005).
244. Tsatmali, M., Ancans, J. & Thody, A. J. Melanocyte function and its control by melanocortin peptides. *Journal of Histochemistry and Cytochemistry* (2002). doi:10.1177/002215540205000201
245. Apalla, Z., Nashan, D., Weller, R. B. & Castellsagué, X. Skin Cancer: Epidemiology, Disease Burden, Pathophysiology, Diagnosis, and Therapeutic Approaches. *Dermatology and Therapy* (2017). doi:10.1007/s13555-016-0165-y
246. American Cancer Society. Cancer Facts & Figures 2018. *Am. Cancer Soc.* (2018). doi:10.1182/blood-2015-12-687814
247. Ali, Z., Yousaf, N. & Larkin, J. Melanoma epidemiology, biology and prognosis. *EJC Suppl.* **11**, 81–91 (2013).
248. Jensen, J. D. & Elewski, B. E. The ABCDEF rule: Combining the ‘ABCDE rule’ and the “ugly duckling sign” in an effort to improve patient self-screening examinations. *Journal of Clinical and Aesthetic Dermatology* (2015).

249. Keohane, S. G. *et al.* The new 8th edition of TNM staging and its implications for skin cancer: a review by the British Association of Dermatologists and the Royal College of Pathologists, U.K. *Br. J. Dermatol.* **0**, (2018).
250. Rastrelli, M., Tropea, S., Rossi, C. R. & Alaibac, M. Melanoma: epidemiology, risk factors, pathogenesis, diagnosis and classification. *In Vivo* (2014). doi:10.1007/s11894-011-0178-8
251. Park, S. L. *et al.* Risk factors for malignant melanoma in white and non-white/non-African American populations: The multiethnic cohort. *Cancer Prev. Res.* (2012). doi:10.1158/1940-6207.CAPR-11-0460
252. Dummer, R., Hauschild, A., Lindenblatt, N., Pentheroudakis, G. & Keilholz, U. Cutaneous melanoma: ESMO Clinical Practice Guidelines for diagnosis, treatment and follow-up. *Ann. Oncol.* (2015). doi:10.1093/annonc/mdv297
253. Weinstein, D., Leininger, J., Hamby, C. & Safai, B. Diagnostic and prognostic biomarkers in melanoma. *J. Clin. Aesthet. Dermatol.* (2014). doi:10.1007/978-1-60761-433-3
254. Leonardi, G. C. *et al.* Cutaneous melanoma: From pathogenesis to therapy (Review). *Int. J. Oncol.* **52**, 1071–1080 (2018).
255. Merlino, G. *et al.* The State of Melanoma: Challenges and Opportunities. *Pigment Cell Melanoma Res.* **29**, 404–416 (2016).
256. Kalal, B. S., Upadhyay, D. & Pai, V. R. Chemotherapy resistance mechanisms in advanced skin cancer. *Oncology Reviews* (2017). doi:10.4081/oncol.2017.326
257. Wilson, M. A. & Schuchter, L. M. in *Cancer Treatment and Research* (2016). doi:10.1007/978-3-319-22539-5\_8
258. Jones, C. *et al.* Unmet clinical needs in the management of advanced melanoma: findings from a survey of oncologists. *Eur. J. Cancer Care (Engl)*. **24**, 867–872 (2015).

259. Mackiewicz, J. What is new in the treatment of advanced melanoma? State of the art. *Contemp. Oncol.* **16**, 363–370 (2012).
260. Ugurel, S. *et al.* Chemosensitivity-directed therapy compared to dacarbazine in chemo-naive advanced metastatic melanoma: a multicenter randomized phase-3 DeCOG trial. *Oncotarget* **8**, 76029–76043 (2017).
261. Quirbt, I., Verma, S., Petrella, T., Bak, K. & Charette, M. Temozolomide for the treatment of metastatic melanoma. *Curr. Oncol.* (2007). doi:10.1634/theoncologist.12-9-1114
262. Daponte, A. *et al.* Temozolomide and cisplatin in advanced malignant melanoma. *Anticancer Res.* (2005).
263. Wichtowski, M. & Murawa, D. Electrochemotherapy in the treatment of melanoma. *Contemp. Oncol.* **22**, 8–13 (2018).
264. Baldea, I. *et al.* Melanogenesis and DNA damage following photodynamic therapy in melanoma with two meso-substituted porphyrins. *J. Photochem. Photobiol. B Biol.* (2016). doi:10.1016/j.jphotobiol.2016.06.012
265. Achkar, T. & Tarhini, A. A. The use of immunotherapy in the treatment of melanoma. *J. Hematol. Oncol.* (2017). doi:10.1186/s13045-017-0458-3
266. Weber, J. *et al.* Adjuvant Nivolumab versus Ipilimumab in Resected Stage III or IV Melanoma. *N. Engl. J. Med.* (2017). doi:10.1056/NEJMoa1709030
267. Redman, J. M., Gibney, G. T. & Atkins, M. B. Advances in immunotherapy for melanoma. *BMC Med.* **14**, 20 (2016).
268. Pol, J. *et al.* Trial Watch—Oncolytic viruses and cancer therapy. *Oncoimmunology* **5**, e1117740 (2016).
269. Corrigan, P. A., Beaulieu, C., Patel, R. B. & Lowe, D. K. Talimogene Laherparepvec: An

- Oncolytic Virus Therapy for Melanoma. *Ann. Pharmacother.* **51**, 675–681 (2017).
270. Wang, R. *et al.* Interferon- $\alpha$ -2b as an adjuvant therapy prolongs survival of patients with previously resected oral mucosal melanoma. *Genet. Mol. Res.* (2015).  
doi:10.4238/2015.October.5.8
271. DI TROLIO, R. *et al.* Update on PEG-Interferon  $\alpha$ -2b as Adjuvant Therapy in Melanoma. *Anticancer Res.* **32**, 3901–3909 (2012).
272. Flaherty, L. E. *et al.* Outpatient biochemotherapy with interleukin-2 and interferon alfa-2b in patients with metastatic malignant melanoma: Results of two phase II Cytokine Working Group trials. *J. Clin. Oncol.* (2001). doi:10.1200/JCO.2001.19.13.3194
273. Tarhini, A. A., Kirkwood, J. M., Gooding, W. E., Cai, C. & Agarwala, S. S. Durable complete responses with high-dose bolus interleukin-2 in patients with metastatic melanoma who have experienced progression after biochemotherapy. *J. Clin. Oncol.* (2007).  
doi:10.1200/JCO.2006.10.2822
274. Amin, A. & White, R. L. High-dose interleukin-2: is it still indicated for melanoma and RCC in an era of targeted therapies? *Oncology (Williston Park)*. (2013).
275. Sasidharan Nair, V. & Elkord, E. Immune checkpoint inhibitors in cancer therapy: a focus on T-regulatory cells. *Immunol. Cell Biol.* **96**, 21–33 (2017).
276. Weber, J. S., Ramakrishnan, R., Laino, A., Berglund, A. E. & Woods, D. Association of changes in T regulatory cells (Treg) during nivolumab treatment with melanoma outcome. *J. Clin. Oncol.* **35**, 3031 (2017).
277. Van Allen, E. M. *et al.* Genomic correlates of response to CTLA-4 blockade in metastatic melanoma. *Science (80-. )*. (2015). doi:10.1126/science.aad0095
278. Snyder, A. *et al.* Genetic Basis for Clinical Response to CTLA-4 Blockade in Melanoma. *N.*

*Engl. J. Med.* (2014). doi:10.1056/NEJMoa1406498

279. Alsaab, H. O. *et al.* PD-1 and PD-L1 checkpoint signaling inhibition for cancer immunotherapy: mechanism, combinations, and clinical outcome. *Frontiers in Pharmacology* (2017). doi:10.3389/fphar.2017.00561
280. Bai, J. *et al.* Regulation of PD-1/PD-L1 pathway and resistance to PD-1/PD-L1 blockade. *Oncotarget* **8**, 110693–110707 (2017).
281. Schwartzentruher, D. J. *et al.* gp100 Peptide Vaccine and Interleukin-2 in Patients with Advanced Melanoma. *N. Engl. J. Med.* (2011). doi:10.1056/NEJMoa1012863
282. Royal, R. E. *et al.* A toll-like receptor agonist to drive melanoma regression as a vaccination adjuvant or by direct tumor application. *J. Clin. Oncol.* **35**, 9582 (2017).
283. Verdegaal, E. M. E. Adoptive cell therapy: a highly successful individualized therapy for melanoma with great potential for other malignancies. *Curr. Opin. Immunol.* **39**, 90–95 (2016).
284. Knudsen, E. S. & Witkiewicz, A. K. The Strange Case of CDK4/6 Inhibitors: Mechanisms, Resistance, and Combination Strategies. *Trends in Cancer* (2017). doi:10.1016/j.trecan.2016.11.006
285. Eliades, P. *et al.* A novel multi-CDK inhibitor P1446A-05 restricts melanoma growth and produces synergistic effects in combination with MAPK pathway inhibitors. *Cancer Biol. Ther.* **17**, 778–784 (2016).
286. Rauf, F. *et al.* Ibrutinib inhibition of ERBB4 reduces cell growth in a WNT5A-dependent manner. *Oncogene* (2018). doi:10.1038/s41388-017-0079-x
287. Cosgarea, I., Ritter, C., Becker, J. C., Schadendorf, D. & Ugurel, S. Update on the clinical use of kinase inhibitors in melanoma. *JDDG J. der Dtsch. Dermatologischen Gesellschaft*

- 15, 887–893 (2017).
288. POPESCU, A. & ANGHEL, R. M. Tyrosine-kinase Inhibitors Treatment in Advanced Malignant Melanoma. *Mædica* **12**, 293–296 (2017).
289. Pappalardo, F. *et al.* Computational Modeling of PI3K/AKT and MAPK Signaling Pathways in Melanoma Cancer. *PLoS One* **11**, e0152104 (2016).
290. Hoops, S. *et al.* COPASI--a COMplex PATHway SIMulator. *Bioinformatics* **22**, 3067–3074 (2006).
291. Miao, H., Wu, H. & Xue, H. Generalized Ordinary Differential Equation Models (). *J. Am. Stat. Assoc.* **109**, 1672–1682 (2014).
292. Gillespie, D. T. Exact stochastic simulation of coupled chemical reactions. *J. Phys. Chem.* (1977). doi:10.1021/j100540a008
293. Fell, D. A. Metabolic control analysis: a survey of its theoretical and experimental development. *Biochem. J.* (1992). doi:10.1042/bj2860313
294. Ingalls, B. P. & Sauro, H. M. Sensitivity analysis of stoichiometric networks: An extension of metabolic control analysis to non-steady state trajectories. *J. Theor. Biol.* (2003). doi:10.1016/S0022-5193(03)00011-0
295. Höfer, T. & Heinrich, R. A Second-order Approach to Metabolic Control Analysis. *J. Theor. Biol.* **164**, 85–102 (1993).
296. Johnson, M. L. & Faunt, L. M. Parameter estimation by least-squares methods. *Methods in Enzymology* (1992). doi:10.1016/0076-6879(92)10003-V
297. Edgar, R. Gene Expression Omnibus: NCBI gene expression and hybridization array data repository. *Nucleic Acids Res.* (2002). doi:10.1093/nar/30.1.207
298. Chelliah, V., Laibe, C. & Le Novère, N. BioModels database: A repository of mathematical

models of biological processes. *Methods Mol. Biol.* (2013). doi:10.1007/978-1-62703-450-0-10

299. Adjiri, A. DNA Mutations May Not Be the Cause of Cancer. *Oncol. Ther.* **5**, 85–101 (2017).
300. Cedar, H. & Bergman, Y. Linking DNA methylation and histone modification: Patterns and paradigms. *Nature Reviews Genetics* (2009). doi:10.1038/nrg2540
301. Robertson, K. D. DNA methylation and human disease. *Nature Reviews Genetics* (2005). doi:10.1038/nrg1655
302. Moore, L. D., Le, T. & Fan, G. DNA methylation and its basic function. *Neuropsychopharmacology* (2013). doi:10.1038/npp.2012.112
303. Liu, H. *et al.* DevMouse, the mouse developmental methylome database and analysis tools. *Database* (2014). doi:10.1093/database/bat084
304. Irizarry, R. A. *et al.* Comprehensive high-throughput arrays for relative methylation (CHARM). *Genome Res.* (2008). doi:10.1101/gr.7301508
305. De Souza, A. P., Planello, A. C., Marques, M. R., De Carvalho, D. D. & Line, S. R. P. High-throughput DNA analysis shows the importance of methylation in the control of immune inflammatory gene transcription in chronic periodontitis. *Clin. Epigenetics* (2014). doi:10.1186/1868-7083-6-15
306. Candido, S., Alessandro, G., Palumbo, P., Pennisi, M. & Russo, G. CO. 1–11 (2018). doi:10.1186/s12859-018-2397-6
307. Weinstein, J. N. *et al.* The Cancer Genome Atlas Pan-Cancer Analysis Project. *Nat. Genet.* **45**, 1113–1120 (2013).
308. Pacini, F., Castagna, M. G., Brillì, L. & Pentheroudakis, G. Thyroid cancer: ESMO clinical practice guidelines for diagnosis, treatment and follow-up. *Ann. Oncol.* (2012).

doi:10.1093/annonc/mds230

309. Vigneri, R., Malandrino, P. & Vigneri, P. The changing epidemiology of thyroid cancer: Why is incidence increasing? *Current Opinion in Oncology* (2015).  
doi:10.1097/CCO.0000000000000148
310. Rahbari, R., Zhang, L. & Kebebew, E. Thyroid cancer gender disparity. *Future Oncol.* (2010). doi:10.2217/fon.10.127
311. Knox, M. A. Thyroid nodules. *Am. Fam. Physician* (2013). doi:10.1016/j.mcna.2012.02.002
312. Ferrari, S. M., Fallahi, P., Antonelli, A. & Benvenga, S. Environmental Issues in Thyroid Diseases. *Front. Endocrinol. (Lausanne)*. **8**, 50 (2017).
313. Vigneri, R., Malandrino, P., Gianì, F., Russo, M. & Vigneri, P. Heavy metals in the volcanic environment and thyroid cancer. *Mol. Cell. Endocrinol.* (2017).  
doi:10.1016/j.mce.2016.10.027
314. Fagin, J. A. & Wells, S. A. Biologic and Clinical Perspectives on Thyroid Cancer. *N. Engl. J. Med.* (2016). doi:10.1056/NEJMra1501993
315. Lloyd, R. V, Buehler, D. & Khanafshar, E. Papillary Thyroid Carcinoma Variants. *Head Neck Pathol.* **5**, 51–56 (2011).
316. Lo, C.-Y., Chan, W.-F., Lam, K.-Y. & Wan, K.-Y. Follicular Thyroid Carcinoma: The Role of Histology and Staging Systems in Predicting Survival. *Ann. Surg.* **242**, 708–715 (2005).
317. Ahmadi, S., Stang, M., Jiang, X. “Sara” & Sosa, J. A. Hürthle cell carcinoma: current perspectives. *Onco. Targets. Ther.* **9**, 6873–6884 (2016).
318. Yu, X.-M., Schneider, D. F., Levenson, G., Chen, H. & Sippel, R. S. Follicular variant of papillary thyroid carcinoma is a unique clinical entity: a population-based study of 10,740 cases. *Thyroid* (2013). doi:10.1089/thy.2012.0453



319. Priya, S. R., Dravid, C. S., Digumarti, R. & Dandekar, M. Targeted Therapy for Medullary Thyroid Cancer: A Review. *Front. Oncol.* **7**, 238 (2017).
320. Roche, A. M., Fedewa, S. A., Shi, L. L. & Chen, A. Y. Treatment and survival vary by race/ethnicity in patients with anaplastic thyroid cancer. *Cancer* **124**, 1780–1790 (2018).
321. Nguyen, Q. T. *et al.* Diagnosis and treatment of patients with thyroid cancer. *Am. Heal. drug benefits* (2015).
322. Liu, J.-W. *et al.* Tyrosine kinase inhibitors for advanced or metastatic thyroid cancer: a meta-analysis of randomized controlled trials. *Curr. Med. Res. Opin.* (2017).  
doi:10.1080/03007995.2017.1368466
323. Fallahi, P. *et al.* Selective use of vandetanib in the treatment of thyroid cancer. *Drug Des. Devel. Ther.* (2015). doi:10.2147/DDDT.S72495
324. Wells, S. A. *et al.* Vandetanib in Patients With Locally Advanced or Metastatic Medullary Thyroid Cancer: A Randomized, Double-Blind Phase III Trial. *J. Clin. Oncol.* **30**, 134–141 (2012).
325. Fallahi, P. *et al.* Cabozantinib in Thyroid Cancer. *Recent Patents on Anti-Cancer Drug Discovery* **10**, 259–269 (2015).
326. Benekli, M. *et al.* Efficacy of sorafenib in advanced differentiated and medullary thyroid cancer: Experience in a turkish population. *Onco. Targets. Ther.* (2014).  
doi:10.2147/OTT.S70670
327. Brose, M. S. *et al.* Sorafenib in radioactive iodine-refractory, locally advanced or metastatic differentiated thyroid cancer: a randomised, double-blind, phase 3 trial. *Lancet (London, England)* (2014). doi:10.1016/S0140-6736(14)60421-9
328. Fisher, R. & Larkin, J. Vemurafenib: A new treatment for BRAF-V600 mutated advanced

melanoma. *Cancer Management and Research* (2012). doi:10.2147/CMAR.S25284

329. Hyman, D. M. *et al.* Vemurafenib in Multiple Nonmelanoma Cancers with BRAF V600 Mutations. *N. Engl. J. Med.* **373**, 726–736 (2015).
330. Batlle, E. & Clevers, H. Cancer stem cells revisited. *Nat. Med.* **23**, 1124 (2017).
331. Nagayama, Y., Shimamura, M. & Mitsutake, N. Cancer Stem Cells in the Thyroid. *Front. Endocrinol. (Lausanne)*. **7**, 20 (2016).
332. Malaguarnera, R. *et al.* Insulin Receptor Isoforms and Insulin-Like Growth Factor Receptor in Human Follicular Cell Precursors from Papillary Thyroid Cancer and Normal Thyroid. *J. Clin. Endocrinol. Metab.* **96**, 766–774 (2011).
333. Ahn, S.-H., Henderson, Y. C., Williams, M. D., Lai, S. Y. & Clayman, G. L. Detection of Thyroid Cancer Stem Cells in Papillary Thyroid Carcinoma. *J. Clin. Endocrinol. Metab.* **99**, 536–544 (2014).
334. Gianì, F. *et al.* Thyrospheres From Normal or Malignant Thyroid Tissue Have Different Biological, Functional, and Genetic Features. *J. Clin. Endocrinol. Metab.* **100**, E1168–E1178 (2015).
335. Todaro, M. *et al.* Tumorigenic and Metastatic Activity of Human Thyroid Cancer Stem Cells. *Cancer Res.* **70**, 8874–8885 (2010).
336. Li, W., Reeb, A. N., Sewell, W. A., Elhomsy, G. & Lin, R.-Y. Phenotypic Characterization of Metastatic Anaplastic Thyroid Cancer Stem Cells. *PLoS One* **8**, e65095 (2013).
337. Reeb, A. N., Li, W. & Lin, R.-Y. Bioluminescent Human Thyrospheres Allow Noninvasive Detection of Anaplastic Thyroid Cancer Growth and Metastases In Vivo. *Thyroid* **24**, 1134–1138 (2014).
338. Giuffrida, R. *et al.* Resistance of papillary thyroid cancer stem cells to chemotherapy. *Oncol.*

*Lett.* **12**, 687–691 (2016).

339. Liotti, F. *et al.* Interleukin-8, but not the Related Chemokine CXCL1, Sustains an Autocrine Circuit Necessary for the Properties and Functions of Thyroid Cancer Stem Cells. *Stem Cells* **35**, 135–146 (2017).
340. Legewie, S., Herzel, H., Westerhoff, H. V & Blüthgen, N. Recurrent design patterns in the feedback regulation of the mammalian signalling network. *Mol. Syst. Biol.* **4**, 190 (2008).
341. Mendes, P. *et al.* in *Methods in molecular biology (Clifton, N.J.)* **500**, 17–59 (2009).
342. Zhang, W., Heinzmann, D. & Grippo, J. F. Clinical Pharmacokinetics of Vemurafenib. *Clin. Pharmacokinet.* **56**, 1033–1043 (2017).
343. Reif, J. H. Depth-first search is inherently sequential. *Inf. Process. Lett.* **20**, 229–234 (1985).
344. Miyoshi, J., Higashi, T., Mukai, H., Ohuchi, T. & Kakunaga, T. Structure and transforming potential of the human cot oncogene encoding a putative protein kinase. *Mol. Cell. Biol.* **11**, 4088–4096 (1991).
345. Lee, J. *et al.* Aberrant Expression of COT Is Related to Recurrence of Papillary Thyroid Cancer. *Medicine (Baltimore)*. **94**, e548 (2015).
346. Gantke, T., Sriskantharajah, S. & Ley, S. C. Regulation and function of TPL-2, an I $\kappa$ B kinase-regulated MAP kinase kinase kinase. *Cell Res.* **21**, 131–145 (2011).
347. Pattison, M. J. *et al.* TLR and TNF-R1 activation of the MKK3/MKK6-p38 axis in macrophages is mediated by TPL-2 kinase. *Biochem. J.* **473**, 2845–2861 (2016).
348. Vougioukalaki, M., Kanellis, D. C., Gkouskou, K. & Eliopoulos, A. G. Tpl2 kinase signal transduction in inflammation and cancer. *Cancer Lett.* **304**, 80–89 (2011).
349. Martel, G. & Rousseau, S. TPL2 signalling: From Toll-like receptors-mediated ERK1/ERK2 activation to Cystic Fibrosis lung disease. *Int. J. Biochem. Cell Biol.* **52**, 146–151 (2014).

350. Sourvinos, G., Tsatsanis, C. & Spandidos, D. A. Overexpression of the Tpl-2/Cot oncogene in human breast cancer. *Oncogene* **18**, 4968–4973 (1999).
351. Kim, K. *et al.* Interleukin-22 promotes epithelial cell transformation and breast tumorigenesis via MAP3K8 activation. *Carcinogenesis* **35**, 1352–1361 (2014).
352. Jeong, J. H. *et al.* TPL2/COT/MAP3K8 (TPL2) Activation Promotes Androgen Depletion-Independent (ADI) Prostate Cancer Growth. *PLoS One* **6**, e16205 (2011).
353. Lee, H. W. *et al.* Tpl2 induces castration resistant prostate cancer progression and metastasis. *Int. J. Cancer* **136**, 2065–2077 (2015).
354. Lee, J.-H. *et al.* TPL2 Is an Oncogenic Driver in Keratocanthoma and Squamous Cell Carcinoma. *Cancer Res.* **76**, 6712–6722 (2016).
355. Lee, H., Choi, H., Joo, K. & Nam, D.-H. Tumor Progression Locus 2 (Tpl2) Kinase as a Novel Therapeutic Target for Cancer: Double-Sided Effects of Tpl2 on Cancer. *Int. J. Mol. Sci.* **16**, 4471–4491 (2015).